

INFORMATION TO USERS

This manuscript has been reproduced from the microfilm master. UMI films the text directly from the original or copy submitted. Thus, some thesis and dissertation copies are in typewriter face, while others may be from any type of computer printer.

The quality of this reproduction is dependent upon the quality of the copy submitted. Broken or indistinct print, colored or poor quality illustrations and photographs, print bleedthrough, substandard margins, and improper alignment can adversely affect reproduction.

In the unlikely event that the author did not send UMI a complete manuscript and there are missing pages, these will be noted. Also, if unauthorized copyright material had to be removed, a note will indicate the deletion.

Oversize materials (e.g., maps, drawings, charts) are reproduced by sectioning the original, beginning at the upper left-hand corner and continuing from left to right in equal sections with small overlaps.

Photographs included in the original manuscript have been reproduced xerographically in this copy. Higher quality 6" x 9" black and white photographic prints are available for any photographs or illustrations appearing in this copy for an additional charge. Contact UMI directly to order.

Bell & Howell Information and Learning
300 North Zeeb Road, Ann Arbor, MI 48106-1346 USA
800-521-0600

UMI[®]

**Holocene Fire History of a Coastal Temperate Rain Forest,
Vancouver Island, British Columbia, Canada**

Daniel Girard Gavin

**A dissertation submitted in partial fulfillment of the
requirements for the degree of**

Doctor of Philosophy

University of Washington

2000

Program Authorized to Offer Degree: College of Forest Resources

UMI Number: 9995371

Copyright 2000 by
Gavin, Daniel Girard

All rights reserved.

UMI[®]

UMI Microform 9995371

Copyright 2001 by Bell & Howell Information and Learning Company.

All rights reserved. This microform edition is protected against
unauthorized copying under Title 17, United States Code.

Bell & Howell Information and Learning Company
300 North Zeeb Road
P.O. Box 1346
Ann Arbor, MI 48106-1346

© Copyright 2000
Daniel Girard Gavin

In presenting this dissertation in partial fulfillment of the requirements for the Doctoral degree at the University of Washington, I agree that the Library shall make its copies freely available for inspection. I further agree that extensive copying of the dissertation is allowable only for scholarly purposes, consistent with "fair use" as prescribed in the U.S. Copyright Law. Requests for copying or reproduction of this dissertation may be referred to Bell and Howell Information and Learning, 300 North Zeeb Road, Ann Arbor, MI 48106-1346, to whom the author has granted "the right to reproduce and sell (a) copies of the manuscript in microform and/or (b) printed copies of the manuscript made from microform."

Signature: David L. Arin

Date: Dec 4, 2000

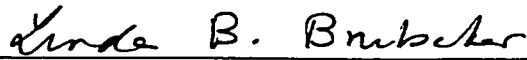
University of Washington
Graduate School

This is to certify that I have examined this copy of a doctoral dissertation by

Daniel Girard Gavin

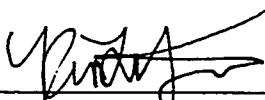
and have found that it is complete and satisfactory in all respects,
and that any and all revisions required by the final
examining committee have been made.

Chair of Supervisory Committee:

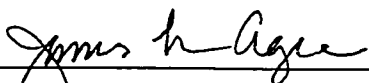


Linda B. Brubaker

Reading Committee:



Kenneth P. Lertzman



James K. Agee

Date: Nov 15, 2000

University of Washington

Abstract

Holocene Fire History of a Coastal Temperate Rain Forest,
Vancouver Island, British Columbia, Canada

Daniel Girard Gavin

Chairperson of the Supervisory Committee:
Professor Linda B. Brubaker
College of Forest Resources

The current lack of information about the temporal and landscape pattern of fires is a key source of uncertainty about natural disturbance regimes in coastal temperate rain forests. Two approaches were employed to examine fire history within a 700 ha low elevation area on the west coast of Vancouver Island: 1) point estimates of time-since-fire from tree ages and radiocarbon dates on soil charcoal, and 2) spatially aggregated estimates of fire occurrence from an 1800-year lake sediment record of charcoal accumulation. To aid with the first approach, the accuracy of the radiocarbon method for dating known fire events was evaluated. It was found that calibrated radiocarbon ages of soil charcoal consistently overestimated fire ages by 100–400 years due to the age of wood at the time of the fire. Estimates of time-since-fire at 83 sites ranged from 64 to ca. 12,220 cal. years before present. Approximately 20% of the sites have not burned for over 6000 years; these are on low fire-susceptibility landforms (i.e., north aspects and low terraces), which burned mainly in the early Holocene. In contrast, all sites on high-susceptibility landforms (i.e., south aspects) burned within the last 800 years. In the second approach, distinct peaks in charcoal in the lake sediment record corresponded with fires within 250 m of the lake. Fire intervals in this area increased from ca. 50 years (AD 200–900) to ca. 350 years (AD 1100–present), corresponding with regional climatic change. The decadal-

scale fire frequency detected in the lake sediment record contrasts with the > 2000-year time-since-fire detected in a large area near the lake. Interpreted together, these records suggest that fires repeatedly burn certain sites. Fire frequency on high-susceptibility landforms was probably sufficient during the late Holocene to support Douglas-fir, a species dependent on fire for regeneration. On low-susceptibility landforms, extremely low fire frequency probably allowed late-successional forest structure to persist throughout the late Holocene. The extremely long time-since-fire detected in a large portion of the study area supports the distinction of the coastal temperate rain forest as affected by a fundamentally different fire history than forests further inland.

TABLE OF CONTENTS

LIST OF FIGURES.....	ii
LIST OF TABLES	iv
CHAPTER 1: OVERVIEW.....	1
CHAPTER 2: ESTIMATION OF INBUILT AGE IN RADIOCARBON-DERIVED AGES OF SOIL CHARCOAL FOR FIRE HISTORY STUDIES	5
Introduction.....	5
Study area	9
Methods	11
Results	21
Discussion.....	28
Conclusions.....	35
CHAPTER 3: HOLOCENE FIRE HISTORY OF A COASTAL TEMPERATE RAIN FOREST BASED ON SOIL CHARCOAL RADIOCARBON DATES	37
Introduction.....	37
Study area	39
Methods	46
Results	53
Discussion.....	72
CHAPTER 4: AN 1800-YEAR RECORD OF THE SPATIAL AND TEMPORAL DISTRIBUTION OF FIRE FROM THE WEST COAST OF VANCOUVER ISLAND, CANADA	84
Introduction.....	84
Clayoquot Lake study area	87
Methods	89
Results	98
Discussion.....	113
LITERATURE CITED.....	121

LIST OF FIGURES

Figure 2.1	Schematic diagram showing terms associated with the inbuilt age of charcoal	8
Figure 2.2	Location of sample sites in the Clayoquot Valley	10
Figure 2.3	Outline of the steps used to simulate the inbuilt-age distribution of charcoal following forest fire	15
Figure 2.4	Time-since-death of coarse woody debris and snags of common tree species in western Washington, British Columbia, and southeast Alaska	20
Figure 2.5	Calibrated radiocarbon ages on single fragments of charcoal from the soil surface	24
Figure 2.6	Mean probability distribution of 26 radiocarbon ages of soil charcoal	25
Figure 2.7	Mean coarse woody debris and fine branch biomass of plots in three forest types in the Clayoquot Valley	26
Figure 2.8	Simulated inbuilt-age distributions of charcoal biomass produced following forest fire	27
Figure 2.9	Example of a radiocarbon age determination adjusted to account for error introduced by inbuilt age	34
Figure 3.1	Location and climate of the study watershed	40
Figure 3.2	Location of sample sites in the Clayoquot Valley	55
Figure 3.3	Time-since-fire at 83 sites in the Clayoquot Valley	56
Figure 3.4	Charcoal mass in soil related to time-since-fire	64
Figure 3.5	Stratigraphic and temporal relationships among soil charcoal radiocarbon dates	65

Figure 3.6	Time-since-fire distribution at 83 sites in the Clayoquot Valley.....	68
Figure 3.7	Box plots of time-since-fire estimates at 83 sites in the Clayoquot Valley .	69
Figure 3.8	Time-since-fire related to the terrain insolation index and terrain type.....	70
Figure 3.9	The proportion of all possible site pairs that have differences in time-since-fire estimates < 300 years in non-overlapping distance classes	71
Figure 3.10	Schematic showing how a time-since-fire distribution may form in areas with a wide range in fire susceptibility	80
Figure 4.1	Map of the study area showing the fire history sampling sites	88
Figure 4.2	Date-of-last fire map for the area within a 500 m buffer around Clayoquot Lake.....	100
Figure 4.3	Age-depth relationship for the Clayoquot Lake sediment core	101
Figure 4.4	Accumulation rates from the Clayoquot Lake sediment core for charcoal, conifer needle macrofossils, and magnetic susceptibility	103
Figure 4.5	Frequency distribution of the charcoal peak component calculated as the positive residuals from a background curve.....	106
Figure 4.6	Comparison of fires detected in the Clayoquot Valley by lake sediment records, tree-ring records, and radiocarbon dates of soil charcoal	107
Figure 4.7	Comparison between the distance of fires to the lake edge and the height of the corresponding CHAR peak in the sediment core.....	109
Figure 4.8	Fire history parameters used for the calculation of the fire hazard ratio ...	111
Figure 4.9	Macrofossil diagram from Clayoquot Lake	112

LIST OF TABLES

Table 2.1	Descriptions of decay classes for coarse woody debris and snags	16
Table 2.2	Radiocarbon dates on western redcedar wood taken directly beneath the bark on standing snags	19
Table 2.3	Radiocarbon dates of soil charcoal from recent fires.....	23
Table 3.1	Tree-ring dates of fire events in the Clayoquot Valley	57
Table 3.2	Radiocarbon dates of soil charcoal obtained from the Clayoquot Valley....	58
Table 3.3	Frequency of sites with different numbers of dates per site in different soil horizons	63
Table 4.1	Radiocarbon dates and Pb-210 age determinations from the Clayoquot Lake sediment core	102
Table 4.2	Cross-correlation of three time series from the Clayoquot Lake sediment record	108

ACKNOWLEDGEMENTS

I am deeply indebted to my major advisor, Linda Brubaker, for training me in paleoecology, for providing me with the tools and freedom to conduct my research, and for guidance and criticism at all stages of research and writing. Ken Lertzman served as a second advisor; the original concept and many of the ideas in this dissertation are his. I am grateful for the flexibility, support, and additional research opportunities from both Linda Brubaker and Ken Lertzman. I also wish to thank my other committee members, Jim Agee, David Ford and Richard Gammon, for their advice at various stages of this research and for reviewing this dissertation.

For help in the field, Melanie Konradi, Cheryl Takahashi, Teresa Opalka, and Len Koehler assisted me for long periods and Ken Lertzman, Doug Hallett, and Wyatt Oswald for shorter periods. Field work in the remote study area would have been impossible without logistical support from Josie Cleland and the Clayoquot Biosphere Project. The cabin, canoes, and radios provided by the Clayoquot Biosphere Project were essential. Jan Heine and Brian Sherrod loaned gear for coring lake sediments.

Cheryl Takahashi and Gladys Baptiste in the Archaeology Department at Simon Fraser University completed many long weeks of laboratory work. Anne Walton, Ramona Maraj and Teresa Opalka also helped with laboratory work. Erle Nelson provided advice on radiocarbon dating and space for much of the laboratory work. Bob Flett of Flett Research performed the Pb-210 analysis. I am grateful to Tom Brown at the Center for Accelerator Mass Spectrometry at Lawrence Livermore National Laboratory for aid in all

steps of radiocarbon dating and ensuring the accuracy of the dates. Special thanks go to Phil Hurvitz for teaching me the basics and many of the complexities of GIS using Arc/Info software. This work was improved and influenced by frequent in-depth discussions with my graduate student peers: Lisa Carlson, Wyatt Oswald, and Doug Hallett. Audrey Pearson provided much background information and shared data on the study site.

This research was funded by Forest Renewal BC with a grant (HQ96235-RE) to Kenneth Lertzman. Additional support during the final phase of this research was provided by a scholarship from the College of Forest Resources and by a grant from Global Forest (Vancouver, B.C.).

Lastly, I am most owing to my wife Melanie whose firm support and love more than anything made this dissertation a reality.

DEDICATION

This dissertation is dedicated to my parents, Paul and Eleanor Gavin, for instilling in me
an appreciation for the natural world.

CHAPTER 1: OVERVIEW

Forests near the west coast of Vancouver Island are noted for a preponderance of late successional characteristics, including stands with a wide range of ages and sizes, an abundance of woody debris, and a scarcity of Douglas-fir (*Pseudotsuga menziesii* (Mirb.) Franco) (Lertzman et al. 1996; Alaback 1996). The apparent absence of even age classes in these forests, which represent the wettest sections of the Coastal Western Hemlock biogeoclimatic zone (Meidinger and Pojar 1991), suggest that stand composition and structure has been influenced by processes operating at small spatial scales (i.e., treefalls) and that large disturbance events (major wind storms and fires) have been of little importance. These forests have been termed "coastal temperate rain forest" because they sharply contrast with those of drier, slightly more inland forests dominated by seral Douglas-fir that presumably colonized after stand-replacing fires within the last several hundred years (Gagnon and Bradfield 1986; Green and Klinka 1994). Though the lack of direct evidence of fire in coastal forests suggests long fire intervals, fire size and frequency has never been investigated in these forests. Knowledge of the past pattern of fire is important to gain an understanding of the origin of old-growth forest structure, processes of species turnover and long-term trajectories of forest composition (Spies and Franklin 1989; Lertzman 1992; Huff 1995). In addition, the pattern of fire is of practical importance for guiding management strategies that attempt to simulate the rate, pattern and patch size of the natural disturbance regime (Scientific Panel 1995a; Lertzman et al. 1997).

Characterization of the fire regime in areas with very long fire intervals has been hindered by the methods employed to reconstruct fire events. In cases where fire intervals are longer than the ages of trees, tree-ring methods are not applicable. In such

cases, dates of fires may be determined by using fine-scale sampling of the charcoal stratigraphy in lake sediments (Clark 1988a; Clark and Royall 1995; Long et al. 1998). Paleoecological studies using lake sediments have the distinct disadvantage of not being spatially explicit because the sediment charcoal stratigraphy represents a spatially aggregated record of all fire events within a certain area near the lake (the charcoal source area), and thus can not be used to reconstruct the pattern of fire on the landscape. However, the potential for developing a spatially explicit record of fire exists in the form of charcoal preserved in soil. In fact, in most areas of coastal temperate rain forest the only recoverable evidence of fire in forest stands is soil charcoal.

The overall goal of this dissertation is to describe the temporal and spatial pattern of fire over the last 10,000 years in low elevation areas of a single watershed near the west coast of Vancouver Island. To best characterize both the temporal and spatial variability in the fire regime, three different fire history methods were used in the same study area: tree-ring dates of the most recent fires, soil charcoal radiocarbon dates of older fires, and a sediment charcoal record from a lake. The combinations of records from the same study area should describe the spatial and temporal pattern of fire more completely than is possible by any single method. Inter-comparisons of these three methods also provide valuable tests on the spatial and/or temporal precision of each fire history method.

Of the three fire history methods used in this dissertation, the soil charcoal method is utilized most extensively. Unlike for the other fire history methods, few fire history studies based on soil charcoal have been conducted (e.g., Carcaillet 1998), and methodological issues remain regarding how to sample for soil charcoal and the temporal precision of radiocarbon ages to estimate fire dates. This study, with a total of 141 radiocarbon dates of soil charcoal, represents one of the largest known efforts to

radiocarbon date soil charcoal for fire history, and can be used to assess the reliability of the soil charcoal method to provide meaningful fire history data, such as the time elapsed since the last fire and intervals between fires. For example, this study explicitly addresses the sampling intensity required to locate charcoal from the most recent fire, the number of charcoal fragments that should be aged per soil profile, and the presence of a charcoal stratigraphy in the soil. In addition, an important error in radiocarbon dates of charcoal to age fire events results from the age of the wood at the time of the fire, which causes charcoal ages to be greater than the age of the fire. This error, termed 'inbuilt age,' is of particular concern in forests with large accumulations of dead wood.

This dissertation is organized into three main chapters that are meant to be read as stand-alone papers, though each chapter builds on ideas and data presented in earlier chapters. Chapter two is an investigation of the inbuilt age errors of radiocarbon dates of soil charcoal used to determine fire dates. Inbuilt age was examined empirically by comparing charcoal radiocarbon dates with actual dates of fires determined by tree-ring methods, and theoretically with a model of charcoal production following a fire. Subsequent chapters incorporate the inbuilt age error into analyses involving soil charcoal radiocarbon dates.

Chapter three addresses the fire history from tree-ring dates and soil charcoal radiocarbon dates over a network of sites in the study area. Fire history is analyzed with respect to site features, such as forest composition, terrain formations, and the exposure to solar radiation. Soil charcoal radiocarbon dates revealed several instances of exceptionally long fire intervals. The implications of this fire disturbance regime are discussed in the context of stand-scale community dynamics as well as the dynamics of the landscape-scale forest mosaic over millennial time scales.

Chapter four provides a more complete view of the spatial and temporal pattern of fire by using a lake sediment record of fire events in conjunction with soil charcoal radiocarbon dates and tree-ring dates in forests adjacent to the lake. Although methods for lake sediment charcoal records have progressed over the last decade (e.g., Long et al. 1998), the dispersal of charcoal to lakes is poorly understood, and therefore the size of the source area that contributes charcoal to lake sediments is also poorly understood. This chapter provides an explicit means of estimating the source area of charcoal using point estimates of fire at a range of distances around the lake. The record of fire dates from the sediment core provides a record of the changes in fire frequency that are likely linked to climatic changes. The comparison of fire history results from the lake sediment record with the results from the soil charcoal dates reveal important features of the spatial distribution of fire over time.

This study addresses important questions regarding the soil charcoal method of fire history: (1) how closely do radiocarbon dates of soil charcoal represent the time of fire? and (2) how must soil charcoal profiles be sampled to obtain meaningful fire history parameters? This study also addresses large questions regarding the disturbance ecology of forests: (3) How long have stands in the coastal temperate rain forest persisted in the absence of fire? and (4) How has fire history varied with terrain features over millennial time-scales?

CHAPTER 2: ESTIMATION OF INBUILT AGE IN RADIOCARBON-DERIVED AGES OF SOIL CHARCOAL FOR FIRE HISTORY STUDIES

Introduction

Radiocarbon ages of wood charcoal from soils are commonly used to determine ages of fire events (Molloy et al. 1963; Turner 1984; Horn and Sanford 1992; Meyer et al. 1992; Hopkins et al. 1993; Carcaillet 1998). Two sources of error must be addressed in this approach. The first, the standard error of a radiocarbon measurement and the calibration from the radiocarbon to the calendar time scale, is internal to the method and can be readily quantified using established techniques (Aitken 1990; Stuiver and Reimer 1993). The second, the age of the measured sample relative to the time-since-fire, is less well understood and more difficult to quantify. This uncertainty occurs because a radiocarbon age represents the time since carbon was removed from the atmosphere and incorporated into the sample, but, in many situations, the wood was already decades to centuries old at the time of the fire. The resulting 'inbuilt age' or 'presample age' error is defined as the difference between the time since wood formation and the age of the event of interest (e.g., fire) (McFadgen 1982). Inbuilt age always biases radiocarbon ages to be older than the event (Waterbolk 1983). Because it is possible for wood to remain intact for centuries before burning, it is possible that the inbuilt age may be large enough that the 2σ confidence interval of a calibrated radiocarbon age does not encompass the time of the fire.

McFadgen (1982), in a review of the potential effect of inbuilt age for the interpretation of radiocarbon ages from archeological sites, described inbuilt age as the sum of two components. The first occurs because charcoal may have resulted from a fire that

happened at some time following the death of the plant. This component is affected by the residence time of dead wood on the ground or as dead branches in trees (i.e., time-since-death). The second occurs because the charcoal may represent wood layers located at some depth within a branch or log, rather than on the most recent growth increments. This component is affected by the number of years of wood growth that occurred subsequent to the formation of the wood that is dated. Thus the inbuilt age can be reduced by choosing species with short life spans and/or sample residence times, such as wood from short-lived species or small twigs (McFadgen 1982; Waterbolk 1983; Lowe et al. 1998). In some cases, however, the material available for radiocarbon dating does not meet these criteria. In these cases, there is an uncertain inbuilt age, and radiocarbon ages should be considered a maximum age of the fire.

As with archeological samples, soil charcoal used to determine the dates of past fires requires the consideration of inbuilt age. Though most fire history studies using soil charcoal acknowledge the effect of inbuilt age (e.g., Molloy et al. 1963), it is often assumed to be less than the confidence interval of the radiocarbon measurement (Turner 1984; Carcaillet 1998). This assumption has never been tested. If inbuilt age is significant, the violation of this assumption will result in underestimation of time-since-fire and will limit the ability to estimate fire intervals from multiple radiocarbon ages from the same location.

The goal of this study is to estimate the magnitude of inbuilt age in radiocarbon ages of soil charcoal used to reconstruct the fire history of a watershed in western Vancouver Island, British Columbia (Canada). Two approaches were used to estimate inbuilt ages. First, inbuilt age was empirically documented using AMS (accelerator mass spectrometry) radiocarbon ages of soil charcoal and tree-ring ages of known fires. The

difference between the known age of a fire and the calibrated radiocarbon age is a direct measure of inbuilt age. Combining inbuilt ages from samples at several sites provides an estimate of the inbuilt ages representative of the study area. Second, inbuilt age was simulated for representative forest types using a model parameterized by a set of forest plot measurements and reasonable estimates of fuel age and consumption by fire. In addition to estimating the range of inbuilt ages that are possible, means of addressing the inbuilt-age error with sampling strategies or statistical methods are also discussed.

Rationale

A key concept for this analysis is the inbuilt-age distribution, defined here as the frequency distribution of charcoal pieces in different age classes (representing different times since wood formation) at the time of a fire. Inbuilt-age distributions indicate the magnitude of the lag between wood formation and the fire event (Figure 2.1). The amount of charcoal produced by the combustion of fuels with different times since formation (e.g., live branches versus dead wood) directly affects the inbuilt-age distribution. For example, a fire that burns mainly live branches will produce more charcoal with little inbuilt age than a fire that burns mainly old decaying logs. The inbuilt-age distribution can also be thought of as a probability distribution for the inbuilt age of a randomly selected piece of charcoal. For example, the probability that a piece of charcoal has an inbuilt age between 50 and 100 years is equivalent to the proportion of all charcoal pieces in that age class. If the general form of the inbuilt-age distribution can be approximated, then radiocarbon ages of soil charcoal can be interpreted with respect to the added error from inbuilt age.

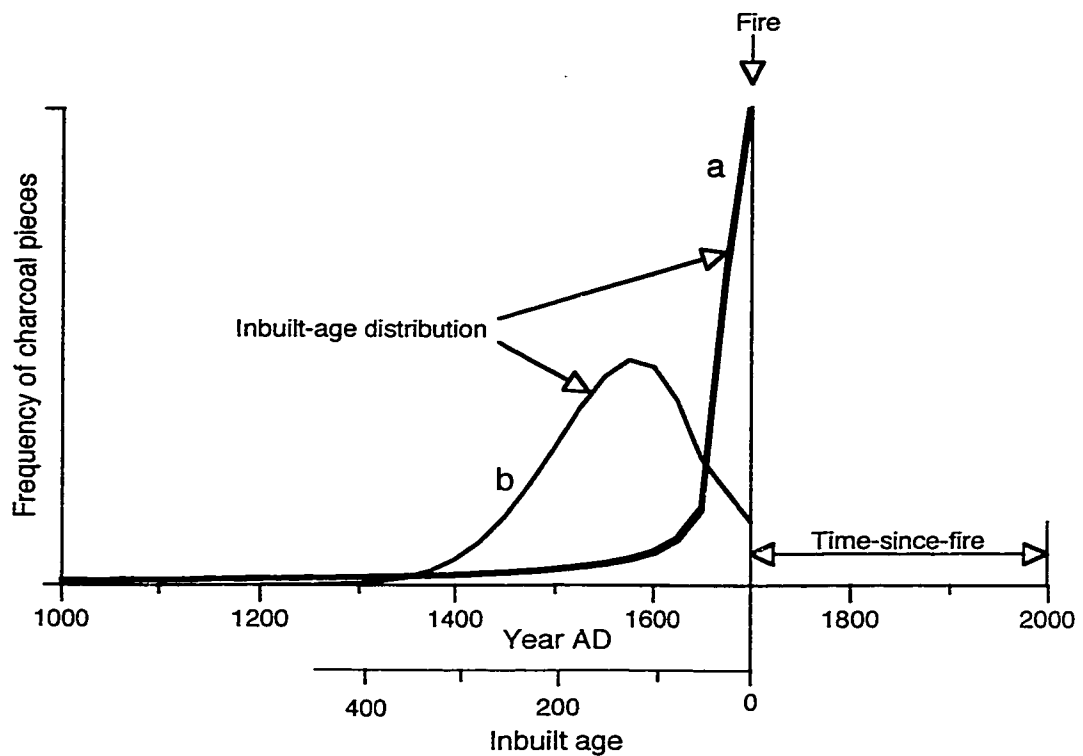


Figure 2.1 Schematic diagram showing terms associated with the inbuilt age of charcoal formed in a fire in AD 1700. The frequency of charcoal pieces across inbuilt-ages can form a variety of inbuilt-age distributions. The two hypothetical inbuilt-age distributions shown here have different consequences for interpreting radiocarbon ages, as described in the text. Distribution (a) indicates inbuilt ages more than 50 years are rare; distribution (b) indicates inbuilt ages are frequently greater than 50 years.

Study area

This study was conducted in the Clayoquot River Valley (49° 15'N, 125° 35'W) located on the west coast of Vancouver Island, British Columbia, Canada (Figure 2.2), where annual precipitation is ca. 5000 mm. In the biogeoclimatic ecosystem classification system of British Columbia (Meidinger and Pojar 1991), the valley is in the very wet maritime variant of the Coastal Western Hemlock zone. The valley contains undisturbed forests dominated by western redcedar (*Thuja plicata* Donn) and western hemlock (*Tsuga heterophylla* (Raf.) Sarg.). Sitka spruce (*Picea sitchensis* (Bong.) Carr.) and red alder (*Alnus rubra* Bong.) occur mainly on floodplains. Forests on better drained terraces and alluvial fans are dominated by western hemlock and Pacific silver fir (*Abies amabilis* (Dougl.) Forbes). Douglas-fir (*Pseudotsuga menziesii* (Mirb.) Franco) has a very patchy distribution, and its presence usually indicates the occurrence of fire in the recent past (Schmidt 1970). In this forest type, western redcedar may exceed 1000 years (Daniels et al. 1995), but western hemlock and Pacific silver fir are usually less than 500 years.

Old-growth western hemlock forests are noted for high accumulation (> 200 Mg ha⁻¹) of down logs and standing dead trees or snags (coarse woody debris, CWD; Harmon et al. 1986; Spies et al. 1988). The biomass of CWD changes predictably following forest fires, with peak accumulations occurring within few to several decades following fire due to mortality from the previous stand, and again after several centuries due to mortality of canopy trees in the new forest (Agee and Huff 1987; Spies et al. 1988). Long-term studies on CWD suggest that decay rates are species-specific and size-dependent, but follow a simple negative exponential curve (Harmon et al. 1986; Stone et al. 1998). Plot remeasurements on Vancouver Island suggest decay constants of 0.067 and 0.012 year⁻¹

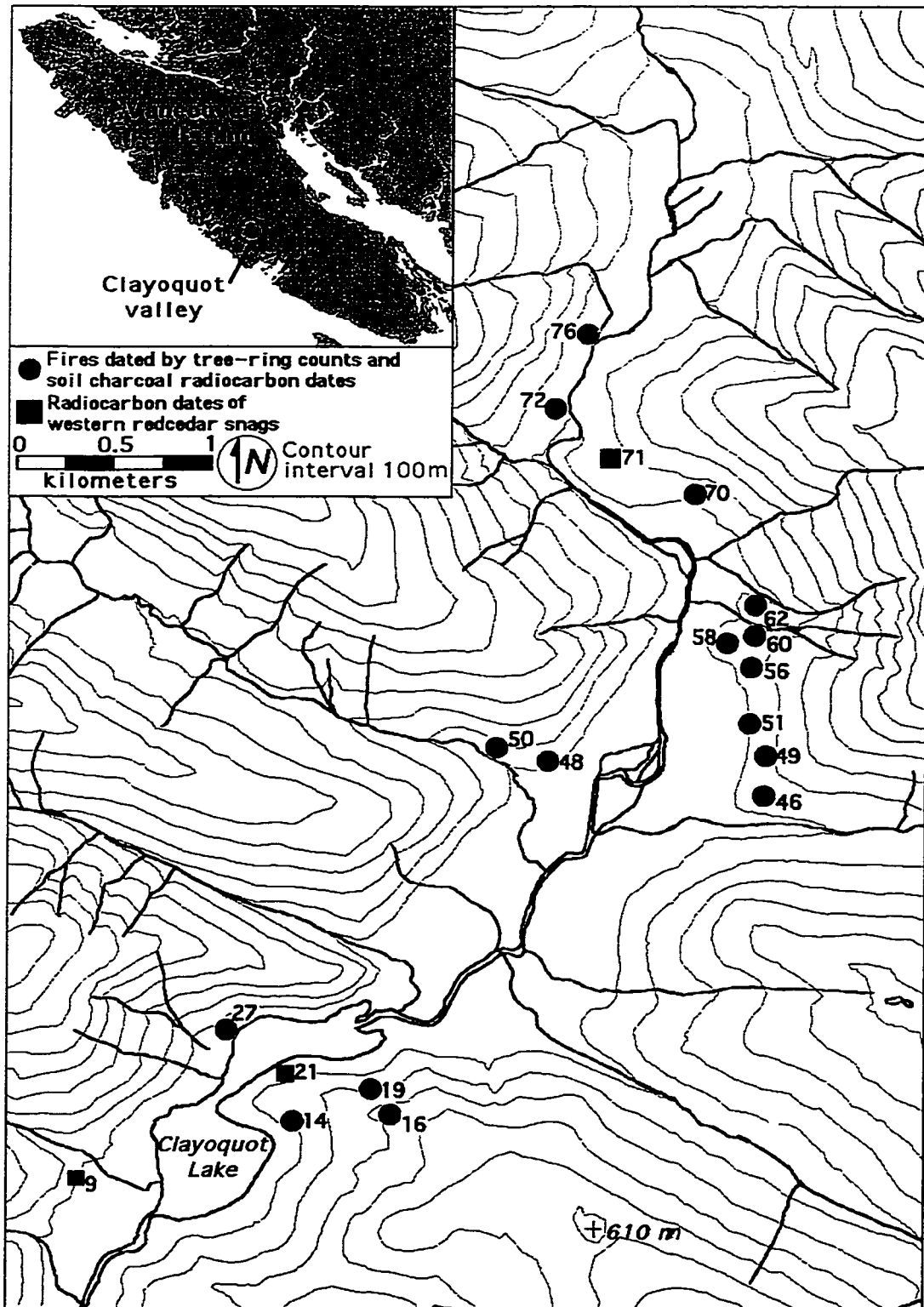


Figure 2.2 The location of sample sites in the Clayoquot River Valley, British Columbia, Canada.

for Douglas-fir logs < 20 and > 80 cm in diameter, respectively (Stone et al. 1998). In the absence of large stand-replacing disturbances, CWD biomass should reach an equilibrium level controlled by rates of tree mortality and decay, though an equilibrium might not be reached until 1000 years following disturbance (Agee and Huff 1987).

Few forest fires have occurred in historical times in the Coastal Western Hemlock zone (Veblen and Alaback 1996). These have been high intensity events consuming dead wood as well as foliage and branches of living trees (Agee 1993). However, fuel consumption is generally a small proportion of the total stand biomass, because high moisture in the inner bark and sapwood prevents the combustion of live fuel with a diameter > 1 cm (Chandler et al. 1983; J.K. Agee, *personal communication*). Large CWD is also not completely consumed (Chandler et al. 1983; Stocks and Kauffman 1997). As a result, fuels are derived predominantly from a portion of CWD, litter (fine woody debris; FWD), and small diameter branches (< 1 cm).

Methods

Inbuilt-age measurements

Rationale The inbuilt-age distribution for the study area was directly assessed by comparing the radiocarbon ages of soil charcoal pieces with the age of the most recent fire determined from tree-ring records. This analysis involved four steps: 1) Forest fires at 16 locations were aged using tree-ring records, 2) Surficial soil charcoal from these sites was aged (total of 26 radiocarbon ages), 3) Each radiocarbon age was calibrated to yield a probability distribution, and 4) The probability distribution of each calibrated age was expressed relative to the known age of the fire, and all probability distributions were

combined. This mean distribution was interpreted to represent the inbuilt-age distribution typical for these forests.

To estimate the inbuilt age of a charcoal sample collected at a given site, one would ideally need to know the probability distribution of inbuilt ages of all charcoal from a fire event at that site. Considering the difficulty of estimating inbuilt-age distributions (expense of dating large numbers of charcoal pieces) and the fact that these distributions are likely to vary across sites depending on fuel loads and fire behavior, it is impossible to construct such distributions for every site. The use of a composite probability distribution derived from data for several sites is a reasonable approach under these circumstances, as it should capture the potential range and central tendencies of inbuilt-age distributions that occur within a forest type.

Field methods I determined fire dates at 16 sites located > 200 m apart along an 8 km transect in low elevation forest (< 200 m above sea level; Figure 2.2). At nine sites, I determined the exact year of fire based on tree-ring counts of western hemlock or Douglas-fir that regenerated following the fire (10–16 trees cored/site), in conjunction with abrupt growth changes recorded in 3–7 large Douglas-fir trees that survived the fire. The first year of abrupt growth change was the same among trees within a site, and was considered the year following the fire. At seven sites, I estimated fire dates based on the ages of at least seven dominant Douglas-fir. I aged each tree by extrapolating the age of the inner-most ring in the core to the age of the pith (using concentric circles) and adding one year for every 15 cm of the core height above ground. The ages of Douglas-fir trees always clustered within 12–38 years at each site, suggesting that the fire date is close (ca. 10 years) to the age of the oldest individual. If the date of a fire estimated by a stand age was very close to the year of a fire dated exactly at a nearby site, I used the exact-year

date. For comparison with tree-ring dates of fires, I obtained 26 AMS radiocarbon ages on single pieces of charcoal collected from surficial soil at the 16 tree-ring sites (1–3 ages per site). I collected charcoal pieces as close to the soil surface as possible in an effort to age material originating from the most recent fire. At sites with > 1 charcoal age determination (7 sites), locations of charcoal samples were ca. 5 m apart.

Data analysis Radiocarbon ages were calibrated (Stuiver and Reimer 1993 [v4.1]) with the INTCAL98 calibration curve (Stuiver et al. 1998). A calibrated radiocarbon age yields an irregular probability distribution that typically spans 100 to 500 years, depending on the standard error of the radiocarbon age and the position in the calibration curve (Stuiver and Reimer 1993). The first step in creating the composite inbuilt-age distribution was to express the individual calibrated-age distributions as years-before-fire (rather than years BP) by subtracting the tree-ring age of the fire from each age represented in the probability distribution. Then, individual distributions were summed from different sites into a mean probability distribution (MPD), weighting each radiocarbon age equally. Because only the general form of the MPD is important, I removed the high frequency variation with a LOWESS filter, a smoothing method using locally weighted regression, with a 200-year window. This smoothed MPD is regarded as an estimate of the inbuilt-age distribution.

Inbuilt-age simulation model

Rationale Simulation of inbuilt age may show the level of inbuilt age that is to be expected based on our current understanding of fire behavior and fuel loads. The simulation approach may also show what processes contribute the most to observed inbuilt ages. If the simulation results match observed values of inbuilt age, the simulation

approach may be a reliable means of assessing inbuilt age that can be applied to other forest types. I simulated inbuilt-age distributions following fire events using measurements of fuel loads from plots in the study area (Pearson 2000), predictions of fuel consumption and charcoal production based on empirical studies (Sandberg and Ottmar 1983; Ottmar et al. 1993; Clark et al. 1998) and estimates of the time elapsed since the growth of woody fuels (Figure 2.3).

Modeling charcoal production and ages I calculated fuel loads from plots established in the Clayoquot Valley for a separate study of forest structure (data provided by A.F. Pearson; Pearson 2000). Plots were representative of three broad forest types: Sitka spruce forest (6 plots), cedar–hemlock forest (5 plots), and hemlock–fir forest (10 plots). Western hemlock usually codominated the plots with the other species. The cedar–hemlock plots most closely resembled the species combination at sites used for direct measures of inbuilt age. In each plot, I calculated CWD volume using equations for a cylinder for logs, or a cone with a taper value of 0.012 cm cm^{-1} for standing snags (Spies et al. 1988). I calculated CWD biomass using wood density estimates of species in different decay classes (Triska and Cromack 1979) (Table 2.1), which ranged from 0.43 g cm^{-3} for decay class I Sitka spruce to 0.13 g cm^{-3} for decay class V western hemlock (Graham and Cromack 1982; Sollins 1982; Spies et al. 1988). If a piece of CWD was not identifiable to species, I randomly assigned it to a species using the proportions of identified CWD in the plot. I assumed smaller diameter fuel loads (i.e., forest floor litter) to be 10 Mg ha^{-1} for all plots, a value from similar stands (Agee and Huff 1987). I estimated live branch biomass for all trees in each plot (Pearson 2000) using species-specific allometric equations in Gholz et al. (1979), of which 5% was considered available fuel < 1 cm diameter (approximate proportion from coastal old-growth Douglas-fir; Ishii et al. 2000).

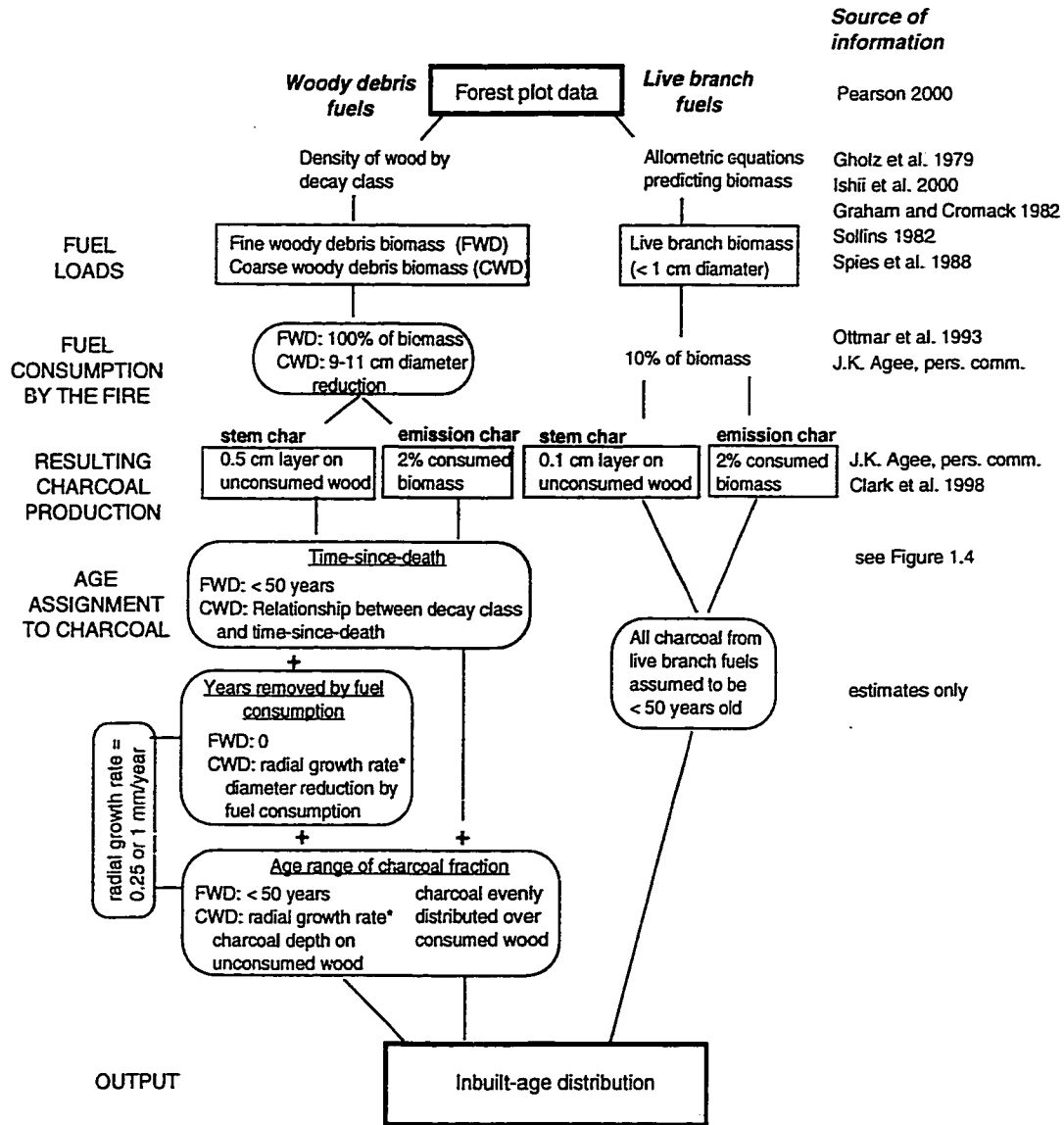


Figure 2.3 Outline of the steps used to simulate the inbuilt-age distribution of charcoal following forest fire in western Washington and British Columbia.

Table 2.1 Descriptions of decay classes for coarse woody debris and snags used in this study. From Triska and Cromack 1980.

Category	Decay class				
	I	II	III	IV	V
Bark	Intact	Bark more or less intact	Bark sloughing or absent	Detached or absent	Detached or absent
Structural integrity	Sound	Sound	Heartwood sound, supports own weight Snags broken	Heartwood rotten, does not support own weight	None Snags broken near base
Twigs < 3 cm	Present	Absent	Absent	Absent	Absent
Texture of rotten portions	Intact	Mostly intact; sapwood partially soft	Hard, large pieces	Soft, small blocky pieces	Soft, powdery when dry
Invading roots	Absent	Absent	Sapwood only	Throughout	Throughout
New vegetation	None	None	< 2 m height	< 15 cm DBH; moss	Up to 200 cm DBH.

I calculated CWD fuel consumption using an empirically derived relationship in which moisture of 1000-hour time-lag fuel (CWD 7.6–15.2 cm diameter) predicts diameter reduction (Sandberg and Ottmar 1983; Ottmar et al. 1993). This relationship, developed for summer-like (i.e., dry, late season) burning conditions, predicts diameter reduction in inches, C , as

$$C = -0.125 * (\% \text{ 1000-hour fuel moisture}) + 6.27 \quad (1)$$

Conditions necessary for wildfire in coastal forests of western British Columbia require moisture of the 1000-hour time-lag fuel class to drop below 20%, conditions usually met only after several weeks of no rain within summers of below-average rainfall (Huff and Agee 1980; Pickford et al. 1980). I used two fuel moisture levels, 15% and 21%, corresponding to 11 cm and 9 cm diameter reduction, respectively. I assumed decay class V CWD and FWD (< 2.5 cm diameter) were completely consumed (J.K. Agee *personal communication*). I also assumed fire intensity to be high, causing crown fires, consuming 10% of live branch biomass < 1 cm diameter, but no live fuels > 1 cm diameter (Fahnestock and Agee 1983).

I calculated charcoal production from CWD as a 0.5 cm layer on unconsumed wood, and from a portion (2% by mass) of all consumed fuels that was lifted off the fire by convection (J.K. Agee, *personal communication*; Clark et al. 1998). Crown fuels have a greater moisture content, do not burn as long as understory fuels, and therefore should produce a more shallow charcoal layer on branch wood. I calculated charcoal production from small diameter live branches as a 0.1 cm layer, assuming an average branch

diameter of 0.5 cm following fire (equivalent to charcoal comprising 36% by volume of unconsumed small-diameter branches).

The inbuilt-age of charcoal differs among fuel types. For CWD fuels, the inbuilt age of charcoal is affected by its residence time following death, depth of consumption of the outer wood, and the diameter growth rate of the outer consumed wood. I obtained species-specific residence time estimates from studies that measured the time-since-death of CWD in different stages of decay (Graham and Cromack 1982; Sollins et al. 1987; Hennon and Loopstra 1991; Daniels et al. 1997). These studies used tree-ring analysis and radiocarbon ages to measure the time-since-death of individual pieces of CWD. Because western redcedar CWD decays more slowly than other species (Daniels et al. 1997), the age of older western redcedar CWD has rarely been studied and western redcedar comprises a large proportion of the CWD in the study area, I obtained three radiocarbon ages from the last ten years of growth on decay class 4 and 5 western redcedar snags (Table 2.2). Together, these various studies indicate that both the average time-since-death and range of times-since-death of CWD increase exponentially with decay class (Figure 2.4; see also Harmon et al. 1986). Time-since-death estimates for Pacific silver fir were not available in the literature, and were assumed to be the same as for western hemlock, a species with similar wood properties (Hoadley 1990). I assumed live branch fuels and FWD to be less than 50 years old.

Radial growth rate (G) and diameter reduction from fuel consumption (C) determine the number of years of growth removed from the outer wood by fire. Therefore, these parameters control the effect of fuel consumption on inbuilt age. To simplify interpretation, I ran two scenarios in which G and C were assumed to be constant over the plot. The first scenario (fast-growth) assumes 45 years removed by consumption ($G = 1$

Table 2.2 Radiocarbon ages on western redcedar wood taken directly beneath the bark of standing snags.

Site code	Field code	Decay class	Lab code (CAMS #)	¹⁴ C Age (year BP)	Cal. date ^a (year AD)
9	LW01	IV	43866	270 ± 60	1650
71	RT01	IV	43871	490 ± 60	1430
21	UE02	V	43886	950 ± 50	1140

^a Median age intercept only, rounded to nearest decade (Stuiver and Reimer 1993; Stuiver et al. 1998).

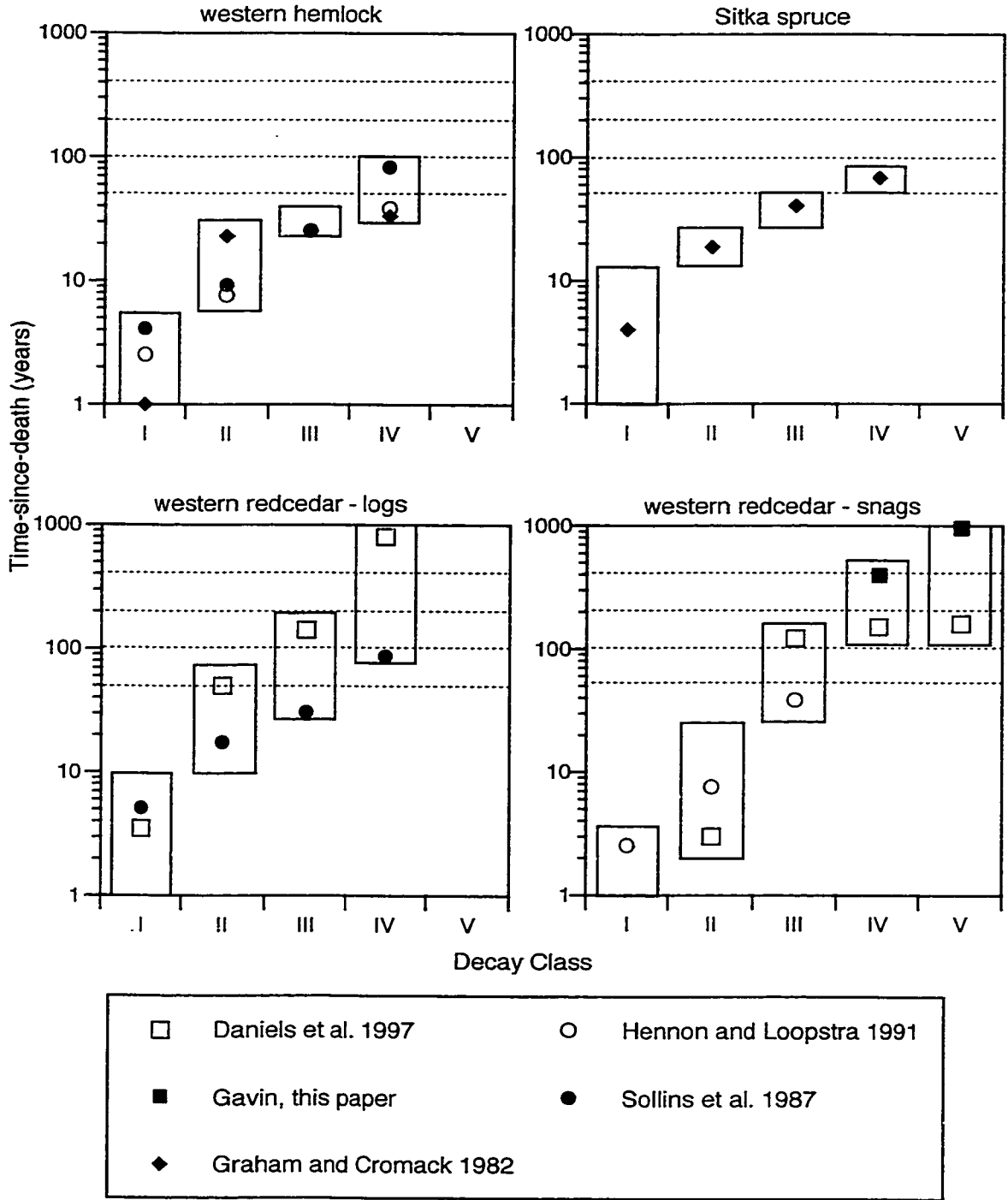


Figure 2.4 Time-since-death of coarse woody debris and snags of common tree species in western Washington, British Columbia, and southeast Alaska. Data were limited to studies that directly measured time-since-death using tree-ring analysis on the fallen tree or on neighboring trees affected by the death of the tree, by plot remeasurements, or by radiocarbon age determinations. Solid rectangles represent the time-since-death ranges of coarse woody debris and snags used in this study. Dashed lines indicate classes used to summarize the simulation results.

mm year⁻¹; C = 9 cm). The second scenario (slow-growth) assumes 220 years removed by consumption (G = 0.25 mm year⁻¹; C = 11 cm). For each piece of CWD, I calculated the amount of charcoal in each of five age classes (0–50, 50–100, 100–200, 200–400, 400–1000 years) based on the sum of the time-since-death (Figure 2.4), the number of years removed by fuel consumption, and the number of years comprising the 0.5 cm layer of charcoal on the unconsumed wood. Charcoal was also produced from 2% of the consumed biomass (Figure 2.3); this charcoal was assumed to be evenly distributed over the consumed wood. The time-since-death estimates may range several decades to centuries for individual pieces of CWD, causing the inbuilt ages to encompass more than one age class; in these cases charcoal was divided among age classes based on the proportion of the estimated age range in each age class.

In addition to the two main scenarios of the model described above, I ran additional scenarios to examine the sensitivity of the inbuilt-age distribution to several parameters. In these scenarios, I varied the radial growth rate (0.1–2 mm year⁻¹), diameter reduction by fuel consumption (5–15 cm), the depth of the charcoal layer on CWD (0.1–1 cm) or live branches (0.05–0.5 cm), and the percentage of consumed wood contributing to emission charcoal (0.5–10%). To examine the sensitivity of the model output on each variable, I kept all other variables constant using the values in the slow-growth scenario (above), and recorded the proportion of charcoal produced in ages classes > 200 years.

Results

Inbuilt-age measurements

The 26 calibrated radiocarbon ages of charcoal overestimated the age of the fire between 0 and 676 years (Table 2.3; Figure 2.5). The majority of the radiocarbon ages (21) had

inbuilt ages between 150 and 450 years; but two radiocarbon ages yielded inbuilt ages over 600 years. Inbuilt ages of charcoal from 19th century fires (average = 353 years) were generally greater than inbuilt ages of charcoal from earlier fires (average = 193 years) (Table 2.3). The MPD of the calibrated radiocarbon ages, expressed relative to the age of the fire, peaks at 200 years (median = 270 years; 25th-75th percentile = 180–380 years; 5th-95th percentile = 30–610 years) (Figure 2.6). Overall, the composite curve implies that 69% of the charcoal overestimates the time-since-fire by > 200 years, and 22% of the charcoal overestimates the time-since-fire by > 400 years.

Inbuilt-age simulation model

Measured CWD and estimated small branch fuel loads varied widely among plots (77–1060 and 1.5–16.3 Mg ha⁻¹, respectively), but the average fuel loads were similar among forest types (169–180 and 6.1–7.0 Mg ha⁻¹, respectively) (Figure 2.7). Likewise, simulated CWD fuel consumption varied considerably among plots (12–47%), but the average was similar among forest types (25–31%). An average of 6.2 Mg ha⁻¹ of wood biomass was converted to charcoal in each plot (3.8–12.9 Mg ha⁻¹), with charcoal from CWD the major source of charcoal in each plot (average 90%; 67–98%). Increasing the CWD diameter reduction from 9 to 11 cm caused fuel consumption to increase by 4% and charcoal mass to decrease by 3%.

The simulated inbuilt-age distributions varied greatly between the two model scenarios (Figure 2.8). The fast growth scenario produced almost no charcoal in the > 100 year age classes, but the slow growth scenario produced 85% and 25% of the charcoal in the > 200 and > 400 year age classes, respectively. In contrast to the large differences between model scenarios, inbuilt-age distributions were similar within and among forest types,

Table 2.3 Radiocarbon ages of soil charcoal in the Clayoquot Valley. Lines separate sites with different fire dates.

Site code	Field code	Tree-ring method	Year of fire	Lab code (CAMS #)	¹⁴ C Age (year BP)	Cal. date ^a (year AD)	Inbuilt-age (years)
48	URW04	Stand age	1550	32248	320 ± 60	1557	0
50	URW83	Stand age	1550	53499	610 ± 50	1350	200
72	RT04	Stand age	1620	53473	420 ± 50	1450	170
	RT04		1620	53474	450 ± 50	1440	180
	RT04		1620	32339	520 ± 60	1420	200
46	URE13	Stand age	1655	32239	350 ± 60	1600	55
	URE13		1655	53482	440 ± 60	1440	215
	URE13		1655	53483	970 ± 50	1030	625
56	URE63	Growth response	1683	43899	370 ± 60	1490	193
60	URE64	Stand age	1683	43914	340 ± 50	1590	93
14	PR03	Growth response	1805	32342	530 ± 60	1410	395
16	PR06	Stand age	1805	39387	410 ± 40	1450	355
	PR06		1805	32343	430 ± 60	1445	360
19	UE80	Stand age	1805	53481	310 ± 60	1545	260
76	RT51	Growth response	1805	43873	350 ± 40	1600	205
	RT51		1805	43875	350 ± 40	1600	205
	RT51		1805	43876	420 ± 50	1450	355
70	SBC	Growth response	1830	32233	420 ± 60	1450	380
	SBC		1830	32234	510 ± 90	1420	410
51	SBA	Growth response	1872	32348	320 ± 60	1560	312
58	SBB	Growth response	1872	32231	390 ± 50	1480	392
	SBB		1872	32232	490 ± 60	1430	442
62	URE69	Growth response	1872	43921	500 ± 50	1430	442
49	URE70	Growth response	1872	43922	230 ± 50	1660	212
27	RSA	Growth response	1886	43870	850 ± 50	1210	676
	RSA		1886	53472	300 ± 50	1640	246

^a Median age intercept only, rounded to nearest decade (Stuiver and Reimer 1993; Stuiver et al. 1998).

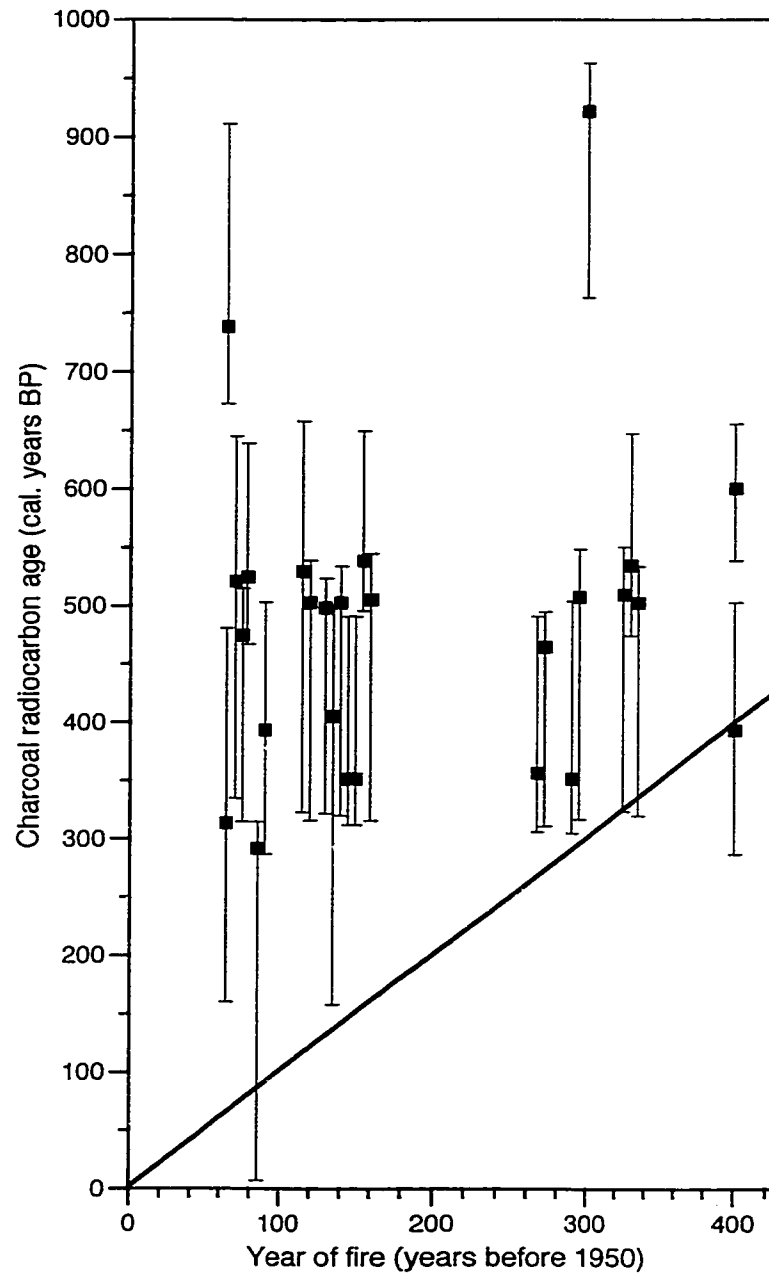


Figure 2.5

Calibrated radiocarbon ages (± 2 SD) on single fragments of charcoal from the soil surface from the Clayoquot Valley study area. The known year of fire was determined using tree-ring records. The diagonal line shows the expected calibrated radiocarbon age with no inbuilt-age. Multiple ages from the same fire year are offset for clarity. In cases of multiple calibrated age intercepts or multiple calibrated age ranges, only the median intercept and maximum and minimum of the age ranges are shown.

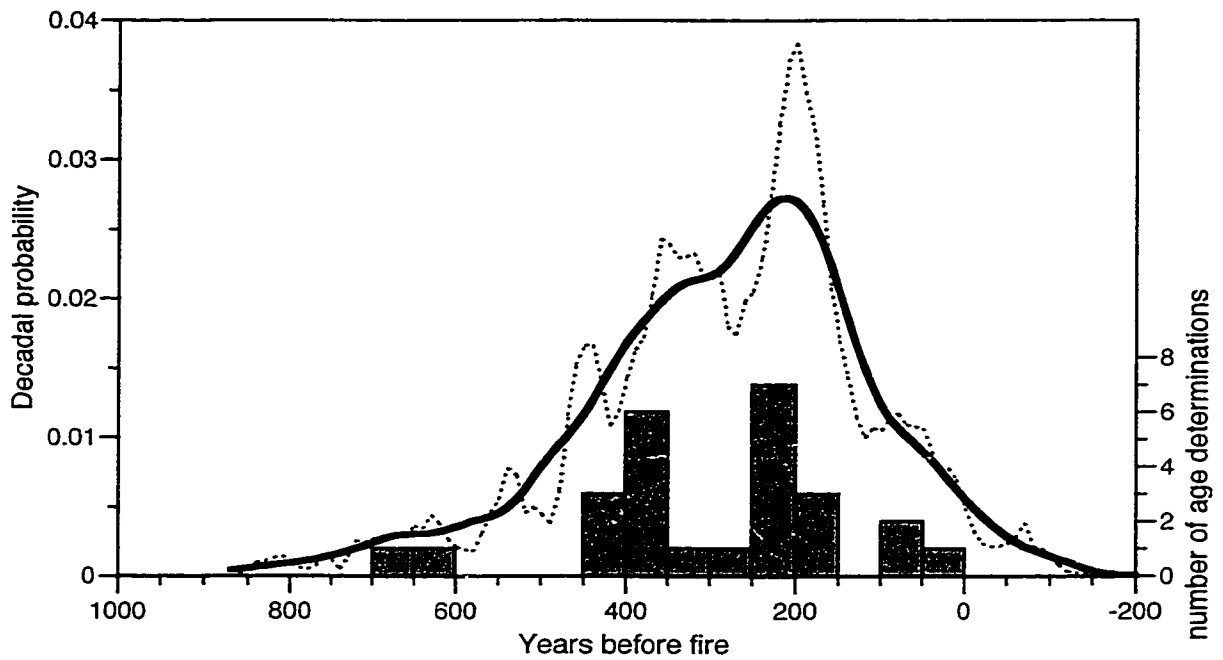


Figure 2.6 Mean probability distribution (MPD) of 26 calibrated radiocarbon ages of soil charcoal. The known ages of fire were subtracted from each age in the calibrated age probability distributions before combining into the MPD. The MPD (dashed line) was smoothed using a LOWESS filter with a 200 year window (solid line). The distribution of the calibrated age intercepts is shown with gray bars.

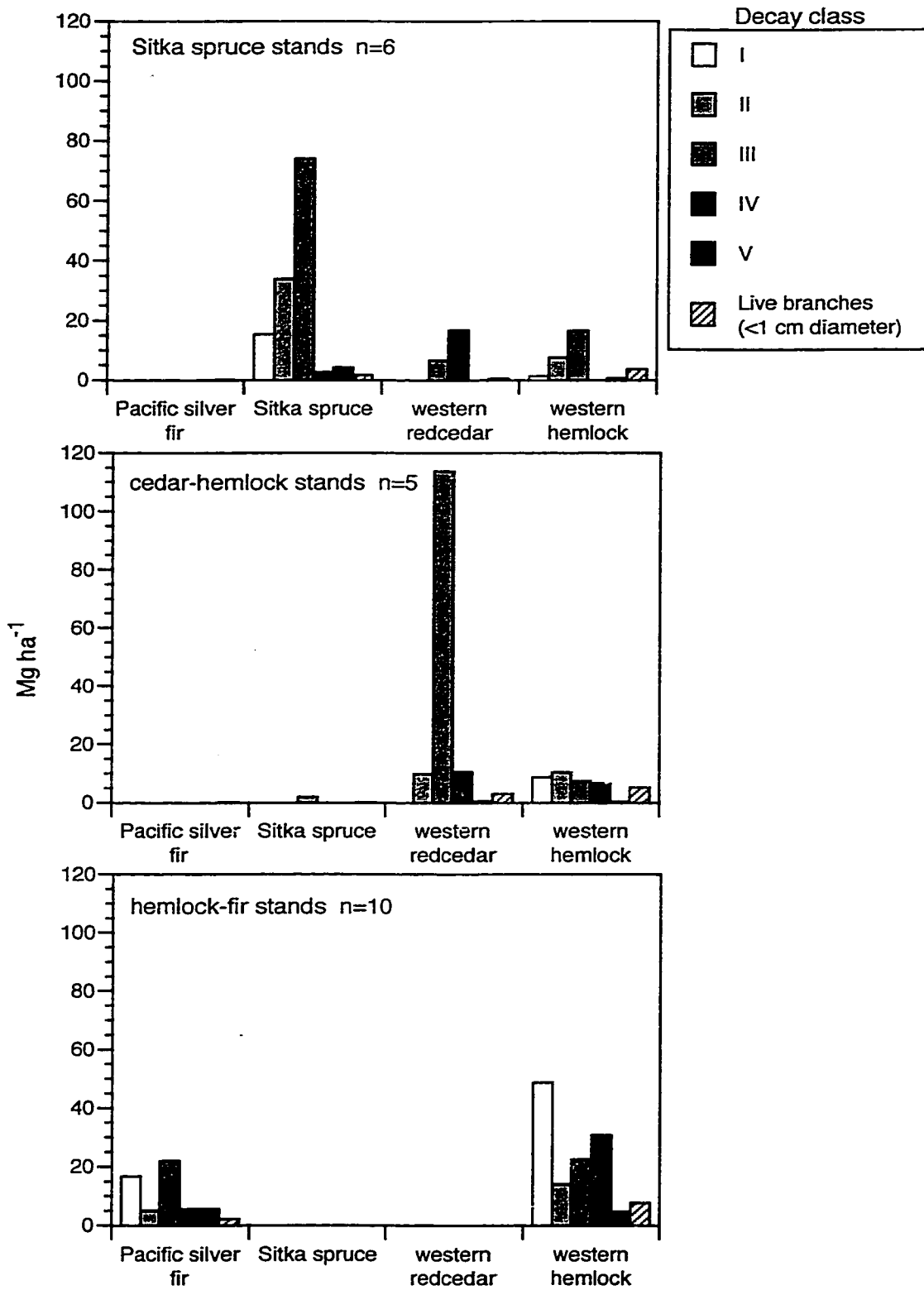


Figure 2.7 Mean coarse woody debris and fine branch biomass of plots in three forest types in the Clayoquot Valley (Plot measurements from Pearson 2000).

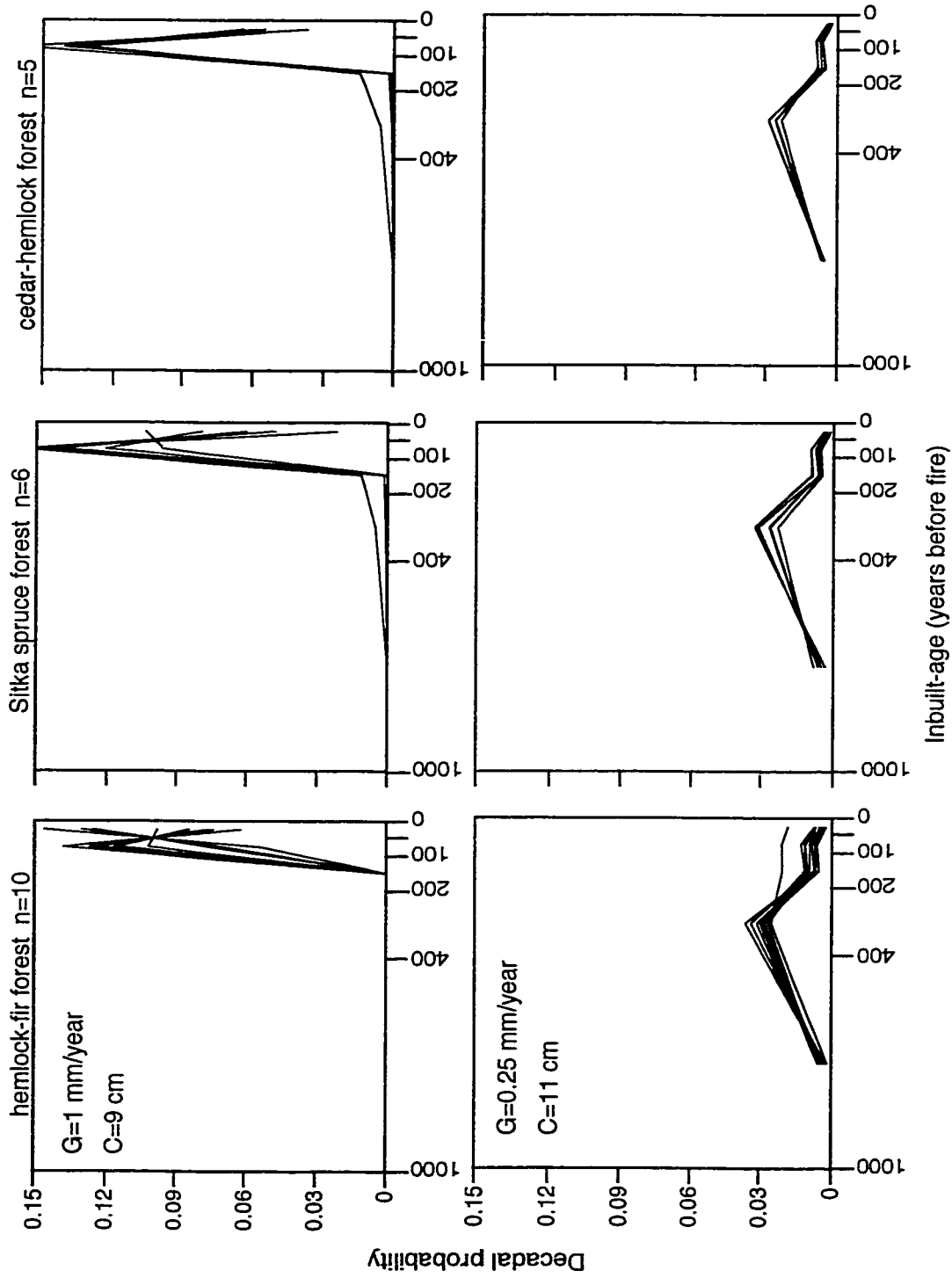


Figure 2.8 Simulated inbuilt-age distributions of charcoal biomass produced following forest fire in the Clayoquot Valley. Each line represents the charcoal age distribution for a forest plot. Two scenarios are shown for different diameter growth rates (G) and diameter reduction by fuel consumption (C).

nearly always peaking in the same age class. Most variability within forest types was in the < 50 year age classes.

Sensitivity analysis of the model output indicated that the magnitude of inbuilt-age was mainly affected by the combined effect of radial growth rate and depth of consumption of outer wood. The proportion of charcoal in age classes > 200 years increased from very low (ca. 5%) to high (ca. 90%) levels when parameters for growth rates and/or fuel consumption were increased to result in ca. 200 years of outer wood removed by fuel consumption. In contrast, the proportion of charcoal in age classes > 200 years changed by < 10% when varying the parameters for the depth of charcoal on unconsumed wood or the parameter for the proportion of consumed wood contributing to emission charcoal.

Discussion

Implications of the inbuilt-age error

The error introduced by inbuilt age potentially affects the interpretation of fire dates in the study area because the magnitude of these errors typically exceeds the 2σ confidence interval of a calibrated age distribution. In all but one case, the radiocarbon ages of soil charcoal are significantly greater than the actual age of the fire, suggesting that inbuilt ages of charcoal in the watershed are often > 180 years (25th percentile), most are < 610 years (95th percentile), though some may be as large as 670 years (greatest observed value) (Figure 2.6). Such potentially large errors in estimating a fire date can prevent the correlation of a fire date with other short-lived events. For example, a large inbuilt age limits the ability to correlate fire dates with known climatic periods (e.g., periods < 300 years). On the other hand, a certain amount of inbuilt age may be acceptable in some studies. For example, to claim that a piece of charcoal represents a fire that burned at

least 1000 years ago, the age of charcoal should exceed 1000 years by the maximum inbuilt age that is likely to be encountered. The present study suggests that radiocarbon ages would have to be > 1610 cal. BP to claim that fires have not burned in the last 1000 years.

The inbuilt-age error also affects the minimum interval between fires that can be detected with radiocarbon ages of charcoal. For example, two fires that occur 300 years apart may produce charcoal with the same radiocarbon age. In contrast, two calibrated radiocarbon ages from charcoal pieces at a given location can differ by 300 years (suggesting a fire interval of ca. 300 years), though both pieces of charcoal actually originated from the same fire event. Thus, it is impossible to determine whether two radiocarbon ages originated from the same fire or from different fires if the dates differ by less than the maximum inbuilt age. However, in cases where there is stratigraphic evidence suggesting different fires (e.g., two charcoal lenses in an organic soil), the effect of inbuilt age is to increase the error of the fire interval estimate.

Simulation of inbuilt age

The simulations used many parameters to capture the key processes affecting the inbuilt-age distribution (Figure 2.3). The estimates of fuel loads and fuel consumption used in the simulations are similar to loads estimated in other studies from the Pacific Northwest (Fahnestock and Agee 1983; Agee and Huff 1987; Spies et al. 1988; Stocks and Kauffman 1997). However, the parameters used for charcoal production and the assignment of inbuilt age to charcoal are only estimates because few studies are available against which to calibrate these values. For example, no studies have estimated the total quantity of charcoal produced in a fire, or the amount of charcoal from different types of

fuel. Furthermore, the radial growth rates of the wood consumed by fire, which have a large effect on inbuilt age, are variable within and among trees and therefore were difficult to incorporate into the simulation model.

Despite these uncertainties, parameter estimations of several simulated inbuilt-age distributions resembled the measured inbuilt ages (i.e., similar proportions of charcoal were > 200 and > 400 years old; Figures 2.6 and 2.8). These scenarios assumed that the majority of charcoal originates from CWD, the growth rate of the outer consumed portions of fuels is slow ($0.25 \text{ mm year}^{-1}$), and there is a large diameter reduction due to fuel consumption (11 cm). This set of conditions is reasonable, given the forest structure and expected fire behavior in the Clayoquot Valley. Although fires in this region typically kill most trees, crown fires are very patchy (Agee 1993). At some sites, high moisture in crown foliage may result in very little combustion of crown fuel, resulting in even less charcoal in the younger age classes than used in this simulation. In contrast, fire duration and intensity in the understory may be sufficient to completely consume FWD and the outer wood of CWD. Slow, smoldering fires in dead wood and forest floor material can continue for days to weeks after the passing of the fire line, and thus produce a large quantity of charcoal from CWD (Chandler et al. 1983).

In coastal temperate rain forests such as the Clayoquot Valley, the charcoal produced from CWD may be centuries old. Western redcedar, one of the most common species in the study area, is more resistant to decay than other species (Figure 2.4; Daniels et al. 1997). The slow decay of this species may explain the two radiocarbon ages that suggest inbuilt ages of ca. 600–700 years (Figure 2.6). In addition, most charcoal probably originates from inner (older) layers of CWD because the outer sapwood decays more rapidly than the inner heartwood and can slough off within a few decades of tree death

(Table 2.1). Thus processes of decay, fragmentation, and consumption by fire cause little of the outer wood to turn into charcoal. Contributing further to a large inbuilt age, this outer wood can represent more than a century of tree-ring growth because large CWD is derived from canopy-dominant trees that often persist for centuries with slow radial growth (e.g., DeBell and Franklin 1987). For example, the outer 5 cm of wood of 130 large Douglas-fir and western hemlock trees cored in the Clayoquot Valley contained an average of 125 years (0.4 mm year^{-1} ; D. Gavin, unpublished data).

Sampling strategies and quantitative treatment of the inbuilt-age error

Given that inbuilt ages might have large effects on determining ages of fires, what methods can aid the interpretation of such charcoal radiocarbon ages? Two different strategies discussed below may be used to help reduce inbuilt age, or to statistically treat radiocarbon ages to better reflect inbuilt age. First, inbuilt age may be reduced by determining the radiocarbon ages of several charcoal pieces and using the minimum age as the best estimate of the fire event. Second, an estimate of the inbuilt-age distribution may be incorporated into the error of a calibrated radiocarbon age such that the new, adjusted error encompasses the age of the fire.

Using several radiocarbon ages to minimize inbuilt age If the minimum of several charcoal radiocarbon ages at a site is selected as the best estimate of the age of a fire, then the minimum radiocarbon age would have, on average, a lower inbuilt age than that of a single radiocarbon age. However, if charcoal with little inbuilt age is rare, obtaining several radiocarbon ages would have limited potential for reducing the inbuilt age. For example, of the 26 radiocarbon ages of charcoal used in the present study, only three (11%) had inbuilt ages < 100 years (Figure 2.6). With this proportion of charcoal pieces

with small inbuilt ages, the ages of six pieces of charcoal must be determined to ensure a 50% probability of obtaining one radiocarbon age with < 100 year inbuilt age (i.e., $1 - \text{the probability that six randomly chosen charcoal pieces have inbuilt ages} > 100 \text{ years} = 1 - (23/26)^6 = 0.52$). Given the expense of AMS dates, most researchers could not afford six radiocarbon ages for each fire event. The alternative of using fewer radiocarbon ages does not significantly reduce this error. Researchers must therefore weigh the importance of reducing the inbuilt-age error against the number of fire events that need to be dated.

Adjusting calibrated radiocarbon ages to reflect the uncertainty due to inbuilt age The inbuilt-age distribution obtained in this study is used to describe the range and relative abundance of inbuilt ages expected for charcoal produced by fires in the forests of the study area. Thus it also represents the probability distribution of inbuilt age associated with a randomly chosen piece of charcoal. This distribution can, therefore, be added to the error of a calibrated radiocarbon age, resulting in a wider distribution that more accurately shows the error of the radiocarbon-derived estimate of the fire date. This adjustment is calculated as a weighted moving average of the probability distribution of a calibrated radiocarbon age using the inbuilt-age distribution as the set of weights. The probability distribution of a calibrated radiocarbon age, $P(T)$ (in years AD/BC), adjusted for inbuilt age is calculated as

$$P_{adj}(T) = \sum_{i=m}^n W(i) \cdot P(T - i) \quad (2)$$

where $P_{adj}(T)$ is the probability distribution of the adjusted age, $W(i)$ is the inbuilt-age distribution ranging from m to n years before fire, and $\sum W(i) = 1$. Calibrated radiocarbon

ages adjusted for inbuilt age will have a lower median age and a larger error than unadjusted calibrated dates (Figure 2.9).

Adjusting radiocarbon ages is an explicit means of uniformly applying error from inbuilt age to all radiocarbon ages in a study. Using the $P_{adj}(T)$ distribution incorporates the range of expected inbuilt ages into the final estimate of the fire date, and, therefore, graphically shows the uncertainty of the estimate of the fire date (Figure 2.9). The adjusted probability distribution can be used in statistical tests that compare fire dates. For example, it provides a means of determining whether the effect of inbuilt age causes two estimates of fire dates to overlap, and thus whether the two charcoal pieces originated from the same fire. One caveat with this method occurs, however, because the adjusted probability distribution is only as reliable as the inbuilt-age distribution on which it is based. As a result of the uncertainty in defining inbuilt-age distributions, a marginally significant difference between two adjusted probability distributions should be interpreted with caution.

Inbuilt age in other forest types

Coastal western hemlock forests contain some of the largest accumulations and oldest mean age of CWD of forests worldwide (Harmon et al. 1986). Due to the dominance of shorter-lived species, faster decay rates, and/or a greater contribution of live fuels, most other forest types may have younger fuels. For example, most species in deciduous hardwood forests of the eastern United States seldom reach 300 years (Burns and Honkala 1990). CWD decays at a significantly faster rate in areas with warm and moist conditions for at least part of the year (e.g., tropical forests and temperate deciduous forests) than in the cool maritime forests of Vancouver Island (Harmon et al. 1986).

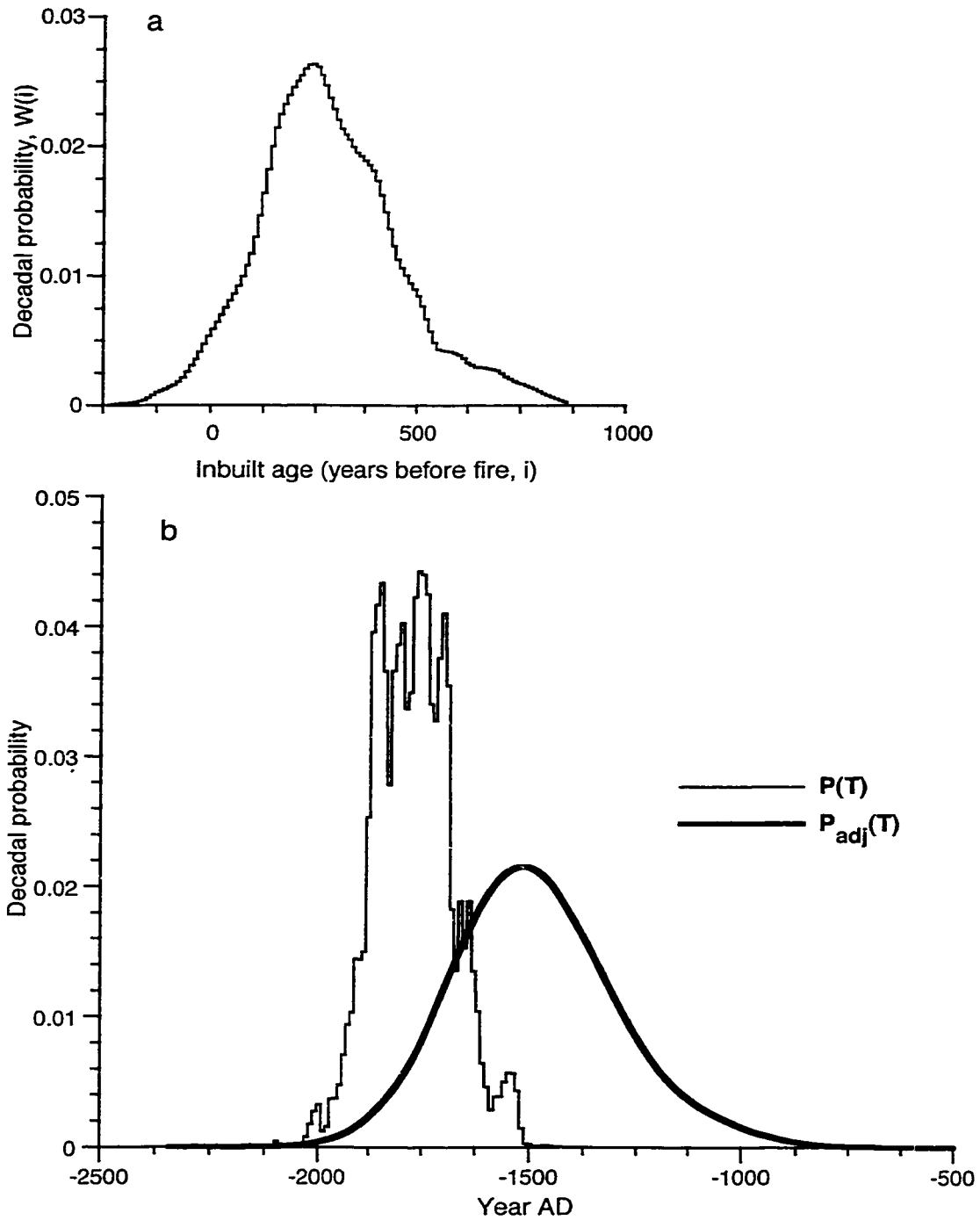


Figure 2.9 Example of a radiocarbon age determination adjusted to account for error introduced by inbuilt age. a. A smoothed inbuilt-age distribution determined from 26 radiocarbon dates (see Figure 2.6). b. Probability distribution of a calibrated radiocarbon date (3460 ± 70 radiocarbon years BP) before ($P(T)$) and after ($P_{adj}(T)$) adjustment for inbuilt age using the values in (a) as weights in a weighted moving average filter.

Similarly, CWD is not persistent and young FWD comprises the majority of fuels in pine forests that experience frequent low-intensity fires (e.g., ponderosa pine of interior Pacific Northwest or slash pine of the southeastern United States) (Chandler et al. 1983). Live material comprises a large component of fuels in other vegetation types, such as resinous vegetation in Californian chaparral or Australian dry sclerophyll *Eucalyptus* forest. Despite these observations, investigations such as this one need to confirm a lower inbuilt age of charcoal dates in other vegetation types. This is necessary to assess the resolution of fire history studies in any given forest type.

Conclusions

Direct measurements of inbuilt age in coastal western hemlock forests of British Columbia suggest that the period elapsed between wood formation and combustion to charcoal may increase the radiocarbon age of charcoal beyond the age of the fire by several centuries. The inbuilt age measured in this study was mainly between 30 and 610 years (95% confidence interval), though an upper extreme of 670 years was detected. These large inbuilt ages result from the long residence times of coarse woody debris, the consumption of the outer wood during fire, and the slow growth rates in the old trees typical of this area. Inbuilt ages typically place the actual date of a fire outside of the 2 σ confidence interval of a calibrated date, therefore significantly affecting the precision of radiocarbon estimates of the dates of past fires.

The magnitude of the inbuilt age detected in this study has three main implications for using soil charcoal to reconstruct fire history. First, inbuilt age can increase the uncertainty of a date by as much as 670 years, and thus greatly limits the ability to correlate fire events among sites. Second, to detect different fires calibrated radiocarbon

ages must be at least 610 years apart (high level of certainty; 95th percentile), or 380 years apart (lower level of certainty; 75th percentile). Therefore, radiocarbon methods do not reliably measure fire intervals within these ranges. Lastly, though soil charcoal radiocarbon ages can be useful for determining the time-since-fire, the temporal precision is coarse.

CHAPTER 3: HOLOCENE FIRE HISTORY OF A COASTAL TEMPERATE RAIN FOREST BASED ON SOIL CHARCOAL RADIOCARBON DATES

Introduction

The coastal temperate rain forest of the Pacific Northwest of North America is noted for the near absence of fire and the dominance of late-successional forest communities that experience a disturbance regime of small-scale tree-fall gaps (Veblen and Alaback 1996; Lertzman et al. 1996; Wells et al. 1998). These forests are also noted for the rarity of Douglas-fir (*Pseudotsuga menziesii*), a long-lived seral species that, in the maritime Pacific Northwest, establishes almost exclusively following fire (Munger 1940; Franklin and Dyrness 1988; Agee 1993; Wells et al. 1998). In the windward portions of coastal mountain ranges in British Columbia, evidence of fire is limited to the scattered occurrence of Douglas-fir on specific topographic features, e.g., south-facing hillslopes (Schmidt 1960; 1970; Veblen and Alaback 1996). This pattern contrasts with most maritime areas of the Pacific Northwest, where a large proportion of the presettlement landscape was dominated by forests that almost invariably contained evidence of large fires in the form of even-aged stands of Douglas-fir. Thus, the rarity of Douglas-fir and stand-structural evidence of fire distinguishes coastal temperate rain forest in the regional context of Pacific Northwest forests. However, it is not known whether the modern fire regime is a long-term feature of the coastal temperate rain forest landscape that has existed over several generation of trees (e.g., > 1000 years).

Factors affecting the fire regime of the coastal rain forest operate at different temporal and spatial scales. At large spatial scales, fire regimes are influenced by long- and short-term climatic changes and at more local scales by topographic features and vegetation

types (e.g., Romme and Knight 1981; Lertzman and Fall 1998; Heyerdahl et al. *in press*). The interaction of these factors causes the location and size of areas susceptible to fire to vary over time (Turner and Romme 1994). For example, during climatic periods marked by generally cool and moist conditions, fires may be restricted to a small portion of the landscape (e.g., south-facing hillslopes), but during climatic periods with generally warm and dry conditions, fires may burn a large portion of the landscape. In addition, characteristics of forest vegetation (e.g., crown closure and fuel dynamics) may change with the climate and fire regime, further affecting susceptibility to fire (Cwynar 1987; Clark et al. 1996). If climate undergoes major fluctuations, large areas of the coastal temperate rain forest that currently appear at very low risk of burning may become more susceptible to fire. This has been shown in drier regions of the maritime Pacific Northwest where several studies have found that millennial-scale climatic change has greatly altered the fire regime (Sugita and Tsukada 1982; Cwynar 1987; Wainman and Mathewes 1987; Long et al. 1998). The goal of this study is to examine the long-term roles of climate, topography, and vegetation in the fire regime of a coastal temperate rain forest that receives some of the highest annual precipitation in North America.

Fire history studies in areas with very long fire intervals must overcome significant challenges. Traditional fire history methods focus on particular spatial and temporal scales that might not be relevant to studying the landscape pattern of past fires in coastal temperate rain forest (Lertzman and Fall 1998). The use of tree-ring analysis and observations of modern fire to understand the pattern of fire at small temporal and spatial scales has limited application in coastal regions, where the time since the last fire may exceed the ages of trees. Over longer time scales, fire occurrence may be addressed with charcoal records in lake sediments. However, this method is not spatially explicit, because lake-sediment records integrate fires within large source areas (Clark 1988a).

Neither of these methods can provide the spatial information needed to describe the landscape-wide controls of a fire regime over long time periods.

The present study overcomes the spatial and temporal constraints of traditional fire history studies by using radiocarbon dates of soil charcoal to describe the spatial pattern of fire over long time scales in low-elevation area on western Vancouver Island (British Columbia, Canada). Although charcoal is inert and should be preserved in stable soils, this method has rarely been used and questions remain regarding sampling issues and the temporal resolution available from soil charcoal records. In addition to examining the utility of radiocarbon dated soil charcoal records for fire history, I examined (1) the length of time since the last fire in relation to topographic features and forest types, and (2) the temporal pattern of fire over the last ca. 10,000 years.

Study area

The research was conducted in the Clayoquot River watershed, on the western edge of the Vancouver Island Range and 20 km from the west coast of Vancouver Island, British Columbia (49°15' N; 125°30' W; Figure 3.1). The 7700 ha, 12 km-long watershed ranges in elevation from 15 to ca. 1200 m. Unforested high-elevation tundra and rock covers 16% of the watershed. Bedrock is of volcanic and igneous origin (Muller 1968). The watershed contains many glacial features, including multiple terraces 5–40 m above the river and steep valley walls with slopes of 40% → 60%, containing many small cliffs. An active floodplain is limited to the lower 4 km of river, and is constricted at several locations by alluvial fans from tributary valleys. Colluvial material is shallow (< 1 m) or absent on slopes above alluvial fans and terraces. Soils are mainly Ferro Humic Podzols (spodosols), classified in the Sugsaw, Reeses, and Hooper soil

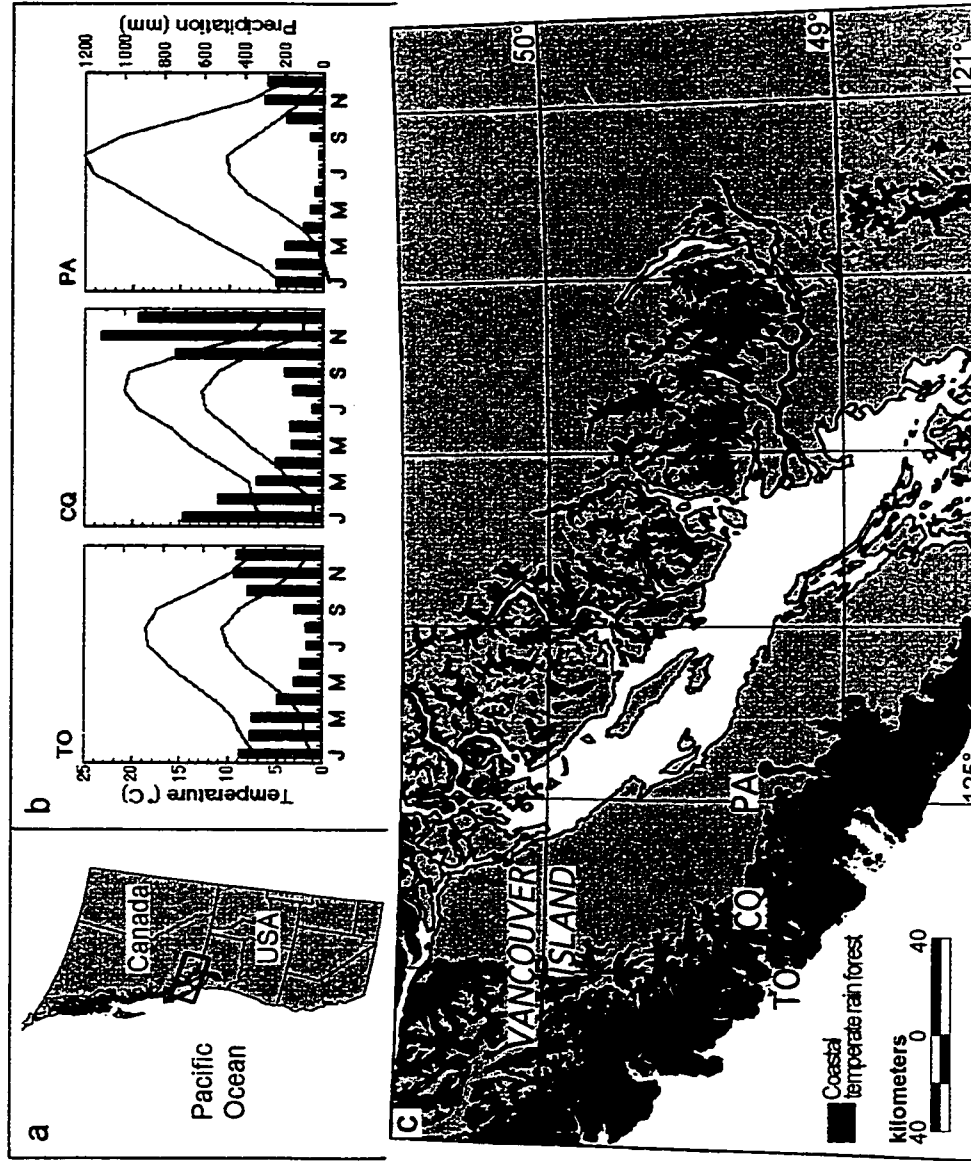


Figure 3.1 Location and climate of the study watershed. (a) Location of Vancouver Island in North America. (b) Köppen climate diagrams for Tofino (TO), Clayoquot Lake (CQ), and Port Alberni (PA). (c) Location of the Clayoquot Valley on Vancouver Island, showing the wettest subzones of the coastal western hemlock zone, sometimes referred to as the coastal temperate rain forest. *Sources:* Clayoquot Lake climate station, 1993-1996 (Clayoquot Biosphere Project, unpublished data); Environment Canada Climate Normals 1961-1990; British Columbia biogeoclimatic zones (British Columbia Ministry of Forests, Research Branch).

associations (Jungen 1985; Canadian System of Soil Classification, Soil Classification Working Group 1998).

The study area was restricted to accessible, low-elevation areas (< ca. 200 m) within the watershed. In the biogeoclimatic ecosystem classification (BEC), this area is in the submontane variant of the very wet maritime subzone of the Coastal Western Hemlock zone (CWHvm1), described as having a wet, humid climate with cool summers and mild winters featuring little snow (Meidinger and Pojar 1991). Because of its location on the western slope of the Vancouver Range, the study area receives significant orographic precipitation from moist air flows off the Pacific Ocean. Mean annual precipitation is 5400 mm, of which approximately 8% falls in June, July and August (Clayoquot Biosphere Project, unpublished data). In contrast, significantly less precipitation occurs on the outer coast (3300 mm at Tofino, 25 km west) and further inland (1770 mm at Port Alberni, 48 km east; Environment Canada 1998). Mean temperatures in the study area are 14.5 and 4.9°C in July and December, respectively (Clayoquot Biosphere Project, unpublished data).

The Clayoquot River watershed is a roadless area, undisturbed by logging and minimally affected by natural disturbances. Between 1950 and 1994, no forest fires occurred in the watershed, and only 19 lightning-ignited fires of limited extent burned in the surrounding 3,500 km² Clayoquot Sound area (Ministry of Forests 1995). Avalanche and debris flows at high elevation affect 7.1% of the forested part of the watershed and no major wind disturbances were detectable over a 50-year aerial photo record (Pearson 2000). Old-growth forest structure is ubiquitous in the watershed, characterized by a wide range of tree sizes and canopy gaps created by small clusters of tree falls or by edaphic constraints (Scientific Panel 1995a; Lertzman et al. 1996). The extent of canopy gaps in an adjacent

watershed suggests that the canopy tree-replacement rate is 350–950 years in the absence of large scale disturbances (Lertzman et al. 1996).

Four broad forest types in the study area are closely associated with landforms and soils. These are described below from personal observations and the literature (Jungen 1985; Green and Klinka 1994). Codes in parentheses are from similar forest types in Green and Klinka (1994).

Sitka spruce forest (Ss) is composed of Sitka spruce (*Picea sitchensis*), western hemlock (*Tsuga heterophylla*), and red alder (*Alnus rubra*). Most of this forest type is subject to frequent flood disturbances which contribute to an open canopy and a dense shrub layer of salmonberry (*Rubus spectabilis*). However, in places this forest type also extends onto low terraces directly above flooded areas. The soils in frequently flooded areas are developed in deep, sandy to gravelly fluvial deposits and have very shallow organic horizons (Rego Humic Gleysols). Soils on better drained sites slightly above the floodplain have a mor humus over a highly weathered dark reddish brown illuvial horizon, and strongly cemented layers below 100 cm (Orstein Ferro Humic Podzols).

Cedar–hemlock forest (CwHw-swordfern; HwBa-Blueberry) is composed of western redcedar (*Thuja plicata*), western hemlock, and minor amounts of Pacific silver fir (*Abies amabilis*) and Douglas-fir. This forest type occurs on terraces, hillslopes, and alluvial fans, and is characterized by large tree sizes (1–1.5 m diameters). The understory is open and consists mostly of deer fern (*Blechnum spicant*) on moist sites and sword fern (*Polystichum munitum*) and huckleberry (*Vaccinium* spp.) on drier sites. Soils on terraces are developed in deep colluvium (Orstein Ferro Humic Podzols), and generally have deeper clay-rich illuvial horizons than in the Sitka spruce forest. These terraces also

show a pit-and-mound microtopography developed from tree tip-ups. Soils on hillslopes are developed on a shallow (50-100 cm) gravelly colluvium over bedrock (Orthic Ferro Humic Podzols). Soils on alluvial fans are aggrading with gravel and cobbles (Orthic Regosols).

Hemlock–fir forest (HwBa-deerfern) is composed of Pacific silver fir with varying amounts of western hemlock and western redcedar. This forest type occurs on terraces and hillslopes. The canopy layer is relatively uniform due to the absence of very large trees. Understory vegetation and soils on terraces and hillslopes are similar to the cedar–hemlock forest type.

Cedar–salal forest (HwCw-salal) is composed of western redcedar (sometimes 100% of the tree layer) and minor amounts of western hemlock, shore pine (*Pinus contorta contorta*), western white pine (*Pinus monticola*), and Douglas-fir. This forest type is restricted to hillslopes, exhibits stunted growth forms, small tree crowns, and has a very dense shrub cover of salal (*Gaultheria shallon*) in the understory indicative of soil nutrient limitations (Klinka et al. 1996). Soils are developed on shallow colluvium (< 50 cm) or directly over bedrock (Orthic Ferro Humic Podzols).

Background: Fire history from radiocarbon dates of soil charcoal

Charcoal in forest soils has been recognized as a source of information about past fires at a single location (e.g., Sanford 1985; Berli et al. 1994; Carcaillet 1998). If soil charcoal profiles are to provide estimates of fire dates to reconstruct a landscape-level fire history, one must consider the spatial and temporal precision of fire dates obtained by this method, especially issues related to charcoal transport following fire, the taphonomic

processes of charcoal burial and mixing within the soil profile, and the accuracy of radiocarbon-derived estimates of fire dates.

Large charcoal pieces in undisturbed soil are most likely formed by fire at that site. Charcoal particles > 0.5 mm are generally not transported by air more than a few tens of meters during fire (Clark and Patterson 1997; Ohlson and Tryterud 2000). In many topographic settings, the natural roughness of forest floors following fire prevents charcoal redeposition by overland flow (Clark 1988b; Lavee et al. 1995). However, soil erosion on steep slopes following fire may transport charcoal large distances (Reneau and Dietrich 1990; Meyer et al. 1992), but such disturbed colluvium is readily distinguished from stable forest soils.

Pedogenic processes and soil disturbances determine whether a soil profile preserves a charcoal stratigraphy that records multiple fires. For example, mor humus horizons aggrade with organic matter and may contain a history of fire (Cruikshank and Cruikshank 1981; Berli et al. 1994). However, fires also may consume humus and obliterate evidence of older fires (McNabb and Swanson 1990; Ohlson and Tryterud 2000). Charcoal occurrence at different depths in mineral soil horizons is usually the result of physical mixing (e.g., tree tip-up disturbances or animal burrowing), which may reduce the reliability of the charcoal stratigraphy for inferring the history of sequential fires (Carcaillet and Talon 1996). Considering the consumption of soil organic matter by fire and the effect of soil mixing over time, charcoal from the most recent fire should be more abundant and occur higher in the soil profile on average than charcoal from previous fires. Therefore, estimates of the time elapsed since the last fire (time-since-fire; TSF) based on the age of the uppermost charcoal should be the most reliable type of

data with which to infer past fires based on a limited number of radiocarbon dates over a range of soil types.

Despite the complexity of charcoal taphonomy in soils, wood charcoal is an ideal material for radiocarbon dates because it is mainly composed of carbon, is chemically inert and thus easily cleaned of contaminants, and is easily identifiable (Aitken 1990). Nevertheless, the accuracy of radiocarbon dates on charcoal for estimating fire dates deserves special attention. In addition to the error inherent in a calibrated radiocarbon date (Stuiver and Reimer 1993), radiocarbon dates also may overestimate the age of the fire because wood may be decades or centuries old at the time of fire. This error (termed inbuilt age) may be substantial in coastal temperate rain forests due to long residence times of woody debris (Spies et al. 1988). As described in Chapter 2, this error limits the estimate of the actual fire date from radiocarbon dates, and thus limits correlation of dates among sites or with other events. It also sets the minimum fire return interval that may be detected based on the difference between two dates.

Soil charcoal radiocarbon dates have aided research on long-term disturbance regimes in a wide range of forest types. For example, in tropical rain forest soil, charcoal dates indicated a TSF of < 1000 years in Brazil (Saldarriaga and West 1986) and in Zaire (Hart et al. 1996). Other studies from Brazil (Sanford et al. 1985) and Costa Rica (Horn and Sanford 1992) have shown TSF may be much longer in these forests. In Australian tropical rain forests, soil charcoal dates often indicated TSF > 8000 years (Hopkins et al. 1993; 1996). Millennial-scale TSF has also been found in temperate forests of New Zealand (Burrows 1996), France (Carcaillet and Thinon 1996; Carcaillet 1998), and Québec (Bussièrès et al. 1996). However, no study of soil charcoal has been conducted in North American coastal temperate rain forest.

Methods

Preliminary site selection

Sampling was primarily confined to a 730-ha area below 200 m elevation (with the exception of six sites extending to 550 m), and excluded recently disturbed areas (i.e., the floodplain and alluvial fans). Ninety-one “target sites” for tree-ring and soil-charcoal sampling were plotted on a map (on a uniform 200 m grid) of the study area. If a tree-ring date was not possible at a target site, this or the nearest suitable microsite was sampled for soil charcoal. Suitable microsites are characterized by a small concavity or level topography 2–20 m in diameter where charcoal is most likely to accumulate following fire (Bassini and Becker 1990). Limiting sampling to these sites should not introduce bias because fire behavior is not affected by such small topographic features (Chandler et al. 1983). I classified each site by forest type (see above) and landform type (hillslope or terrace). Hillslopes were defined as areas with a slope $> 25\%$ and at least one tree height (35 m) above the nearest terrace or floodplain.

Tree-ring dates

I assessed each target site for stand-level evidence of fire, such as the presence of Douglas-fir trees or the appearance of an even-aged western hemlock stand. At sites with such evidence, I collected increment cores as close to the ground as possible from the nearest 7–19 dominant canopy Douglas-fir or western hemlock (average = 11 trees). Fire dates could not be obtained from tree-ring records at some sites because too few (< 7) Douglas-fir were present to core (3 sites) or ages of western hemlock did not cluster and initial growth rates were slow, suggesting that the trees were not a post-fire cohort (3 sites). At sites with evidence of two cohorts, consisting of large Douglas-fir surrounded

by a uniformly smaller cohort of mostly western hemlock, I cored both size classes, though at some sites there were too few trees available in the larger size class (< 7) to estimate the age of the stand-initiating fire. Of the 24 sites sampled, 18 could be dated. Eleven of these sites had 2 cohorts; at 5 of these, both cohorts could be dated. The remaining 7 sites were dated by aging a single cohort of Douglas-fir trees.

Tree cores were air dried, glued to small boards and sanded to a flat surface with progressively finer sandpaper to 400 grit. I assigned calendar dates to tree rings by visually crossdating Douglas-fir cores (Stokes and Smiley 1996), of which a small number were rejected due to poor crossdating (8%). I aged Douglas-fir trees by extrapolating the age of the innermost tree ring to the age of the pith (using concentric circles and assuming a constant growth increment equivalent to the innermost five tree rings) and adding one year for every 15 cm of the core height above ground. This extrapolation resulted in the addition of 7–25 years to the age of the innermost tree ring of individual tree cores. The date of the fire that initiated the Douglas-fir cohort was estimated by the age of the oldest tree. At sites with two age classes, Douglas-fir trees showed nearly synchronous (± 1 year) abrupt decreases in ring widths. These growth declines were used to provide exact-year fire dates, because they corresponded to the approximate age of a western hemlock cohort. Assuming a late-summer fire, the fire year was set to the year preceding the first change in growth rate. If a neighboring target site had a similar fire date (< 10 years difference) based on Douglas-fir ages, that date was rejected in favor of the exact-year date.

The accuracy of these fire dates depended on the tree-ring method used. Stand ages can potentially date fires occurring 400–800 years ago based on the life-span of Douglas-fir. In the study area, the error of fire dates from Douglas-fir stand ages are estimated to be

10–30 years, based on the maximum difference in Douglas-fir tree ages at each site (12–38 years) and the assumption that Douglas-fir establishment initiated within a few years of the fire. In contrast to stand-age data, the growth response of surviving trees provides an exact-year fire date, but these fire dates were mainly limited to the 19th century because trees which survived older fires are now rare.

Isolation of soil charcoal and final site selection

I obtained soil cores using a 5 cm diameter tube at 75 target sites that 1) lacked stand-level evidence of fire (67 sites), 2) were not successfully dated using tree-ring methods (6 sites), and 3) were successfully dated using tree-ring records but where buried charcoal layers suggested that earlier fires could be dated (2 sites). I disaggregated the soil by hand in the first 3–5 cores taken at a site and looked for charcoal fragments, paying careful attention to the organic horizon because charcoal from this horizon most likely dates to the last fire (Carcaillet and Talon 1996). Any charcoal found at this time was labeled separately. I then obtained a second set of 3–5 soil cores spaced 2–5 m apart for later analysis. If the soil was > 10 cm in depth and contained distinct organic and mineral horizons, suggesting that a series of charcoal layers might be detectable, I subdivided the soil cores into 2–5 cm increments (69% of the sites). Otherwise soil cores were not subdivided.

I soaked all soil core sections ($n = 542$) for two hours in a warm 10% KOH solution to disperse organic clumps, and then sieved each section through a 0.5 mm screen. I dried the ≥ 0.5 mm fraction in a warm oven, identified charcoal under a binocular microscope, and measured the weight of charcoal. The total mass of charcoal at each site was expressed relative to the volume of all sieved core sections. Eighteen sites yielded

insufficient charcoal for a date (< 1 mg); resampling within 50 m of these target sites during later field seasons was successful at locating sufficient charcoal in 11 cases. In addition to the 7 target sites with little or no charcoal, one site was rejected due to an anomalous radiocarbon date (see below), totaling 8 of the original 91 target sites that were excluded from the final set of sites. These represent true “holes” in the spatial distribution of samples. In summary, fire dates were available from 83 sites, consisting of 65 sites with radiocarbon dates, 16 sites with tree-ring records, and 2 sites with both radiocarbon dates and tree-ring records.

Because site selection was based on a number of criteria that could affect the spatial distribution of sample sites, I examined the spatial point pattern of the final set of sites to verify that the spatial distribution was random at scales in the range of the initial spacing of sample sites (ca. 200 m). I calculated all site-to-nearest-site distances (nearest-neighbor distances; nnd's). The nnd's were sorted and expressed as a cumulative empirical distribution function, \hat{G} (Diggle 1983). To assess clumped, random, or over-dispersed distributions at different spatial scales, I compared \hat{G} to simulated random point patterns generated by randomly choosing points from a list of 18,250 points on a 20 m grid in the irregularly shaped study area. I assessed clumping or inhibition at scales where the \hat{G} distribution fell outside the envelope generated from 99 simulations.

Radiocarbon dates of soil charcoal

The piece of charcoal closest to the surface of any soil core at a given site was selected for AMS (accelerator mass spectrometry) radiocarbon dating. Abundant charcoal near the soil surface was assumed to represent the most recent fire. I obtained more than one date at sites with less clear evidence of the most recent fire, e.g., where charcoal was

present only in the mineral horizon and/or at low abundance, or where the first date was exceptionally old (> 2000 years BP). Additional dates were also obtained at sites with evidence of multiple fires, e.g., multiple layers of charcoal in a mor humus horizon. In all, a total of 120 radiocarbon dates were obtained for 67 sites. Each charcoal sample was cleaned using a warm 1M HCl rinse, several 1M KOH rinses, and a final 1M HCl rinse. If charcoal pieces were sufficiently large, radiocarbon dates were obtained from a single piece (80 dates). If all charcoal fragments were < 1 mg following cleaning, two or more pieces from the same depth in the soil were combined for a single radiocarbon date (40 dates). Charcoal was stored in 0.1M HCl before radiocarbon dating at the Center for Accelerator Mass Spectrometry, Lawrence Livermore National Laboratory. I calibrated radiocarbon dates to calendar years (Stuiver and Reimer 1993, v4.1) using the INTCAL98 calibration curve (Stuiver et al. 1998). Two radiocarbon dates on samples with low total carbon (~0.2 mg) were rejected (CAMS-53488 and CAMS-53491) because they were anomalous for their location (deep in a mineral horizon in a forest with dominated by very large trees suggesting a very long time-since-fire) and were probably contaminated with non-charcoal carbon.

The error due to inbuilt age (number of years between date of wood formation and the date of fire; McFadgen 1982) was estimated and added to each calibrated radiocarbon date. This estimated error shows, with coarse resolution, the uncertainty of a fire date that is based on a radiocarbon date of a piece of charcoal produced by that fire. The inbuilt-age error was estimated by comparing the ages of 26 radiocarbon dates with the known age of fires based on tree-ring dates (see Chapter 2). In the study area, inbuilt-age error ranged from 0–670 years with a median of 270 years (Figure 2.4).

Time-since-fire and fire return intervals in different forest types and landforms

The time-since-fire (TSF) was estimated by the tree-ring date or the youngest calibrated radiocarbon date (see Chapter 2) for each site. I calculated fire return intervals (number of years between fires) for sites with tree-ring evidence of two fires and for sites with multiple radiocarbon dates that did not show age/depth reversals. The error of calibrated radiocarbon dates and inbuilt-age precludes the detection of fire return intervals < 450 years of each other (Chapter 2). TSF was compared to forest vegetation and terrain characteristics in two ways, as described below.

First, significant differences of median TSF among categories of forest and landform types were tested using Monte Carlo randomization tests. Sites were grouped into categories in three ways: by both forest type and landform type, only by forest type, and only by landform type. Each test consisted of comparing the difference in median TSF between two categories to a distribution of differences from 3999 randomizations generated by randomly allocating TSF dates to the two categories (Manly 1997). Significance was assessed as the proportion of randomizations (adding the observed result as a value in the randomization distribution) that have differences in median TSF as large or larger as that observed.

Second, the relationship of TSF to topographic characteristics of hillslope sites was tested for each vegetation type with exponential regression. For this, I quantified topography in terms of exposure to solar radiation by computing topographically-distributed potential incoming solar radiation (terrain insolation), using the SOLARFLUX program in ARC/INFO GIS software (Rich et al. 1995). Terrace sites were excluded from this analysis because terrace forest had denser canopies and understory moisture levels were

substantially higher than hillslope sites with similar terrain insolation. SOLARFLUX uses a digital elevation model (10 m grid cells) and the sun track to compute insolation at each grid cell accounting for the effects of slope, aspect, and hillshading. Since only the relative amount of insolation at different sites was important, atmospheric transmissivity was assumed to be constant and surface albedo negligible, and the calculations were based only on direct and indirect radiation. Mean daily terrain insolation for August was computed using the average of SOLARFLUX calculations for August 1, 8, 15, 22, and 31. I calculated a terrain insolation index (TII) as the proportion of terrain insolation at a site relative to the amount of terrain insolation on a horizontal surface with a full sky view computed using the same methods (Antonic 1998). TII values > 1 indicate south-facing aspects and little hillshading, while values < 1 indicate north-facing aspects, hillshading, or both. The effect of hillshading and slope on terrain insolation is substantial in the study area, as shown by the imperfect correlation between TII and an index based only on aspect using $(\cos(-\text{aspect angle})+1)$; Beers et al. 1966) ($r = 0.79$; $n = 73,000$ grid cells).

Fire extent

I analyzed the spatial pattern of TSF to assess the scale at which fires burned. TSF cannot show the sizes of all fires because recent fires partially burn over and obscure the extent of older fires. However, if the sizes of the most recent fires were similar, adjacent sites should have similar TSF up to the scale of these fires. Thus, as a means of assessing fire extent, I compared TSF at adjacent sites to see if sites with similar dates were spatially aggregated. For all possible pairs of sites in non-overlapping 250 m distance classes, I computed the proportion of site pairs with TSF < 300 years apart (i.e., sites with effectively the same date). I assessed significant clumping of similar TSF using a Monte

Carlo randomization test (Manly 1997). This test consisted of comparing the proportion statistic for each distance class to a distribution of 3999 proportion statistics generated from randomly allocating TSF dates to sites. Significance was assessed by constructing 95% confidence intervals from the randomization distribution, including the observed proportion statistic in the distribution. This analysis was run for all sites and by landform type (i.e., hillslope and terrace sites).

Results

Site characteristics

The 83 sites were dispersed over 8 km and represented a range of forest types and terrain insolation (Figure 3.2). Approximately half of the sites (53%) were in the cedar–hemlock forest type, occurring mostly on east or west aspects (mean TII = 0.74). Hemlock–fir forests were also well represented (27%), roughly equally common on terraces 10–60 m above the river and on hillslopes with north aspects (mean TII = 0.65). The remaining sites were in the cedar–salal forest type (12%), all of which were on south aspects (mean TII = 1.03), or the Sitka spruce forest type (8%) on terraces. Nearest-neighbor distances among sites ranging from 85 to 500 m, and evenly distributed relative to a random point pattern at scales < 210 m. Sites were randomly distributed at scales of 210–500 m.

Tree-ring dates of fire

Tree-ring estimates of fire dates ranged from ca. AD 1550 to AD 1886 (Table 3.1). Taken together, these dates indicated 15 fire events. In five instances, similar tree-ring dates at adjacent sites suggest that fires spread between sites, though never more than 1 km (Table 3.1; Figure 3.3). In two instances, the pattern of fire dates suggested synchronous

fires from multiple ignitions, because intervening sites did not show evidence of fire. First, exact-year fire dates in AD 1805 were determined at three sites that were separated by > 1 km. Second, stand-initiating fires in ca. AD 1620 were also found at three sites separated by > 1 km (Figure 3.3).

Soil charcoal radiocarbon dates of fire

The 120 radiocarbon dates on soil charcoal (67 sites) ranged from 280 to 10,330 radiocarbon years BP (calibrated to 310–12,220 years BP; Table 3.2). The highest stratigraphic location of charcoal was in the organic horizon at 17 sites, and in the mineral horizon at 50 sites (Table 3.3). Charcoal abundance was similar at sites where charcoal was in the organic horizon and sites where charcoal was only in the mineral horizon, though charcoal in organic horizons generally dated to < 2500 years BP, while dates in the mineral horizons ranged from 470 to 12,220 years BP (Figure 3.3). Charcoal abundance was weakly related to TSF ($r^2 = 0.09$), with a particularly wide range of charcoal abundance for shorter TSF (Figure 3.4). Although sites with > 1 g l⁻¹ of charcoal usually burned in the last 5000 years, sites with < 1 g l⁻¹ represented the full range of TSF (310–12,220 years).

Where ≥ 2 dates were obtained from different depths in the same core (21 sites), adjacent dates were similar (< 300 year difference) for half of the pairs of dates compared and dating-reversals occurred in only 4 cases (Figure 3.5a). Charcoal found in the organic horizon was always younger or the same age as charcoal at lower depths. At sites with dates from multiple cores, radiocarbon dates from the mineral horizon were similar to each other at five of 12 cases (Figure 3.5b). At sites with a single date from the mineral

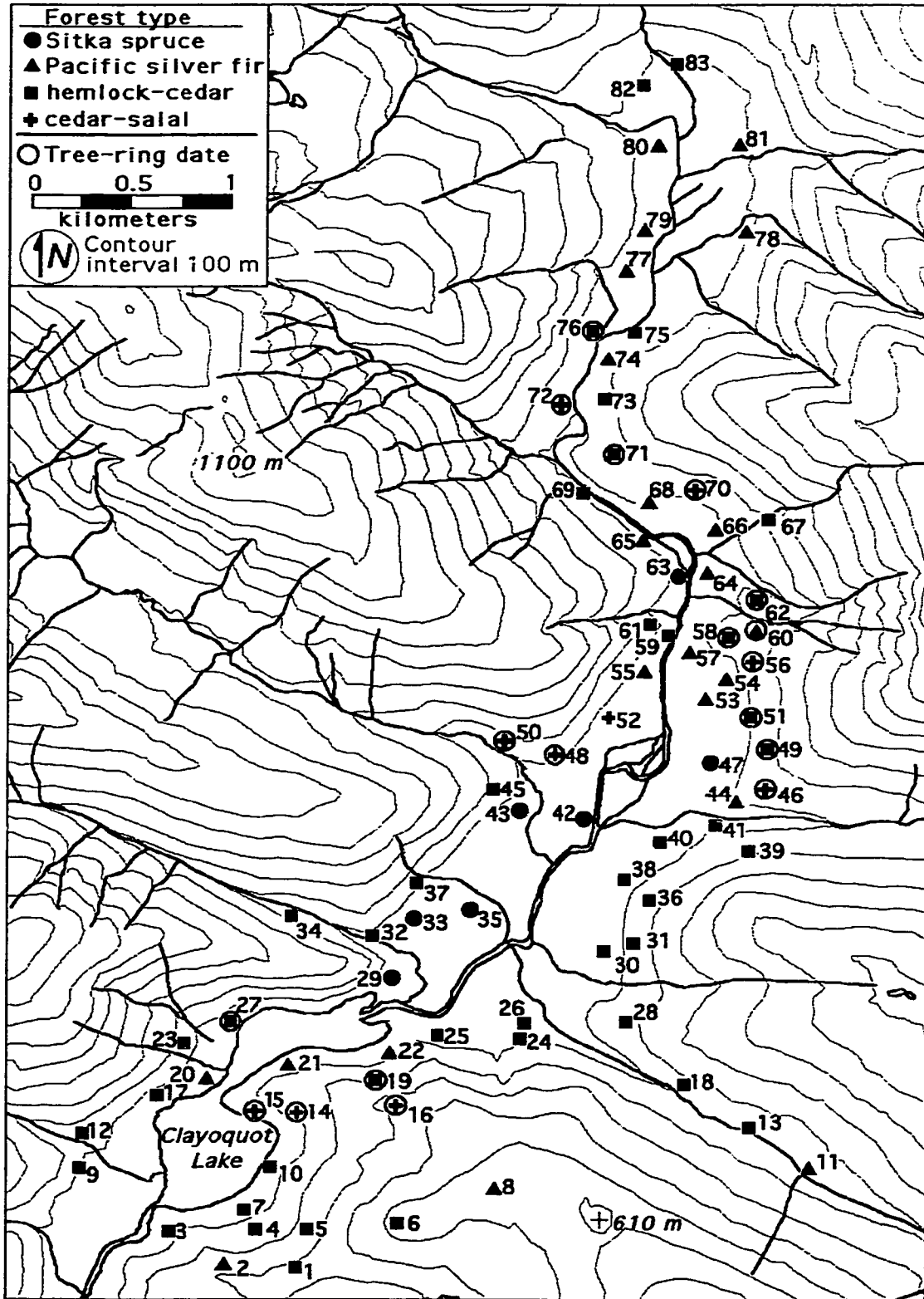


Figure 3.2 Location of sample sites in the Clayoquot Valley, Vancouver Island, British Columbia.

Table 3.1 Tree-ring dates of fire events obtained by coring at least seven trees per cohort. Dates were determined from stand ages or from abrupt growth responses to fire injury in surviving trees. All sites occurred on hillslopes. The site code refers to locations on Figure 3.2.

Site code	Field code	UTM coordinates		Vegetation type ^a	Dating method	Fire date (year AD)
		Easting	Northing			
14	PR03	316615	5452341	CS	Growth response	1805
					Stand age	1620
15	PRB	316403	5452350	CS	Stand age	1805
16	PR06	317114	5452379	CS	Stand age	1805
19	UE80	317013	5452516	CH	Growth response	1805
27	RSA80	316280	5452841	CH	Growth response	1886
46	URE13	318988	5454122	CS	Stand age	1655
48	URW04	317904	5454311	CS	Stand age	1550
49	URE70	318996	5454340	CH	Growth response	1872
50	URW83	317649	5454386	CS	Stand age	1550
51	SBA	318913	5454516	CH	Growth response	1872
					Stand age	1683
56	URE63	318921	5454826	CS	Stand age	1683
58	SBB	318798	5454959	CH	Growth response	1872
					Stand age	1610
60	URE64	318937	5455000	HF	Growth response	1683
62	URE69	318939	5455164	CH	Growth response	1872
70	SBC	318626	5455771	CS	Growth response	1830
					Stand age	1620
71	RT01	318210	5455965	CH	Growth response	1805
					Stand age	1620
72	RT04	317933	5456238	CS	Stand age	1620
76	RT51	318098	5456642	CH	Growth response	1805

^a CH=cedar-hemlock, HF=Hemlock-fir, CS=cedar-salal

Table 3.2 Radiocarbon dates of soil charcoal obtained from the Clayoquot Valley, Vancouver Island.

Site code	Field code	Site coordinates		Vegetation type	Hillslope	Soil horizon	Depth (cm)	Depth in horizon (cm)	Number pieces dated	Sample code ^a	Lab # (GAMS #)	$\delta^{13}C$	Radiocarbon date	cal age intercept (year BP) ^b	95.4% cal age ranges ^c
		UTM zone 10	UTM Easting Northing												
1	LE06		316615 5451494	CH	H	O	3	3	1	LE06ChO	32224	-27.64	840 ± 60	730	910-670
						B	13	2	2	LE06ChB1	32225	-25.89	4280 ± 50	4840	5030-4650
						B	17	6	1	LE06ChB2	32226	-25.49	5460 ± 60	6280	6400-6010
2	LE03		316246 5451514	HF	H	B	20	10	1	LE03G	32345	-26.87	7690 ± 50	8440	8590-8390
3	LE02		315977 5451691	CH	H	O	35	35	1	LE02hmid	32223	-26.18	2980 ± 60	3150	3330-2970
						O	40	40	1	LE02hbottom	39386	-24.44	4920 ± 40	5620	5720-5590
4	LE61		316410 5451700	CH	H	B	5	3	2	LE61A	43865	-24.90	7320 ± 50	8120	8280-7980
5	LE07		316672 5451703	CH	H	B	13	2	3	LE07AhB	32227	-27.36	2360 ± 50	2350	2660-2180
6	PR08		317123 5451733	CH	H	A	7	2	1	PR08AhA	39389		1200 ± 50	1140	1260-990
						B	12	2	1	PR08AhB1	32340		990 ± 50	930	1040-770
7	LE60		316353 5451808	CH	H	B	5	2	1	LE60A	43864		2780 ± 40	2870	2950-2780
8	PR07		317603 5451928	HF	H	B	12	2	2	PR07BhB	32230	-26.07	2690 ± 50	2780	2910-2740
9	LW01		315531 5452040	CH	H	B	15	9	1	LW01BhB2	32228	-27.54	1370 ± 60	1290	1390-1180
						B	30	26	1	LW01BhB4	32341	-23.51	1150 ± 50	1060	1180-960
10	MR		316481 5452043	CH	H	O	3	3	1	MR1h3-4A	26978		2400 ± 60	2360	2710-2340
						O	4	4	1	MR1h4-5A	26979		2360 ± 70	2350	2710-2160
						O	13	13	1	MR1h13-14	26980		2390 ± 60	2360	2710-2330
						O	14	14	1	MR1h14-15	26981		2360 ± 80	2350	2710-2160
11	TA82		319211 5452044	HF	T	B	15	1	1	TA82ChB1	53479		8780 ± 60	9850	10150-9560
12	LW60		315543 5452228	CH	H	B	5	1	3	LW60ChB1	43868	-22.62	1140 ± 50	1030	1170-950
						B	9	5	10	LW60ChB2	43869	-26.88	1060 ± 50	960	1070-800
13	TA81		318912 5452260	CH	T	B	11	4	2	TA81ChB2	53478		9210 ± 50	10340	10500-10240
16	PR06		317114 5452379	CS	H	B	6	2	1	PR06AhB1	32343	-27.81	430 ± 60'	510	550-320
						B	11	7	1	PR06AhB2	39387		410 ± 40'	500	520-320
						B	17	13	1	PR06AhB3	39388		1060 ± 50	960	1070-800
						B	22	18	1	PR06AhB4	32344	-25.73	1590 ± 60	1520	1610-1340
17	LW06		315914 5452439	CH	H	A	10	5	2	LW06C	32229	-22.59	1120 ± 60	1030	1170-940
18	TA03		318578 5452498	CH	T	B	15	10	1	TA03C	53477		9410 ± 50	10610	11040-10430
						B	23	20	1	TA03BhB2	39510		9670 ± 70	11140	11200-10750

Table 3.2 (cont.)

Site code	Field code	Site coordinates		Vegetation type	Hillslope	Soil horizon	Depth (cm)	Depth in horizon (cm)	Number pieces dated	Sample code ^a	Lab # (CAMS #)	$\delta^{13}C^b$	Radiocarbon date	cal age intercept (year BP) ^c	95.4% cal age ranges ^d
		UTM zone 10 Easting	UTM zone 10 Northing												
20	CR	316159	5452534	HF	T	O	15	15	1	CR1h15-16	27019		1080 ± 50	970	1170-920
						O	17	17	1	CR1h17-18	27020		1060 ± 50	960	1070-800
						O	19	19	1	CR1h19-20	27021		910 ± 70	820	930-700
						O	24	24	1	CR1h24-26	27022		1020 ± 50	930	1050-790
						B	27	1	1	CR1h27-28	27023		3600 ± 70	3690	4090-3700
21	UE01	316568	5452604	HF	H	O	4	4	1	UE01A	43885	-22.26	1970 ± 50	1910	2050-1820
22	UE03	317080	5452672	HF	H	B	5	1	1	UE03D	53480		2950 ± 60	3130	3320-2950
						B	5	1	1	UE03C	32346	-25.43	5730 ± 60	6500	6710-6400
23	LW50	316048	5452723	CH	H	B	13	4	8	LW50B	43867	-25.55	1410 ± 50	1300	1410-1240
24	URE17	317729	5452746	CH	H	B	11	2	1	URE17ChB1	32244	-27.39	2220 ± 60	2200	2350-2070
						B	17	8	3	URE17ChB2	32245	-24.42	8190 ± 60	9180	9400-9010
25	LU	317317	5452764	CH	H	O	12	12	1	LU1	25013		1630 ± 70	1530	1700-1360
						O	10	10	1	LU1A	25014		4150 ± 60	4690	4830-4530
						O	10	10	1	LU2B	25015		1290 ± 70	1240	1320-1060
						O	15	15	1	LU2C	25016		1420 ± 50	1310	1410-1270
26	URE56	317753	5452830	CH	T	B	5	2	2	URE56BhB	43893	-24.80	2920 ± 50	3080	3240-2890
						B	5	2	1	URE56AhB	53497		5310 ± 50	6070	6270-5940
28	URE55	318279	5452843	CH	H	B	13	8	2	URE55ChB3	53488		860 ± 60*	750	910-680
						B	21	10	2	URE55BhB3	43892	-24.50	9030 ± 50	10210	10360-9920
29	URW53	317091	5453081	SS	T	B	8	3	1	URW53AhB	43924	-26.99	1210 ± 50	1160	1260-990
30	TA02	318168	5453230	CH	T	B	20	13	2	TA02BhB2	32347	-22.60	4060 ± 50	4560	4810-4420
						B	33	25	8	TA02BhB3	32236	-26.09	4150 ± 50	4690	4830-4530
31	URE57	318320	5453274	CH	T	B	7	5	6	URE57BhB3	43894		2590 ± 50	2750	2790-2480
32	URW82	316995	5453312	CH	T	B	8	6	1	URW82B	53498		6170 ± 40	7090	7210-6940
33	URW02	317200	5453405	SS	T	B	9	5	1	URW02BhB	54628		500 ± 50	520	640-470
						B	10	6	4	URW02C	32246	-25.83	3070 ± 50	3290	3390-3080
34	URW80	316584	5453419	CH	H	O	4	4	1	URW80A	53496		1300 ± 50	1260	1300-1090
35	URW63	317479	5453455	SS	T	B	5	3	2	URW63BhB2	43926		1120 ± 50	1030	1170-940
						B	7	5	1	URW63BhB3	43927		1340 ± 50	1280	1340-1170

Table 3.2 (cont.)

Site code	Field code	Site coordinates		Vegetation type	Hillside Terrace	Soil horizon	Depth (cm)	Depth in horizon (cm)	Number pieces dated	Sample code ^a	Lab # (CAMS #)	$\delta^{13}\text{C}^b$	Radiocarbon date	cal age intercept (year BP) ^c	95.4% cal age ranges ^d
		UTM zone 10	Eastings												
36	URE54	318398	5453509	CH	H	O	2	2	1	URE54BhO1	43890	-24.28	2790 ± 50	2910	3000-2770
37	URW62	317211	5453600	CH	H	A	5	5	1	URE54BhB1	43891	-25.76	4550 ± 50	5300	5450-5000
38	URE52	318269	5453624	CH	H	A	3	3	3	URE52A	53487		2710 ± 50	2780	910-670
						A	3	3	1	URE52B	43889		4330 ± 50	4870	5040-4830
39	URE16	318902	5453780	CH	H	A	8	6	1	URE16C	53485		3050 ± 70	3300	3430-3000
						A	6	6	1	URE16A	32243	-26.08	3470 ± 50	3710	3860-3630
40	URE51	318454	5453831	CH	H	A	7	1	3	URE51EhAE1	43888		450 ± 40	510	540-340
41	URE15	318739	5453923	CH	H	B	4	5	1	URE15D	53484		3190 ± 50	3430	3550-3270
42	URW60	318062	5453958	SS	T	B	6	4	1	URW60A	53495		960 ± 70	920	1050-730
43	URW03	317723	5454001	SS	T	B	8	6	4	URW03A	32247	-27.30	3420 ± 40	3660	3830-3570
44	URE14	318837	5454056	HF	T	B	8	2	1	URE14ChB1	32240	-27.45	6900 ± 60	7690	7910-7610
						B	13	7	1	URE14ChB2	32241	-26.54	3880 ± 60	4330	4440-4100
						B	16	10	2	URE14ChB3	32242	-29.72	3860 ± 60	4250	4420-4090
45	URW52	317590	5454117	CH	H	O	4	4	1	URW52A	43923	-25.01	850 ± 50	740	910-670
47	URE50	318709	5454267	SS	T	B	8	2	8	URE50ChB2	43887	-24.45	9560 ± 50	10960	11110-10690
						B	14	3	1	URE50BhB2	53486		10030 ± 50	11440	11920-11260
52	URW65	318186	5454518	CS	H	O	3	3	1	URW65A	43928	-26.04	440 ± 40	510	540-330
53	URE61	318682	5454624	HF	T	B	5	3	10	URE61ChB2	43895	-25.30	8690 ± 60	9630	9890-9540
						B	9	7	1	URE61ChB4	43896		3250 ± 50	3470	3630-3370
						B	11	9	7	URE61ChB5	43897		8460 ± 60	9490	9550-9300
54	URE65	318785	5454734	HF	T	B	12	6	2	URE65A	43915	-24.01	6570 ± 50	7450	7570-7380
						B	10	5	1	URE65C	53490		7180 ± 50	7970	8150-7870
55	URW06	318368	5454774	HF	H	B	13	3	2	URW06BhB	53494		4750 ± 50	5540	5590-5320
						B	12	2	1	URW06C	39390		4900 ± 50	5610	5740-5490
57	URE62	318598	5454878	HF	T	B	7	7	1	URE62C	43898	-24.75	2400 ± 50	2360	2710-2340
						B	7	7	1	URE62A	53489		10240 ± 50	11790	12350-11690
59	URW66	318488	5454970	CH	T	B	10	4	1	URW66AhB2	43929	-24.75	4680 ± 50	5380	5580-5310
61	URW67	318401	5455033	CH	H	O	3	3	2	URW67A	43930	-23.32	640 ± 50	580	660-550

Table 3.2 (cont.)

Site code	Field code	Site coordinates		Vegetation type	Hillslope	Soil horizon	Depth (cm)	Depth in horizon (cm)	Number pieces dated	Sample code ^a	Lab # (CAMS #)	$\delta^{13}\text{C}^b$	Radiocarbon date	cal age intercept (year BP) ^c	95.4% cal age ranges ^d
		Easting	Northing												
63	URW01	318540	5455295	SS	T	B	13	5	1	URW01BhB1	53492		8190 ± 50	9180	9400-9020
						B	27	19	1	URW01BhB3	53493		8150 ± 50	9060	9270-9010
64	URE07	318687	5455317	HF	T	B	18	15	1	URE07BhB2	32237	-24.66	9180 ± 50	10320	10480-10230
						B	27	22	4	URE07BhB3	32238	-26.97	8710 ± 50	9640	9890-9550
65	URW07	318359	5455498	HF	H	A	9	2	4	URW07BhA1	32249	-26.19	390 ± 40	470	510-320
						A	17	10	6	URW07BhA3	32250	-24.01	3110 ± 60	3350	3470-3160
66	URE67	318728	5455554	HF	T	O	2	2	1	URE67AhO	43917		600 ± 90	600	700-480
						B	8	5	1	URE67AhB3	43918		8340 ± 50	9400	9480-9140
						B	12	9	6	URE67AhB5	43919	-23.06	8280 ± 50	9370	9460-9090
67	URE68	318999	5455608	CH	H	O	2	2	1	URE68A	43920	-24.34	400 ± 50	480	520-320
68	URE66	318389	5455707	HF	T	B	13	2	2	URE66BhB	43916		8120 ± 90	9030	9400-8720
						B	6	2	1	URE66ChB	54629		9440 ± 70	10640	11080-10430
69	URW08	318051	5455754	CH	H	B	12	8	1	URW08ChB3	39509		9120 ± 70	10240	10490-10180
						B	16	12	1	URW08ChB4	39391		9210 ± 50	10340	10500-10240
73	RT60	318160	5456270	CH	H	O	3	3	3	RT60ChO	43883	-25.80	520 ± 50	530	650-500
						B	9	5	12	RT60BhB2	43884	-26.32	750 ± 50	670	780-560
74	RT50	318176	5456490	HF	H	O	10	10	4	RT50A	43872		270 ± 50	305	470-10
75	RT05	318315	5456634	CH	H	B	15	2	1	RT05AhB	53475		8320 ± 50	9350	9470-9130
76	RT51	318098	5456642	CH	H	O	7	7	1	RT51hO3	43875	-23.93	350 ± 40'	350	490-310
						O	9	9	1	RT51hO4	43876	-23.94	420 ± 50'	500	530-320
						A	11	1	1	RT51hA1	43873	-24.4	350 ± 40'	350	490-310
						A	17	7	1	RT51hA4	43874	-27.13	5860 ± 50	6700	6790-6510
77	RT53	318268	5456976	HF	H	B	14	6	1	RT53ChB2	43877	-22.95	480 ± 50	520	630-340
78	RT12	318878	5457186	HF	H	B	17	9	1	RT12AhB2	39394		10330 ± 50	12220	12770-11770
79	RT55	318360	5457197	HF	T	B	10	5	2	RT55AhB3	43879		8890 ± 190	10060	10420-9530
80	RT57	318429	5457658	HF	T	O	2	2	3	RT57AhO1	43880		8300 ± 50	9360	9470-9130
						B	10	3	3	RT57AhB2	43881		9130 ± 60	10240	10470-10190
						B	14	7	12	RT57AhB4	43882	-25.48	8640 ± 50	9550	9770-9530
81	RT54	318842	5457661	HF	T	O	5	5	1	RT54C	43878		460 ± 70	510	630-320
82	RT81	318351	5457983	CH	T	O	8	2	1	RT81A	53476		430 ± 50	510	540-320

Table 3.2 (cont.)

Site code	Field code	Site coordinates		Vegetation type ^a	Hillside Terrace	Soil horizon	Depth (cm)	Depth in horizon (cm)	Number pieces dated	Sample code ^b	Lab # (CAMS #)	$\delta^{13}\text{C}^b$	Radiocarbon date	cal age intercept (year BP) ^c	95.4% cal age ranges ^d
		UTM zone 10	Easting Northing												
83	RT07	318522	5458099	CH	T	B	13	5	1	RT07BhB1	39392		9560 ± 60	10960	11150-10690
						B	33	25	1	RT07ChB4	39393		5910 ± 40	6700	6850-6650
reject	URE81			HF		B	5	2	1	URE81ChB	53491		280 ± 50 ^e	310	480-10

^a CH=cedar-hemlock, HF=hemlock-fir, SS=Sitka spruce, CS=cedar-salal

^b assumed to be -25 where not measured

^c median cal age intercept only, rounded to nearest decade (Stuiver and Reimer 1993; Stuiver et al. 1998)

^d minimum and maximum of ranges only, rounded to nearest decade

^e date rejected (n=2)

^f more accurate tree-ring date available; date not used (n=5)

^g the core identification is the first letter in the sample code following the field code.

Table 3.3 Frequency of sites with different numbers of dates per site in different soil horizons. Two rejected dates are not included.

Soil horizon	Number of dates per site				
	1	2	3	4	5
Organic only	7	1	0	2	0
Organic and mineral	-	2	3	1	1
Mineral only	25	22	2	1	0
Total no. sites	32	25	5	4	1

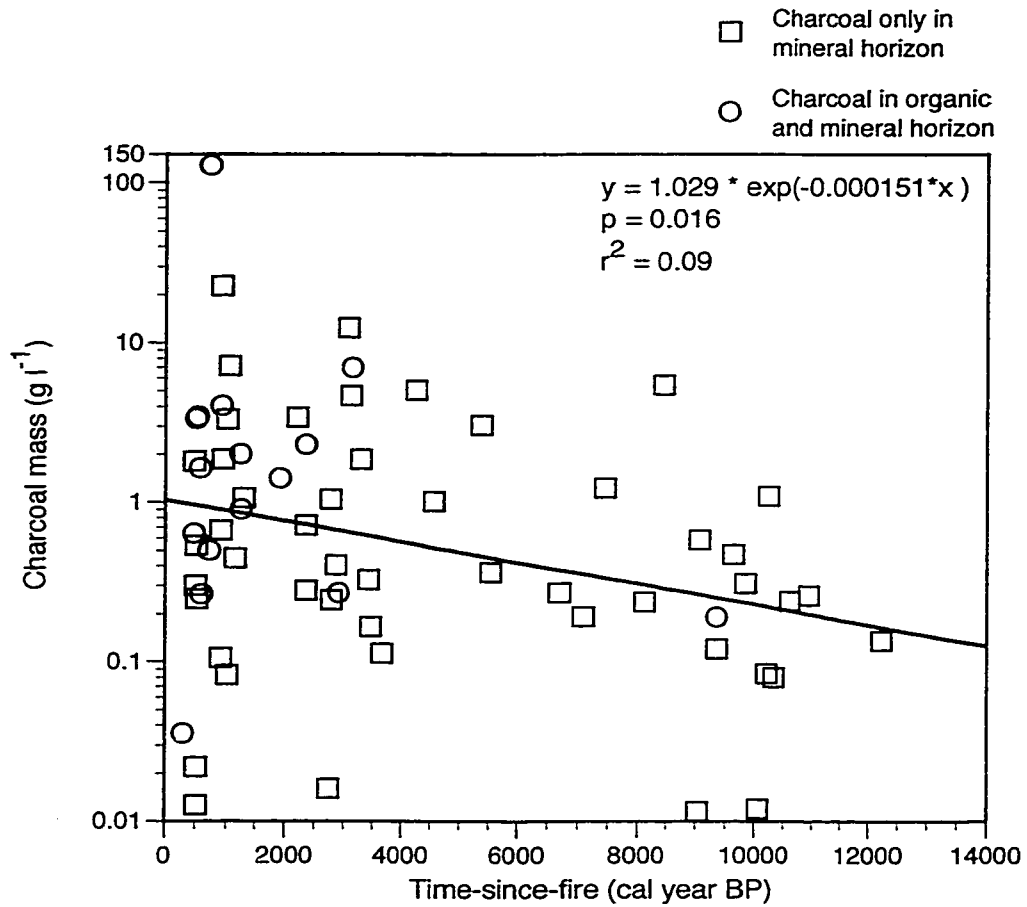


Figure 3.4 Charcoal mass in soil related to time-since-fire at 65 sites in the Clayoquot Valley. Charcoal mass was determined from 3-7 cores (5 cm diameter).

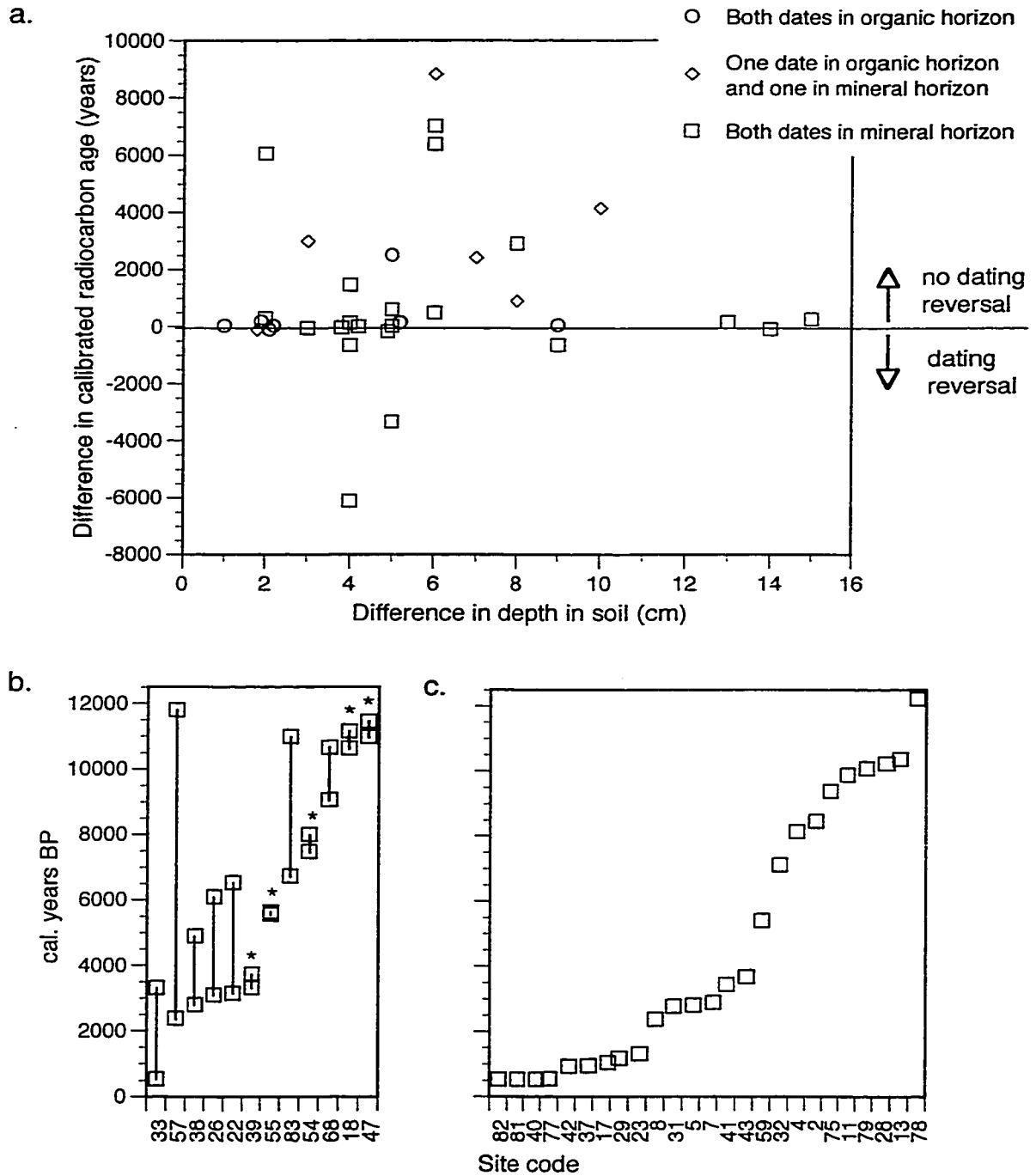


Figure 3.5

a. Stratigraphic relationships among soil charcoal radiocarbon dates from sites with multiple radiocarbon dates from the same soil core. All adjacent dates were compared (up to 4 dates or 3 comparisons per soil core), for a total of 35 comparisons from 21 cores. b. Difference in dates from sites with dates from different cores. Only dates from the mineral horizon are shown. Sites with similar dates are indicated with an asterisk. c. Distribution of dates from sites with only one date from the mineral horizon.

horizon, radiocarbon dates ranged to 12,200 cal. years BP, but were < 3000 cal. years BP at 13 of 25 sites (Figure 3.5c).

Time-since-fire

The frequency distribution of TSF differed greatly between hillslope and terrace sites, though dates at both landform types extended across the entire Holocene (Figure 3.6). On hillslopes, the majority of sites (56%) burned within the last 1000 years, with only a few (11%) not burning over the past 6000 years. In contrast, terraces have a nearly even distribution over TSF age classes, with relatively few sites (21%) burning within the last 1000 years compared to those without evidence of fire (43%) in the past 6000 years. Over both landforms, 18 sites (21%) have TSF > 6000 years; 12 of these date between 11,000 and 9000 years BP. Adjusting radiocarbon dates for inbuilt-age shifts the TSF distribution forward in time, but does not affect the overall form of the distribution for either landform type (Figure 3.6).

Median TSF differed significantly between some but not all vegetation types and landforms (Figure 3.7). In the cedar–hemlock, hemlock–fir and Sitka spruce forest types, TSF encompassed the entire Holocene. TSF in the cedar–salal forest type had a narrower range (to 510 years BP), and significantly shorter median value than for all other forest types on hillslopes or terraces ($P < 0.001$, except for cedar–hemlock hillslope forest, $P = 0.111$). Overall, the median TSF on terraces was six times greater than on hillslopes ($P < 0.001$), reflecting the > 4000 year longer TSF on cedar–hemlock terraces ($P = 0.004$) and hemlock–fir terraces ($P = 0.002$) compared to cedar–hemlock hillslopes. Fewer differences were found between forest types across both landform types (Figure 3.7). TSF in cedar–hemlock forest was shorter than in hemlock–fir forest ($P = 0.043$). TSF in

cedar–salal forest was shorter than in Sitka spruce forest ($P < 0.001$), but only weakly shorter than in hemlock–fir forest ($P = 0.095$).

All hillslope sites with high TII values (> 0.95) have burned within the last 1000 years (Figure 3.8a). In contrast, only 42% of hillslope sites with low TII values (< 0.95) have burned within the last 1000 years. The slope parameter for the exponential regression between TSF and TII was significant for all 83 sites ($\beta = -2.48$, $t = -3.3$, $P = 0.002$). For individual forest types, this relationship was marginally significant for the 44 cedar–hemlock forest sites ($\beta = -2.06$, $t = -2.1$, $P = 0.058$), but improved after removing an outlier with a TII of 0.15 ($\beta = -3.29$, $t = -3.3$, $P = 0.005$). Slope parameters were not significantly different from zero for cedar–salal and hemlock–fir forest ($P = 0.88$ and 0.94 , respectively).

Fire return intervals

Trends in fire return intervals are similar to those for TSF even though few reliable intervals were detected ($n = 16$ intervals) (Figure 3.8b). Fire return intervals varied from 185–570 years in cedar–salal forests to 700–ca. 9000 years in cedar–hemlock forests at low TII values and hemlock–fir forests on terraces. Too few fire-interval estimates were available for statistical comparisons among vegetation types and landforms.

Fire extent

The frequency of site pairs with a similar TSF was significantly higher than expected for randomly distributed fire dates only at scales < 250 m, suggesting that fires rarely extended 250 m in the study area (Figure 3.9). However, fires frequently spread up to 250 m on hillslopes, as ca. 60% of the site pairs in this landform had similar TSF at scales

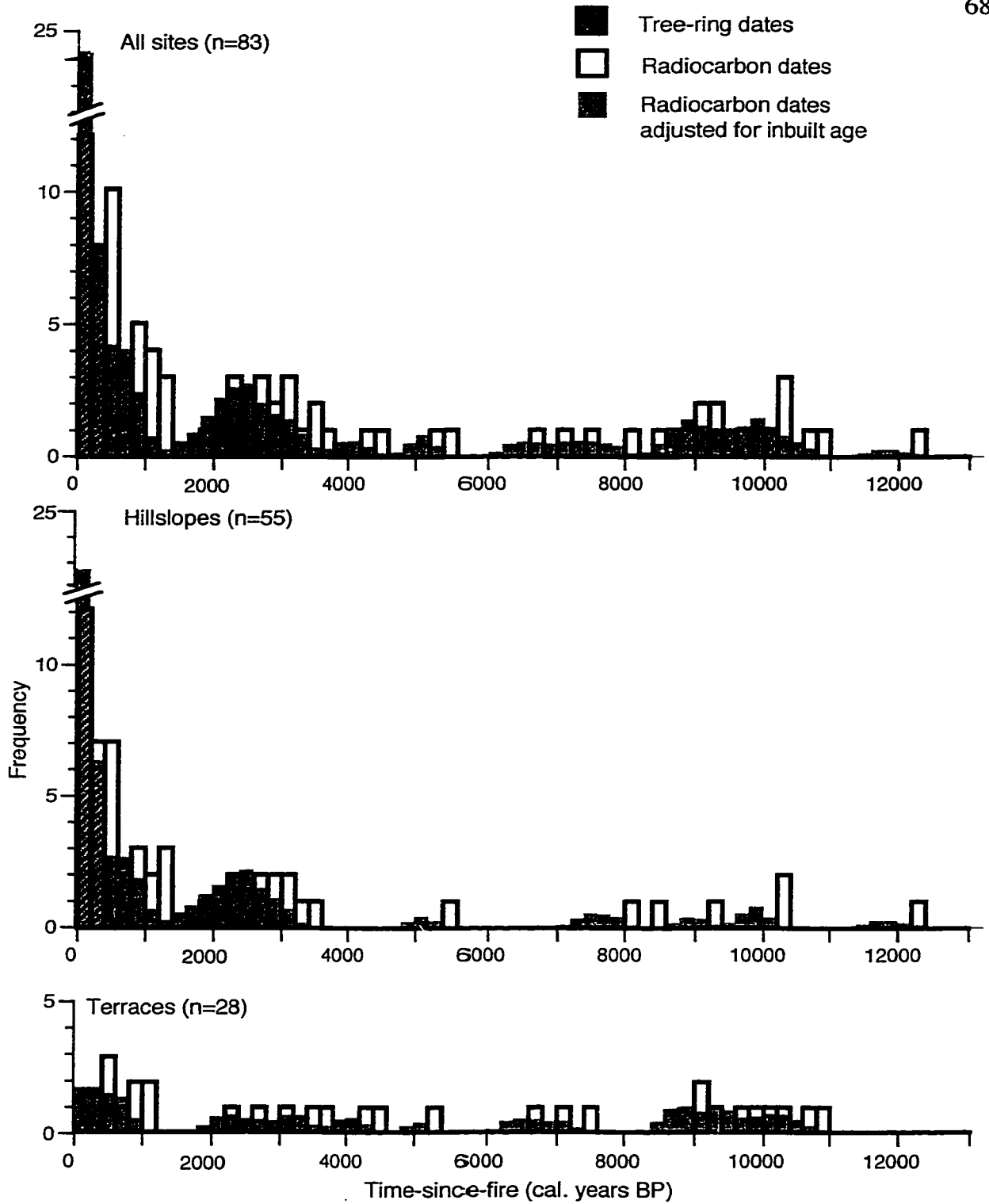


Figure 3.6 Time-since-fire distribution at 83 sites in the Clayoquot Valley study area. Shaded bars represent the range of uncertainty in radiocarbon dates from radiocarbon calibration and from inbuilt age (age of wood at time of fire).

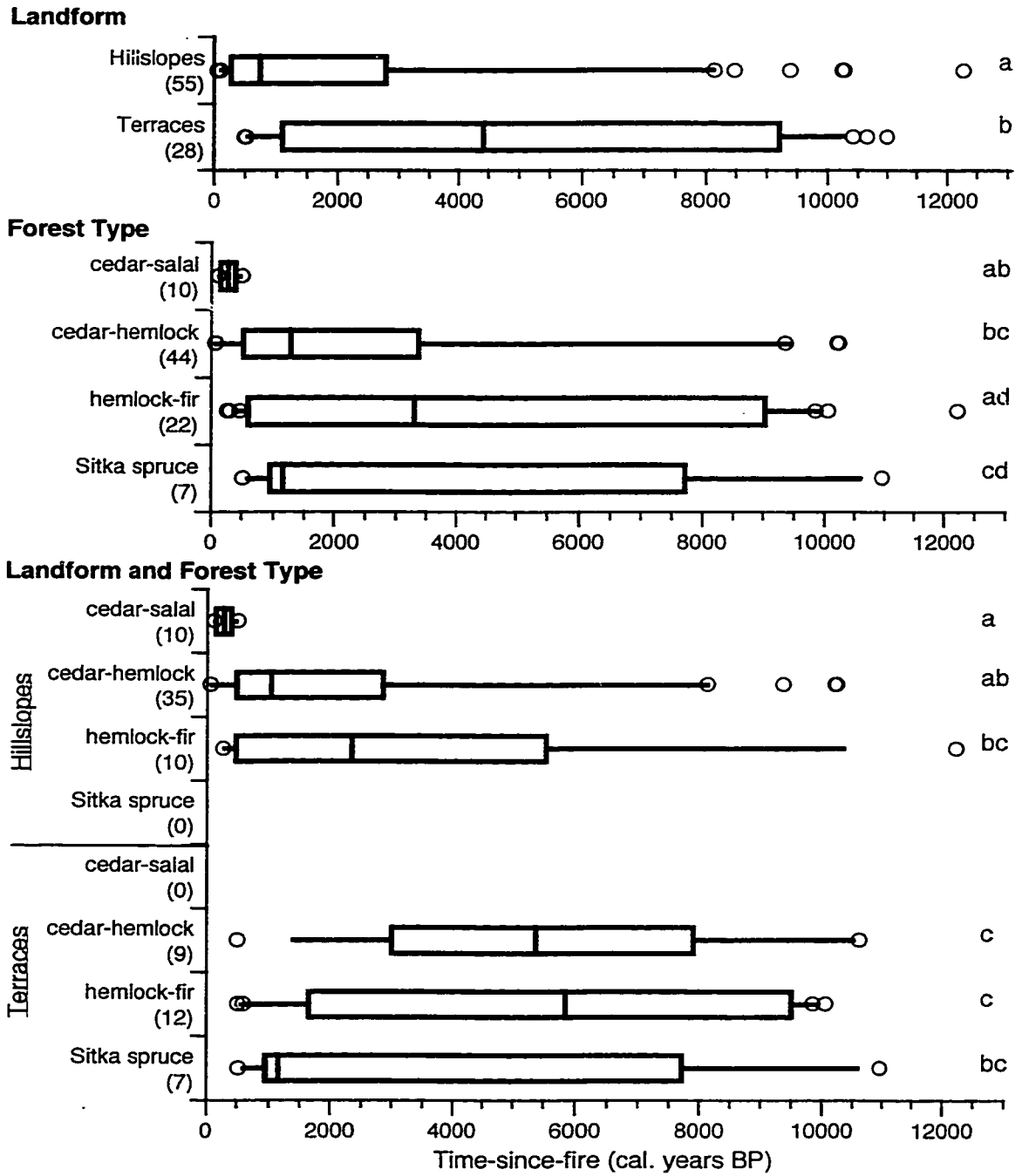


Figure 3.7 Box plots of time-since-fire by landform, vegetation type, and landform and vegetation type for 83 sites in the Clayoquot Valley. The number of sites in each class is indicated in parentheses. Differences in letter codes indicate a significant difference ($P < 0.05$) in median time-since-fire determined with randomization tests.

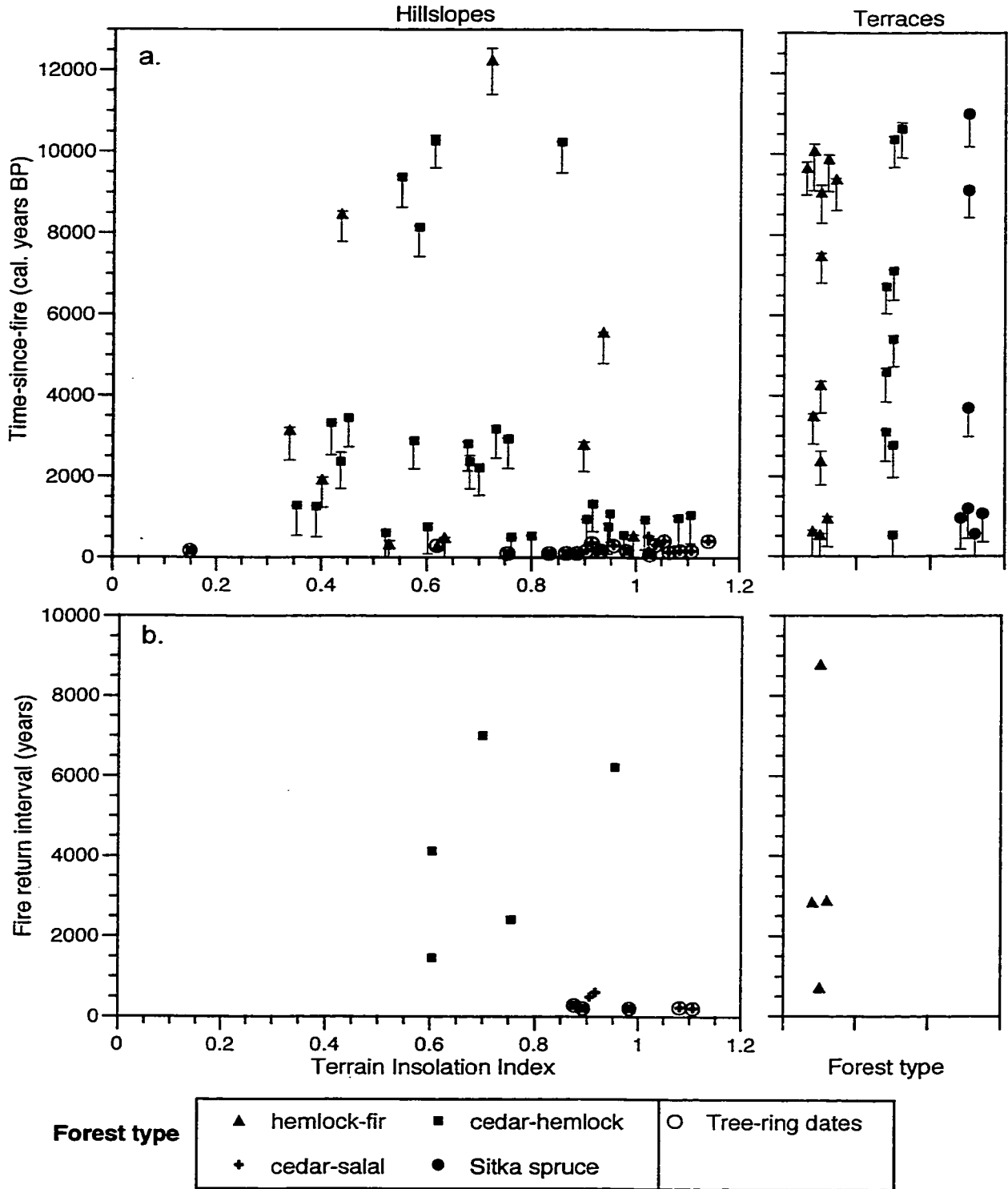


Figure 3.8 (a) Time-since-fire estimates relative to the terrain insolation index on hillslopes (August solar radiation relative to a flat unobstructed surface) and on terraces. Error bars represent the 95% confidence interval of charcoal radiocarbon dates after adjusting for potential inbuilt age (see *Methods*). (b) Fire intervals at sites with multiple tree-ring dates or with multiple radiocarbon dates from undisturbed soil profiles.

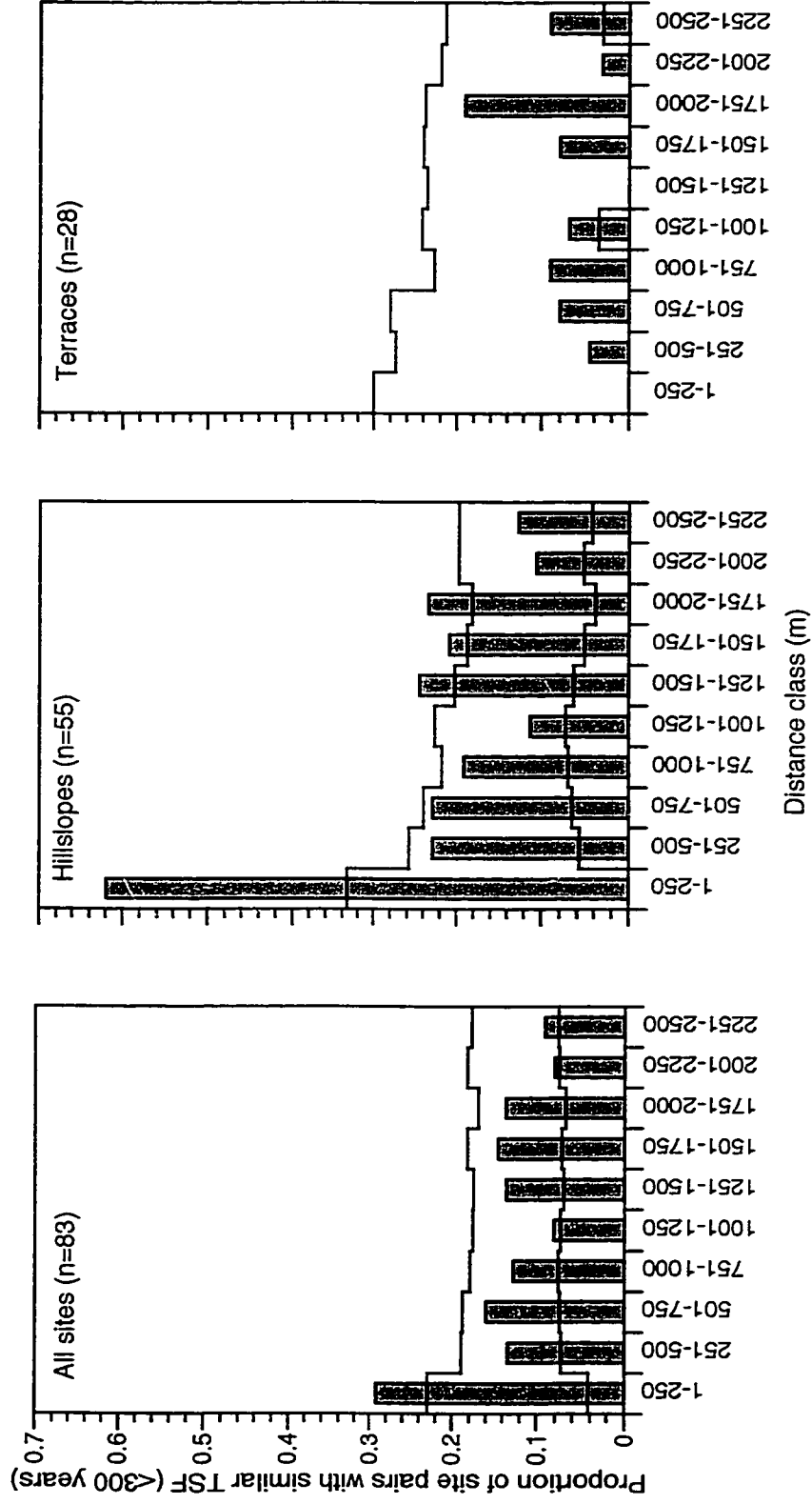


Figure 3.9 The proportion of all possible site pairs that have differences in time-since-fire < 300 years in non-overlapping distance classes. Solid lines indicate 95% confidence intervals based on 3999 Monte Carlo randomizations of time-since-fire among sites.

< 250 m. TSF was similar among sites at scales of 1250–2000 m suggesting an underlying regular pattern of fire in the study area, possibly due to the regular spacing of landforms that burned close to the same times. In contrast, no clumping of sites was observed on terraces, suggesting fire extent was rarely larger than the smallest distances between sites (100–250 m). However, sampling on terraces may have been too sparse to detect a strong spatial pattern at this scale.

Discussion

Obtaining fire history data from soil charcoal

Charcoal is ubiquitous and well preserved in the Clayoquot Valley, as it was found at nearly all of the targeted sites, sometimes occurring as large pieces embedded in highly weathered clay-enriched mineral horizons of podzols. The widespread occurrence of large and old charcoal pieces (> 0.5 mm; > 1000 years) is consistent with the observation that charcoal would not be fragmented by freeze-thaw cycles at this elevation (Carcaillet and Talon 1996). Furthermore, the poor correlation between charcoal abundance and TSF suggests that the controls of charcoal abundance are unrelated to time (e.g., *in situ* fragmentation) (Figure 3.4). Charcoal abundance in the Clayoquot Valley may be less affected by degradation processes than by random processes and controls operating at small spatial scales, such as the locations of large pieces of fuel and the effects of microtopography on local charcoal deposition.

Soil charcoal is most useful for reconstructing fire histories when the dates of charcoal pieces are in stratigraphic order (i.e., progressively older with increased soil depth). However, processes of soil genesis and disturbance sometimes disrupts this ideal situation (Carcaillet and Talon 1996). In mor organic horizons, which aggrade over time,

the uppermost piece of charcoal should date the most recent fire. Indeed, this study shows that pieces of charcoal located in the organic horizons closest to the soil surface were always the youngest charcoal encountered at a site (Figure 3.5). In contrast, the charcoal stratigraphy in the subsurface mineral horizons may be more complex because these horizons do not aggrade by continuous deposition of material. Soil mixing is a means of moving charcoal into the mineral horizon, and may explain the several instances of dating reversals found in this horizon by this study (Figure 3.5). An important mechanism that could move charcoal into mineral horizons is the action of tree tip-ups that can lift large root plates to a vertical position, greatly mixing the surface soil, leading to the incorporation of organic material into the mineral horizon and the eventual development of a new organic horizon (Bormann et al. 1995). Other mechanisms that could move charcoal into the mineral horizon include bioturbation from animal activity and roots burning *in situ* (Carcaillet and Thimon 1996).

Overall, the methods of site selection and prioritizing radiocarbon dates in this study were designed to assure a representative sample of the distribution of TSF in the study area. Sites were evenly spaced to capture the diversity and relative abundance of terrain and forest types in the study area. Because charcoal was located and dated at most of these sites regardless of the time elapsed since the last fire there was no bias introduced by excluding sites with a very long TSF due to the progressive loss of fire evidence, a common problem in tree-ring studies of fire disturbance (Fox 1989; Finney 1995; Weisberg 1998). Furthermore, in most cases, at least one of the radiocarbon dates at each site had a high likelihood of being from the most recent fire. Charcoal in the organic horizon (which most likely dates the most recent fire) or tree-ring dates were available at 44% of the sites. Although the remainder of the sites were dated by charcoal in the mineral horizon and thus represent a potentially less accurate estimate of TSF, the

increased number of dates at these sites (either by obtaining additional dates from the same core or from different cores) yielded similar fire dates 75% of the time (Figure 3.5). In all, only 25 sites were dated by a single date from the mineral horizon. It is reasonable to assume that additional sampling would have corroborated these single dates 75% of the time. Based on these results, ca. 90% of the sites represent sampling conditions that assure the most recent fire was dated with a high level of confidence.

Controls over fire extent

This study indicates that terrain features exert strong controls on fire susceptibility. Terrain controls are complex, operating both directly and indirectly on fuel moisture and fire behavior. First, the degree of slope affects fire behavior as fires on steep hillslopes preheat fuels upslope (by radiant energy and by updrafts) and propagate faster than fires on flat terrain (Agee 1993). Fires may also spread downslope at a fast rate if burning logs on steep slopes are dislodged during fire (Agee and Huff 1980; Chandler et al. 1983). Because lightning and fire ignitions are more common at higher than lower elevations (Pickford et al. 1980; Romme and Knight 1981; Fowler and Asleson 1984), spotting from burning logs rolling down steep slopes may be an important mechanism affecting fire occurrence at lower elevations. Second, terrain can indirectly affect fire susceptibility by controlling the insolation available for drying understory fuels. For example, August insolation on north-facing and south-facing hillslopes may be 30% and 115% of insolation on flat ground, respectively (Antonic 1998). Furthermore, major landform types may affect the canopy structure of forests and thus influence understory fuel moisture; for example, terraces may support productive forests with dense multi-tiered canopies, causing the understory on terraces to be moister than on less productive hillslope sites (Swanson et al. 1988). One would expect areas with low fire susceptibility

to occur on terraces due to a combination of slow rates of spread of fire and shading by dense canopies, and on north-facing hillslopes due to limited insolation. In contrast, the most fire-susceptible areas should be south-facing hillslopes with high insolation and more open canopies.

In the Clayoquot Valley, the clearest indication of the influence of terrain on the fire regime is the close association of fires with south-facing hillslopes during the last 600 years, and the co-occurrence of Douglas-fir trees at these sites (Figure 3.3; Figure 3.8). This finding supports conclusions based solely on the distribution of Douglas-fir (Schmidt 1960; 1970) that recent fires on western Vancouver Island were limited to well-drained and exposed south-facing hillslopes. Furthermore, the existence of isolated patches of Douglas-fir in the Clayoquot Valley suggest a long-term history of fire at such locations. Douglas-fir requires a seed source from local live trees to reestablish following disturbance, as the seed rain from non-local sources probably contains very little input from Douglas-fir. Therefore, for Douglas-fir to persist for multiple generations at a site, fires must reoccur locally at intervals within the typical life-span of the oldest trees, approximately 700–800 years (Franklin and Hemstrom 1981; Huff 1995). This suggests that the persistence of Douglas-fir in the Clayoquot Valley depends on the long-term existence of isolated fire-susceptible patches in the landscape. If more extensive Douglas-fir stands occurred during previous climatic periods of higher fire frequency (e.g., the early Holocene, see below), then it is possible that the modern stands are relicts of a former larger population (Schmidt 1970).

Many fires in the Clayoquot Valley could have been larger than that documented by this study if they were ignited at dry sites at higher elevations outside the study area and spread down slope in narrow bands (i.e., on exposed ridge-lines). This possibility is

supported by the spatial distribution of forest types within the watershed. Specifically, the cedar–salal forest was restricted to the highest hillslopes in the study area and consistently burned within the last 500 years (Figure 3.7), suggesting that extensive areas of this forest type at higher elevations may have a similar fire history, and may even have burned in the same fire events with the low elevation sites. Extending sampling to higher elevations would be necessary to determine the size of fires for this forest type at the scale of the whole watershed.

Similar to the pattern of recent fires, the evidence for very long TSF is strongly associated with terrain features. All sites that have not burned in over 6000 years were restricted to terraces and north-facing hillslopes. Most sites on such low-susceptibility terrain have not burned for more than 1000 years (Figure 3.8). Although north-facing hillslopes (i.e., $TII < 0.95$) and terraces have similar distributions of TSF (Figure 3.6), the large range in TSF at these sites may have resulted from two different processes. First, susceptibility to fire may vary within a given type of terrain. On terraces, for example, the Sitka spruce forest type had a much lower median TSF than the hemlock–fir or cedar–hemlock forest type (though not statistically significant; Figure 3.7), suggesting that the more open canopy of the Sitka spruce forest may have caused these sites to be more fire-susceptible than other terrace forest types with a denser and more uniform canopy (Lertzman et al. 1996). Second, the range of TSF on both terraces and north-facing hillslopes may have resulted from fire in adjacent high fire-susceptibility areas that infrequently spread into these low-susceptibility areas before extinguishing. Spotting and radiant heat from adjacent fires may cause fires to penetrate short distances into low-susceptibility terrain; thus fires may not always extinguish exactly at the transition from high- to low-susceptibility terrain types (e.g., Agee and Huff 1980).

If past fires affected stand composition and structure indirectly by reducing soil quality and nutrient pools, controls over fire may be even more complex than described above. In the Clayoquot Valley, the low productivity and stunted growth forms in the cedar–salal forest type may be an example of this effect. The productivity of this forest type has been explicitly addressed on northern Vancouver Island where low productivity appears to be due to low soil nutrient availability, possibly resulting from long periods without windthrow-caused soil turnover and competition by salal for available soil nitrogen (Keenan et al. 1996; Prescott et al. 1996). The Clayoquot Valley stands are younger (burned more recently), occur on steeper terrain, and have smaller stature than the north Vancouver Island stands (Prescott et al. 1996). Recurrent fires in these stand types at Clayoquot Valley would volatilize soil nitrogen and promote erosion on steep rocky slopes contributing to poorer stand and site conditions than at the north Vancouver Island stands (McNabb and Cromack 1990; McNabb and Swanson 1990). If past fires indirectly contributed to the structure of mature cedar–salal forest, this feedback mechanism might promote fire on such sites. Similar fire–vegetation–fire feedback mechanisms that affect soil fertility have been suggested in tropical (Goldammer and Siebert 1990) and other temperate (Lusk 1996) rain forest. Though it is common at the watershed or regional-scale, the cedar–salal forest type was not adequately sampled in this study because it was rare at low elevations in the study area. Further investigation may provide additional information on the long-term role of fire–vegetation feedback in this forest type.

Annual to decadal-scale controls of fire

Though only 15 recent fires were dated by tree-rings, two instances of synchronous fire at disjunct sites were identified (AD 1805 and ca. AD 1620). Such synchrony in fire is evidence that specific weather events influence fire occurrence (Swetnam 1993; Veblen

et al. 1999). The Clayoquot Valley fires may have been associated with atmospheric circulation patterns similar to those causing fires on the Olympic Peninsula, where several large lightning fires have been well studied (Huff and Agee 1980; Pickford et al. 1980). The Olympic Peninsula fires were ignited after more than three weeks without rain and grew rapidly during dry foehn winds flowing from east of the Cascade Mountains. These “east winds” usually occur when a high surface pressure system over the northeast Pacific moves inland to southern British Columbia, producing strong easterly or northeasterly winds that become warmer and drier when they descend the west slope of the Cascade Mountains (Washington) or Coast Range (British Columbia) (Agee 1993). Such high-pressure ridges may persist for weeks and block moisture-bearing onshore winds (Skinner et al. 1999). In addition, “dry lightning” (cloud-to-ground strikes without significant rainfall), which poses the greatest hazard for fire ignition, may occur when ground-level air masses are dry (Rorig and Ferguson 1999). Though rare along the Pacific coast, a single storm with dry lightning may cause multiple ignitions in its path (Agee 1993).

Climatic patterns that cause synchronous fires within a single watershed may also influence fires at a regional scale. Although old-growth Douglas-fir stands are thought to have originated from such episodic, widespread fire events associated with specific climatic periods (e.g., Sprugel 1991; Agee 1993), little is known about Douglas-fir stand establishment dates on a regional scale, and the best information available is only anecdotal. For example, Schmidt (1970) claimed to have identified eight major fire events after reconnaissance on Vancouver Island, two of which (AD 1610 and AD 1820) are similar to fire dates in the Clayoquot Valley. However, it should be noted that Schmidt (1970) and other studies in Washington (Henderson and Peter 1981; Hemstrom and Franklin 1982) and Oregon (Teensma 1987; Weisberg 1998) did not employ cross-

dating techniques (Stokes and Smiley 1996), limiting the ability to make regional comparisons of fire dates.

Centennial to millennial-scale controls of fire

In this study, frequency distributions of TSF provide coarse temporal information about variations in fire activity during the Holocene. Given the non-random spatial pattern of fire in the Clayoquot Valley, the typical use of TSF frequency distributions to estimate fire frequency is inappropriate (Lertzman et al. 1998). Interpretation of past fire regimes from the TSF distribution in the Clayoquot Valley is based on two assumptions. First, the probability of lightning ignitions did not vary greatly throughout the record. Second, extreme fire weather or long-term climate warming and/or drying could overcome topographic controls of fuel moisture, allowing fires to spread from high- to low-susceptibility areas. Such periods would be represented by the presence of charcoal on sites that seldom burned during cooler and/or wetter periods (Figure 3.10).

The cluster of sites with TSF between 11,000 and 9000 years BP were mainly on terraces, suggesting that climate conditions during the early Holocene made this landform more susceptible to fire than during more recent times (Figure 3.6). Paleoclimate models and empirical evidence support this interpretation. Orbital geometry at 10,000 years BP caused an 8% increase in summer insolation at a latitude of 50°N (Thompson et al. 1993). General circulation models for this period indicate that increased seasonality of solar insolation and the intensification of the subtropical Pacific high pressure system led to higher summer temperatures and increased drought in this region (Thompson et al. 1993). Abundant paleoecological evidence from the Pacific Northwest show drought in the early Holocene directly following the transition to Holocene climate at 11,200 years BP

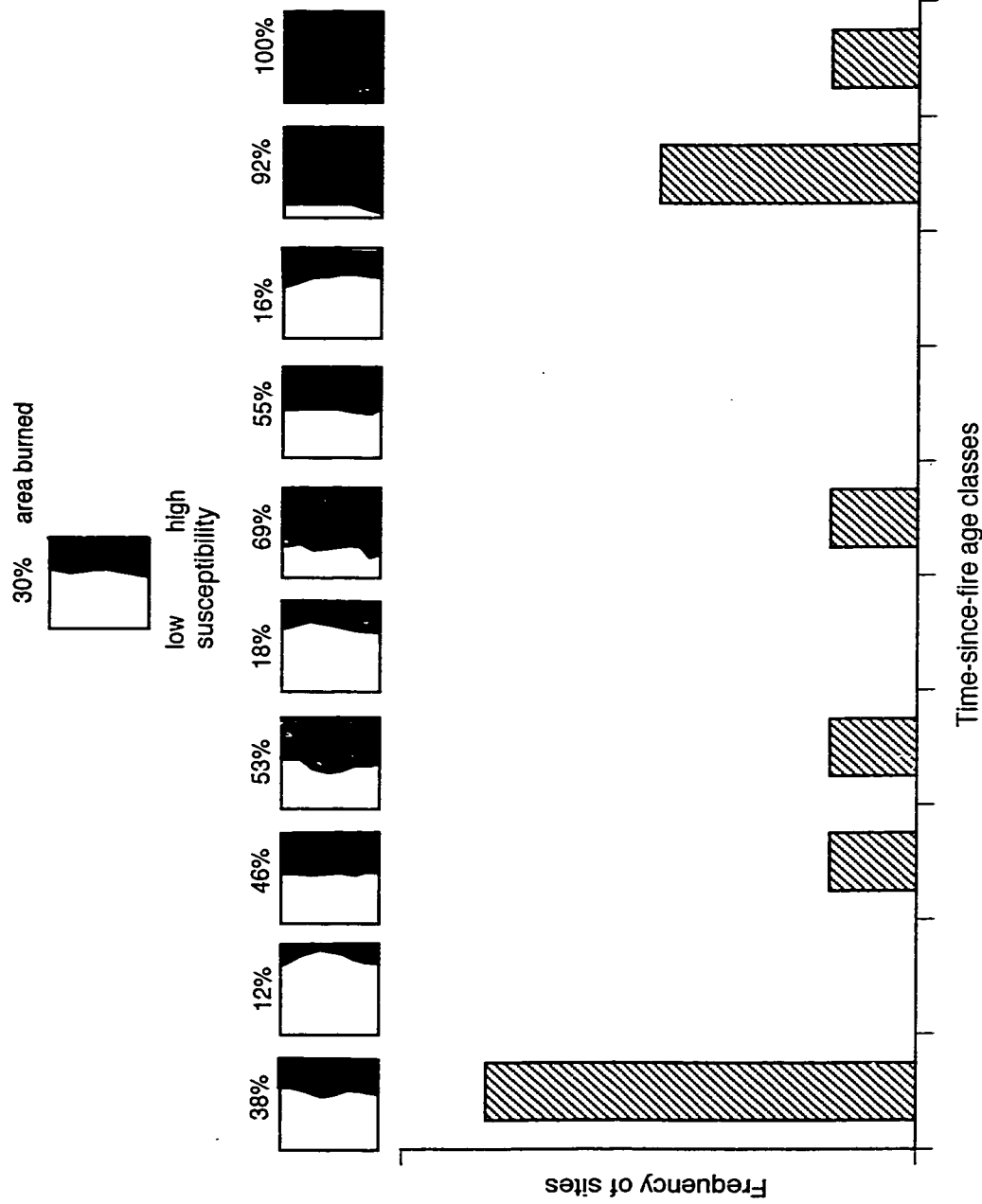


Figure 3.10 Schematic showing how a time-since-fire distribution may form in areas with a wide range in fire susceptibility. This interpretation assumes the probability of ignition did not vary greatly over time, and the maximum extent of fire into low-susceptibility areas is controlled by the severity of fire weather. Small maps show the extent of fire into low-susceptibility areas. Only periods when fires burned into low-susceptible areas to a greater extent than all subsequent periods are represented in the time-since-fire frequency distribution.

(10,000 radiocarbon years BP; Whitlock 1992). For example, pollen records from low elevation sites in southwest British Columbia and the Olympic Peninsula indicate the dominance of Douglas-fir and red alder, both of which require disturbance for regeneration in areas west of the Cascade Mountains (Mathewes 1973; Heusser 1977; McLachlan and Brubaker 1995; Heusser et al. 1999). Forest structure may have also aided fire spread during the early Holocene, as a greater proportion of Douglas-fir would have allowed more light penetration to the understory compared to modern cedar-hemlock forests (Frazer et al. 2000), enhancing the drying of woody fuels.

A second period of high fire activity, though not as strong as in the early Holocene, occurred ca. 3000–2000 years BP (Figure 3.6). This period overlaps with a period of increased fire activity ca. 2200 years BP found in high-resolution lake-sediment charcoal records from the lower Fraser River (southwest British Columbia) and the Olympic Peninsula (D. Hallett, Simon Fraser University, *personal communication*; L. Brubaker, University of Washington, *unpublished data*). However, other paleoclimate evidence suggests this period was the beginning of a cool and wet neoglacial period. For example, many paleoecological studies in the Pacific Northwest show that cooler and wetter conditions began by 3000 years BP (Dunwiddie 1986; Hansen and Engstrom 1996; Pellatt et al. 1998). In addition, evidence of glacial advances from the British Columbia Coast Range suggests cool and moist climate that would not favor fires 3500–1800 years BP (Ryder and Thompson 1986) or 2800–2200 years BP (Clague and Mathewes 1996). The apparent contradiction between these records and the fire records may in part reflect differences in the sensitivity of these records to climatic change. Pollen records typically are of coarse temporal resolution and vegetation change may lag several centuries behind climatic change (e.g., Davis 1986). Similarly, geological evidence of glacial fluctuations (e.g., dates of terminal moraines) is discontinuous and represents a change in climate at

decadal-scales or longer (Porter 1986). In contrast, fire occurrence is much more sensitive to climatic change in general and short-term climatic anomalies in particular, as large fires may occur after a drought of only one month (Pickford et al. 1980). Considering that climate may change substantially within a 1000-year period, a range of climatic trends may have occurred during 3000–2000 years BP. For example, a generally cool and moist climate may have been punctuated by brief periods of favorable fire weather, or relatively long periods of fire weather may have alternated with periods conducive for glacial advances. Unfortunately, the errors associated with radiocarbon dates of soil charcoal precludes the identification of any such intervals in this study.

Role of fire in the landscape dynamics of coastal temperate rain forest

Recent studies (Lertzman and Fall 1998; Heyerdahl et al. *in press*) have emphasized that fire regimes are affected by small-scale terrain features (bottom-up controls) operating within the context of the large-scale (regional) variation in climate (top-down controls). The present study demonstrates that top-down controls have a temporal component, fluctuating with millennial-scale climatic change (Lertzman and Fall 1998). During the early Holocene, bottom-up controls of topography on fuel moisture and stand structure, which are strong under the present climate, were overcome by substantially different top-down controls (i.e., the climate regime), causing fires to be more common on terraces and north-facing hillslopes than in recent centuries. In contrast, during the late Holocene, bottom-up controls of topography effectively limited the extent of fire, so that these types of sites were less often burned. Bottom-up controls also appear to be responsible for the modern mosaic of sites with forest-structural evidence of fire (i.e., Douglas-fir trees, even age classes, and/or cedar–salal forest types), as this evidence was found at the majority of sites that burned in the last 600 years (Figure 3.6).

The present study confirms earlier reviews that suggest recent fires in the coastal temperate rainforest have been mostly restricted to steep south-facing hillslopes (Schmidt 1970; Veblen and Alaback 1996). The results also indicate that a large proportion of low elevation forest has not burned for the last 6000 years. Such remarkably long fire-free intervals have rarely been documented in any forest type worldwide (e.g., Clark and Royall 1996; Kershaw et al. 1997), and have important implications for long-term forest dynamics and regional forest patterns. First, in the absence of other large-scale disturbances, forest composition probably tracked Holocene climatic change primarily through processes of gap-replacement. Species turnover would have occurred through the differential success of shade-tolerant species recruiting into canopy gaps under a given set of climatic conditions (Lertzman 1992; Gray and Spies 1996). Due to the longevity of Pacific Northwest conifer species, compositional changes through gap replacement would have lagged Holocene climatic change by several centuries (Lertzman 1995). Secondly, the absence of recent fire at many sites suggests that old-growth forest structures also predominated on landscapes throughout the late Holocene. This landscape pattern contrasts sharply with forests east of the Vancouver Island Range as well as the majority of forests in the Pacific Northwest, which were dominated by seral Douglas-fir, indicative of recent large fires (Franklin and Dyrness 1988). This study, therefore, supports the distinction of the coastal temperate rain forest as affected by a fundamentally different disturbance history than the large remainder of Pacific Northwest forests.

CHAPTER 4: AN 1800-YEAR RECORD OF THE SPATIAL AND TEMPORAL DISTRIBUTION OF FIRE FROM THE WEST COAST OF VANCOUVER ISLAND, CANADA

Introduction

Spatial variability in the susceptibility of forests to fire is an important aspect of fire regimes, especially in mountainous areas with steep topography and a range of aspects (Romme and Knight 1981; Agee 1993; Turner and Romme 1994; Camp et al. 1997; Heyerdahl et al. *in press*). Similarly, temporal variability in fire frequency is an important aspect of fire regimes, especially during periods of significant climatic or land-use change (Clark 1988c; Swetnam 1993; Kitzberger et al. 1997). These components of variability in fire regimes interact, contributing to the mosaic of age classes in the modern landscape (Shinneman and Baker 1997; Lertzman and Fall 1998). For example, a change in the landscape-level fire frequency would affect the landscape mosaic uniformly if fires were randomly distributed, or patchily if fires preferentially burned certain areas (Clark et al. *in press*). Despite the spatial and temporal variability inherent in fire regimes, few studies adequately address both of these aspects because long-term data on the spatial pattern of fires are difficult to obtain (Niklasson and Granstrom 2000).

Measuring the spatial pattern of fire over long time scales is a particularly difficult challenge in forests that usually experience stand-replacing fires. The two main approaches to studying fire history in such forest types view the fire regime differently. The stratigraphy of macroscopic charcoal particles in lake sediment preserves a history of fire events (discernible peaks of charcoal) over thousands of years, but this method aggregates evidence of fires in the vicinity of the lake (Clark 1990; Millspaugh and

Whitlock 1996). In contrast, tree-ring evidence (stand ages and fire scars) records fire dates at specific points, but the temporal span of this method is limited by tree ages (Arno and Sneek 1977; Johnson and Gutsell 1994). Radiocarbon dating of soil charcoal could potentially record the spatial pattern of fire over long time scales, but soil mixing and the consumption of organic soils by fire usually limit this method to estimating the date of the last fire (Chapter 3; Hopkins et al. 1993; Carcaillet and Talon 1996). No single method effectively estimates both the spatial pattern of fires and their long-term frequency. To overcome the limitation of stand-age data to estimate fire frequency, several fire history studies have used statistical models (e.g., Johnson and Gutsell 1994; Reed et al. 1998), though such models often make unrealistic assumptions about the spatial and temporal distribution of fire events (Lertzman et al. 1998; Huggard and Arsenault 1999). Few studies have used both the sediment charcoal method and the stand age method in the same area to deduce the long-term spatial distribution of fires (Clark 1990).

The use of high-resolution charcoal records from lake sediments to reconstruct fire history has advanced rapidly in recent decades (e.g., Clark 1988a; Long et al. 1998). However, substantial questions remain regarding the spatial scale represented by sediment records. Implicit in the sediment charcoal method is the assumption that most charcoal disperses aurally to the lake surface from a certain source area around the lake, with the size of this source area depending on the size of charcoal particles, because small pieces are convected greater distances than are large pieces (Clark 1988b; MacDonald et al. 1991; Clark et al. 1998; Ohlson and Tryterud 2000). Once dispersed to the lake surface, winds may cause charcoal to be deposited and resuspended in the littoral zone, though mixing in the surface water eventually transports charcoal to the profundal zone (Whitlock et al. 1997). Thus, charcoal must only disperse to the lake edge to be recorded

in sediments at the lake center. More detailed knowledge of the extent of the charcoal source area is needed because fire frequency must be interpreted at the scale in which fires are occurring; in a given forest, a large charcoal source area could record more fires and result in higher fire frequency than a small source area. Despite the importance of determining the charcoal source area for the interpretation of fire frequencies, few studies have explicitly addressed the charcoal source area for particular size classes of charcoal (Clark and Royall 1995; Earle et al. 1996; Whitlock and Millspaugh 1996). In this study, fire dates in a sediment core were compared to fire dates at points at varying distances from the lake to calibrate the charcoal source area and evaluate the spatial pattern of fire.

The overall goal of this study is to better understand the spatial and temporal dynamics of fire disturbance in a coastal temperate rain forest on the west coast of Vancouver Island (British Columbia, Canada). In a previous chapter I investigated the time-since-fire over a network of sites, using tree-ring dates at 18 sites and radiocarbon dates of soil charcoal at 65 sites. That study showed that terrain features and vegetation type have greatly influenced the fire regime (Chapter 3). In the study area, nearly all exposed south-facing slopes burned within the last 800 years; in contrast, several terrace and north-facing sites have not burned in the last 6000 years. This landscape pattern suggests that there is spatial variability in fire frequencies, though the frequency of fire at any one location could not be determined due to the erasure of past fires by the most recent fire (Weisberg 1998). In this chapter, I use these spatially-precise records of the most recent fire in conjunction with charcoal in a lake sediment core as a spatially-aggregated record of all fires within a specific charcoal source area. These data may therefore show if fire frequency was sensitive to known past climate variability, and if fire frequencies varied in relation to terrain controls on fire susceptibility.

The major objectives were to

1. Determine fire dates in the vicinity of the lake by using a spatially aggregated record of fire dates from charcoal accumulation in lake sediment,
2. Determine the area near the lake within which fires are recorded as peaks in sediment charcoal by using point estimates of fire dates from tree-ring records and radiocarbon dates of soil charcoal, and
3. Determine the degree to which fires were more likely to occur in high fire-susceptibility relative to low fire-susceptibility areas near the lake by using a combination of both fire records.

Clayoquot Lake study area

Clayoquot Lake on the west coast of Vancouver Island was formed by an alluvial fan that dams a narrow section of the Clayoquot River Valley (Figure 4.1). A 45-m wide channel connects two basins: a sub-rectangular upper basin (19.2 ha) and a circular lower basin (27.8 ha). Topography around the lake is steep (20–40% slopes) rising from 17 m to 900 m at the top of ridges; a 300 m cliff borders the upper basin. The inflowing Clayoquot River drains ca. 6500 ha upriver. Several times each winter, rain storms cause flooding in a restricted floodplain, typically causing the lake level to rise ca. 1.0 m (maximum observed in 10 years = ca. 3.0 m) (Clayoquot Biosphere Project, unpublished data). A description of the climate, forest types, and soils of the lower elevations of the Clayoquot Valley is given in Chapter 3: *Study area*.

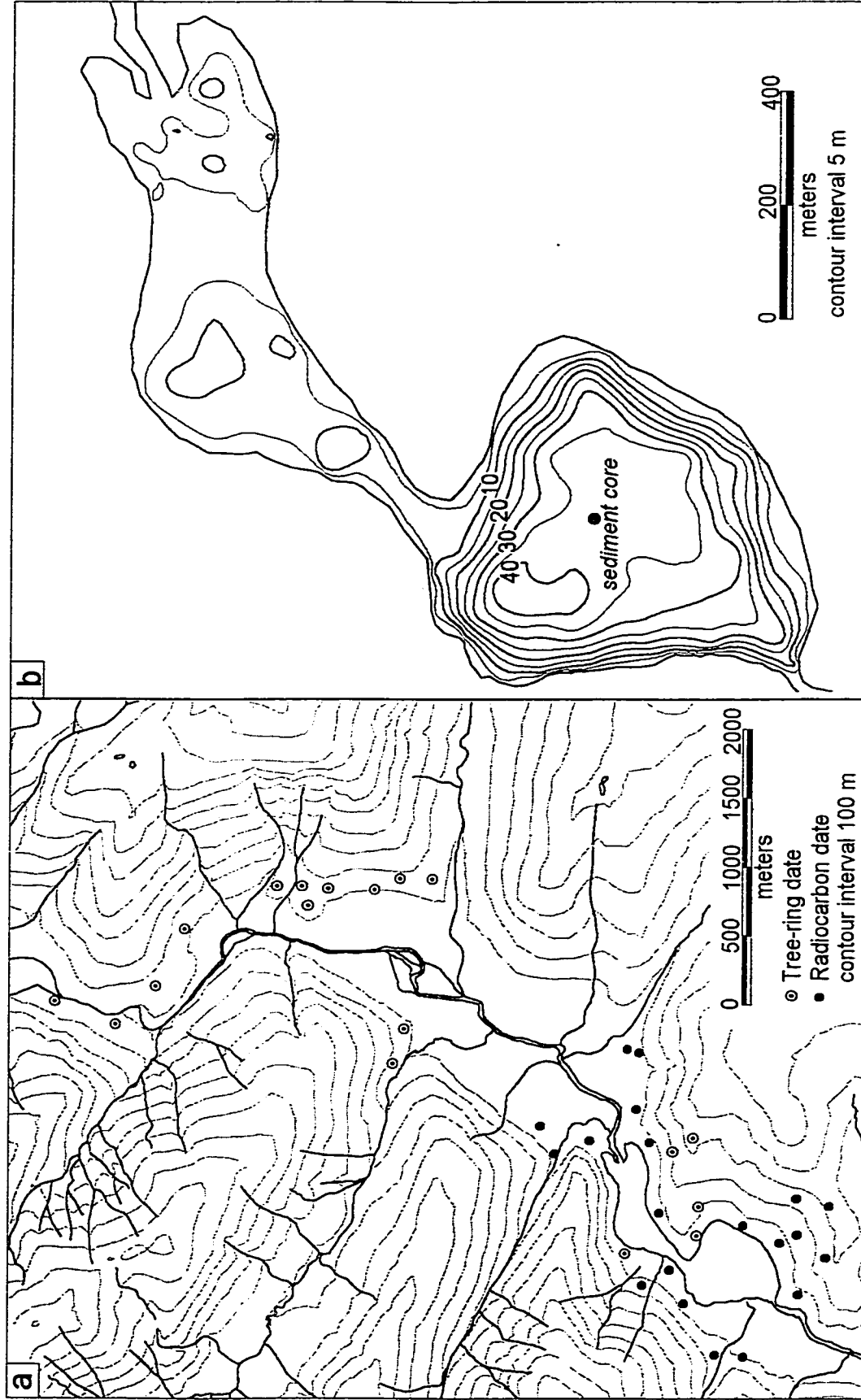


Figure 4.1 a. The study area showing the fire history sampling sites used in this chapter (see Figure 3.2 for all sites and site codes). b. Bathymetric map of Clayoquot Lake.

Methods

Rationale

To describe temporal trends in fire frequency, a lake sediment record was analyzed to reconstruct all the fires that occurred near the lake. To describe how fire frequency varied among areas near the lake, point estimates of fire near the lake were used to place spatial boundaries on the location of the fires detected in the sediment record. The spatial boundaries of fires were determined in two ways: 1) fire dates at points near the lake were associated with dates of charcoal peaks in the sediment core to determine the source area that contributes to large charcoal peaks, and 2) the dates of last fire at points near the lake were mapped to determine whether portions of the charcoal source area escaped all of the fires detected in the sediment record. This combination of approaches reveals whether the fires detected in the sediment record were restricted to a portion of the charcoal source area, in which case fire frequencies would range from zero to high values within different parts of this area. Such differences in fire frequencies could result from terrain-controlled differences in hazards of burning (i.e., probability of fire; Johnson and Van Wagner 1985) over the landscape. To assess the degree to which the hazard of burning varies over the landscape, the fire-hazard ratio, ratio of the probability of burning in two mutually exclusive areas, was calculated. A fire-hazard ratio of 10 would indicate that fire is 10 times more likely to occur in a portion of a study area, causing some areas to escape fire when fire frequency is high in other areas on the landscape. Similarly, a fire-hazard ratio of 1 would indicate that fire occurs randomly over the landscape.

Spatially precise fire dates – tree-ring and soil-charcoal samples

The date-of-last-fire (DLF) was estimated at 25 sites within 500 m of Clayoquot Lake. Site selection and sampling for fire history are described in detail in Chapter 3 (*Methods*). Sampling was limited to elevations below 200 m with the exception of a single ridge where four sites were located at elevations of 200–350 m. DLF was estimated from tree-ring dates of fire or from calibrated radiocarbon dates of soil charcoal (calibrations following Stuiver and Reimer 1993 and Stuiver et al. 1998). Tree-ring records of fire > 1000 m upstream were also used to test whether the charcoal sediment stratigraphy recorded fires at larger distances from the lake through fluvial transport of charcoal.

Radiocarbon dates of the DLF may overestimate the true DLF for two reasons. First, the charcoal from the most recent fire may not be located and dated at each site. The assessment of this error (Chapter 3) suggests that, for a large majority of cases, charcoal from the most recent fire was recovered and dated. Second, the charcoal selected for dates may have been formed from wood that is several centuries old at the time of the fire. Although this “inbuilt age” was found to be up to 670 years (Chapter 2), this bias does not affect the coarse temporal scale evaluation of DLF used in this study.

I constructed a map of DLF for the area within 500 m of the lake edge, assuming that this area encompasses the area that contributes charcoal to the lake through airfall of large pieces or through slope wash from steep slopes above the lake (Clark 1988b; Clark and Royall 1995; Whitlock and Millspaugh 1996). I did not include small areas of bare rock, unsampled floodplain forest, and a portion of the area that drains to the outflowing river. Fire boundaries were determined using Thiessen polygons around sample points (Okabe et al. 2000). I modified polygon boundaries to coincide with natural fire breaks (sharp

ridges and rivers) or distinct changes in forest composition discernible on aerial photographs.

Spatially aggregated fire dates – lake sediment core

Coring and sediment chronology I made a bathymetric map of Clayoquot Lake by surveying transects with an electronic depth sounder and interpolating the mapped data using a spline fit (Figure 4.1). The lower basin was cored in 38 m of water using a percussion corer constructed of 7.6 cm diameter PVC tubing (Reasoner 1993). The core was split lengthwise in the laboratory and contiguous subsamples (ca. 12 ml) were taken at 1 cm intervals from the center of one core-half. ^{210}Pb activity was measured from 20 subsamples from the top 86 cm to date the most recent ca. 200 years of sediment. The remainder of the core was dated with 10 radiocarbon dates on conifer needle samples. I calibrated radiocarbon dates to the calendar time scale (Stuiver and Reimer 1993) using the INTCAL98 calibration curve (Stuiver et al. 1998). Two radiocarbon dates (CAMS-44475 and CAMS-44480) were distinct outliers and were rejected. I assigned the age-depth curve using a cubic spline fit through the ^{210}Pb dated portion and a radiocarbon date at 120 cm, and an ordinary least-squares linear regression for the lower portion of the core.

Laboratory analysis I measured each ca. 12 ml subsample of sediment for magnetic susceptibility, charcoal and macrofossils. Magnetic susceptibility is a measure of iron-bearing minerals that, in lake sediments, is interpreted as an indicator of erosion of mineral soil or fire-created magnetite or maghemite (Thompson and Oldfield 1986). I used volume-specific magnetic susceptibility as a measure of the relative quantity of iron-bearing minerals. The volume of each subsample was measured to the nearest 0.1 ml,

soaked overnight in a 10% sodium hexametaphosphate solution to disperse the sediment, and sieved through 0.5 and 0.15 mm screens using a gentle flow of water. I treated the 0.15–0.5 mm size fraction with 6% hydrogen peroxide for 8 hours to bleach non-charcoal organic material and facilitate charcoal identification (Rhodes 1998). All charcoal was tallied using a binocular microscope (10x–40x). I identified all macrofossils (conifer needles and seeds) in the > 0.5 mm size fraction under a binocular microscope using a modern reference collection and published keys (Dunwiddie 1985; Young and Young 1992). Needle fragments were combined and expressed as needle equivalents and *Thuja* and *Chamaecyparis* branchlets were tallied individually following Dunwiddie (1987).

Charcoal record analysis Charcoal concentrations (pieces cm⁻³) were expressed as charcoal accumulation rates (CHAR; pieces cm⁻² year⁻¹) based on sedimentation rates estimated by ²¹⁰Pb and radiocarbon dates. High variability in CHAR in the top 80 cm of the core reflects high sedimentation rates (ca. 0.4 cm year⁻¹) and low charcoal counts (0–11 pieces per subsample). To make this portion comparable to the remainder of the record, I smoothed the charcoal concentrations for the top 80 cm using a locally-weighted regression (LOWESS; Cleveland 1979) with a 10-year sample window.

Finely-sampled lake sediment records may reveal local fires as distinct peaks in CHAR (e.g., Clark 1988a). Several recent studies have examined peaks in CHAR using a two-step procedure: 1) determine a low frequency background component and calculate a peak component as positive deviations in CHAR from the background levels, and 2) apply a threshold to the peak component that distinguishes peaks due to local fires from peaks due to analytical noise and/or extra-local fires (Long et al. 1998; Millspaugh et al. 2000). The background component may vary over time due to changes in regional fire activity, changes in the local hydrological regime that transports charcoal, or changes in

forest structure and biomass that affect fire behavior and the total quantity of charcoal produced in a fire (Long et al. 1998). Previous studies have modeled the background component using a Fourier transform filter (Clark and Royall 1996) or a LOWESS filter (Long et al. 1998; Millspaugh et al. 2000) that smooth the CHAR record within a specified sample window. Both of these methods allow the size of charcoal peaks to influence the estimated background component. As a result, the background component may be locally elevated and bisect charcoal peaks or pass over small peaks located between larger peaks. Exploratory analysis using both methods suggested there was not a satisfactory compromise between the use of a wide sample window that emphasized large peaks but precluded detection of distinct small peaks located between larger peaks and a narrow sample window that caused the background component to follow the high frequency so closely that small peaks were recognized but the magnitude of large peaks was underestimated.

In this study I used a new approach based on the assumption that the best estimate of the background component is the minimum CHAR value within a temporal window that is equivalent to the duration of approximately one charcoal peak. In this approach, the background component is unaffected by peak height (see also Millspaugh and Whitlock 1995), and the potential for detecting relationships between peak height (magnitude of peaks over the background) to characteristics of the local fire is improved. Careful evaluation of the Clayoquot Lake CHAR record suggests that most peaks span 20–30 years, similar to those observed in a study of modern charcoal accumulation following fire (Whitlock and Millspaugh 1996). Because the time interval represented by each 1-cm subsample varied over the length of the core due to changing sedimentation rates, I first interpolated the CHAR record to 2-year intervals (Long et al. 1998), and from these values, I calculated the minimum CHAR values in 20-, 26-, and 32-year moving

windows. I then smoothed each series of minimum values with a LOWESS filter using a sample window width equal to the window used to calculate the minimum CHAR values. I chose a background curve using a 26-year sample window because it did not follow peaks too closely (20-year sample window) and it did not miss the base of several distinct peaks (32-year sample window). I calculated the peak component as the residuals from this curve.

The peak component of the CHAR record contains a range of peak heights, of which only the large peaks should relate to local fires. A threshold value of the peak component used to distinguish peaks due to local fires was determined by examining the sensitivity of the number of fires detected while varying the threshold (Clark et al. 1996). Increasing the threshold should reduce the number of detected fires because small peaks drop below the threshold values. If local fires are represented by charcoal peaks that are significantly larger than all other charcoal peaks, then a large range of threshold values would result in an identical set of charcoal peaks qualifying as local fires. In this case, the distribution of charcoal peak heights should contain several large peaks from local fires, many small peaks from extra-local fires and analytical noise, and relatively few medium peaks (Clark et al. 1996). I chose a threshold value that occurred within a range that had little sensitivity to the number of peaks detected.

I compared the charcoal, magnetic susceptibility, and macrofossil records to determine if peaks in CHAR were associated with local soil erosion events. Peaks in magnetic susceptibility may be related to erosion of mineral soil following fires within the local lake catchment (Thompson and Oldfield 1986; Millspaugh and Whitlock 1995). Likewise, peaks in macrofossil input may be related to erosion of soil surficial material or needle drop from fire-killed conifers. Each record was compared visually and correlation

coefficients were calculated for a range of lag times (-50 to +50 years). Before the calculation of correlation coefficients, accumulation rates were calculated for magnetic susceptibility (EMAR; electromagnetic units $\text{cm}^{-2} \text{year}^{-1}$) and macrofossils (MFAR; needle equivalents $\text{cm}^{-2} \text{year}^{-1}$). In addition, background components for the MFAR and EMAR records were calculated using the same methods used for the CHAR record, though the EMAR record varied more slowly over time and therefore background was calculated with a 50-year moving window. Correlation was examined separately for the peak components and background components. For the calculation of correlation coefficients, the period of very high sedimentation rates (0–80 cm depth) and thus very high EMAR and MFAR was removed from each record.

Estimate of the charcoal source area

Theoretical and empirical studies of charcoal dispersal suggest that the quantity of charcoal dispersed by convection during a fire should decrease rapidly with increasing distance from the fire, especially for the large size class (0.15–0.5 mm) of charcoal that was analyzed in this study (Clark 1988b; Clark et al. 1998). Slopewash may also transport charcoal at local scales, though this mechanism is probably limited to steep slopes that drain to the lake. In addition to these transport mechanisms, fluvial transport of charcoal from the Clayoquot River may significantly increase the charcoal source area for Clayoquot Lake. Given the two potential categories of charcoal transport at Clayoquot Lake (air and slope wash versus fluvial), I assessed the charcoal source area by examining the correspondence of charcoal peaks in the sediment record with evidence of fires (Chapter 3) from transport by air or slopewash (< 500 m from the lake) and from fluvial transport from the Clayoquot River (> 500 m upriver). To test if charcoal is transported large distances in the Clayoquot River, tree-ring fire dates (Chapter 3) from

sites > 500 m up the river and < 500 m from the lake edge were compared with the date of the closest charcoal peak in the sediment core. I calculated the number of years between each tree-ring date and the closest date of a CHAR peak to identify if charcoal peaks are better matched with local or upriver fires. To test if charcoal is transported at distances < 500 m, I assessed the charcoal source area by comparing the CHAR peak heights with the distance-to-lake of corresponding fires. Specifically, I matched fires determined by soil charcoal or tree-rings to the maximum value of the CHAR peak component in the sediment core within 50 years of the fire date and used regression to evaluate whether peak height decreases with distance of the corresponding tree-ring or soil charcoal sample site to the lake. This method may not capture the actual proximity of older fires to the lake if more recent fires obscured the actual extent of these fires. Therefore, because the proximity of fires to the lake is more reliably estimated for recent fires than for older fires, I tested the relationship between peak height and distance-to-lake separately for the most recent fires (after AD 1100) and for all fires.

Comparing spatially precise and spatially aggregated fire records

The objective of this part of the study was to estimate the range of the hazards of burning near the lake for agreement between the sediment record and the map of DLF. The map of DLF was used to calculate the area within the estimated charcoal source area (250 m from lake edge, see *Results*) that had burned at least once over the length of the sediment record. The burned and unburned areas over this period are denoted as A_s and A_r , comprising s and r proportions of the landscape, respectively ($s+r=1$). Therefore, all fires detected in the sediment record occurred within the area A_s , and not in the area A_r . If one assumes that the hazards of burning (i.e., probability of burning) λ_s and λ_r (in areas A_s and A_r , respectively) are equal, lightning strikes are randomly distributed in the study

area, and fires do not spread between A_s and A_r , the probability (E) of the observed outcome (i.e., that all fires occurred in A_s) is

$$E = \left(\frac{A_s}{A_s + A_r} \right)^F = s^F \quad (1)$$

where F is the number of fire events detected in the sediment core. However, a more realistic scenario is that λ_s is greater than λ_r , reflecting an intrinsic difference between A_s and A_r in susceptibility to fire due to vegetation and terrain. The fire-hazard ratio, $b = \lambda_s/\lambda_r$, may be interpreted as the factor that represents the increased probability that lightning leads to fire in A_s than A_r . An alternative interpretation of b is that all lightning strikes and fire starts occur in A_s and fires have a $1/(b+1)$ chance of spreading into A_r . Regardless of which set of assumptions is more appropriate, b is a measure of the nonrandom occurrence of fire between these areas. The fire hazard ratio may be incorporated into equation 1:

$$E = \left(\frac{bA_s}{bA_s + A_r} \right)^F = \left(\frac{bs}{bs + r} \right)^F \quad (2)$$

Solving equation (2), the fire-hazard ratio for a given probability (E) of the observed outcome is

$$b_E = \frac{r}{s \left(E^{-\frac{1}{F}} - 1 \right)} \quad (3)$$

I calculated b_E for the entire period covered by the lake sediment record and for the last 800 years.

This method only considers the location of fire between two areas; the exact locations and sizes of individual fires were not modeled. Since the goal of this analysis was to examine the spatial distribution of fire at a very coarse scale, this non-spatial approach required fewer assumptions and was less complicated to interpret than approaches such as a spatially explicit simulation model (e.g., Boychuk et al. 1997).

Macrofossil record

I analyzed the macrofossil record to interpret vegetation history. To remove high frequency variation that was probably an artifact of the small sample size in each subsample, I interpolated needle concentrations to 2-year intervals and smoothed the record using a LOWESS filter with a 100-year sample window. Past changes in the composition of the major tree species near the lake was assessed from the relative abundance of macrofossils in the smoothed record.

Results

Tree-ring records and radiocarbon dates of soil charcoal

DLF at 25 sites within 500 m of the lake ranged from BC 6490 to AD 1886 (Figure 4.2). In general, north-facing slopes bordering Clayoquot Lake have not burned since at least AD 200. In contrast, all south-facing slopes have burned since AD 1800. There were two instances of adjacent sites having identical fire dates (AD 1805 and BC 400) and in one instance four adjacent sites had very similar dates of ca. AD 1000. Based on polygon

boundaries, 63% of the area within 500 m of the lake burned at least once during AD 200–present, and 22% burned at least once during AD 1200–present. For a smaller area within 250 m of the lake, these proportions changed very little (56% and 21%, respectively).

Lake sediment core

Core description The 315-cm, 1800-year, sediment core consisted of uniform brown gyttja with abundant macrofossils. The sedimentation rate was fast (ca. 0.43 cm year⁻¹) in the ²¹⁰Pb-dated portion of the core (0–86 cm), slowed considerably between ca. 86–120 cm (ca. 0.09 cm year⁻¹), and was constant (ca. 0.16 cm year⁻¹) for the lower two-thirds of the record (120–315 cm) (Table 4.1; Figure 4.3).

The charcoal, macrofossil, and magnetic susceptibility records show broadly different trends (Figure 4.4). Charcoal counts ranged between 0 and 122 pieces per subsample (median = 14). The CHAR record had distinct peaks composed of 2–4 subsamples (Figure 4.4). The CHAR record varied significantly over time, with a period of large peaks (ca. 1.0 pieces cm⁻² year⁻¹) and high background levels (ca. 0.6 pieces cm⁻² year⁻¹) during AD 400–800, and a period of few peaks (ca. 0.3 pieces cm⁻² year⁻¹) and low background levels (ca. 0.1 pieces cm⁻² year⁻¹) during AD 1100–1600. The period AD 1600–present is marked by three large peaks. Macrofossil counts in each subsample ranged between 0 and 59 needle equivalents (median = 5.75; total in core = 2567). MFAR varied greatly between adjacent samples, with occasional large peaks (ca. 0.3 needle equivalents cm⁻² year⁻¹) in the period AD 200–1300, but few between AD 1300–1800. Background levels of MFAR were low throughout the record (ca. 0.05 needle equivalents cm⁻² year⁻¹) except after AD 1800, when MFAR increased sharply with

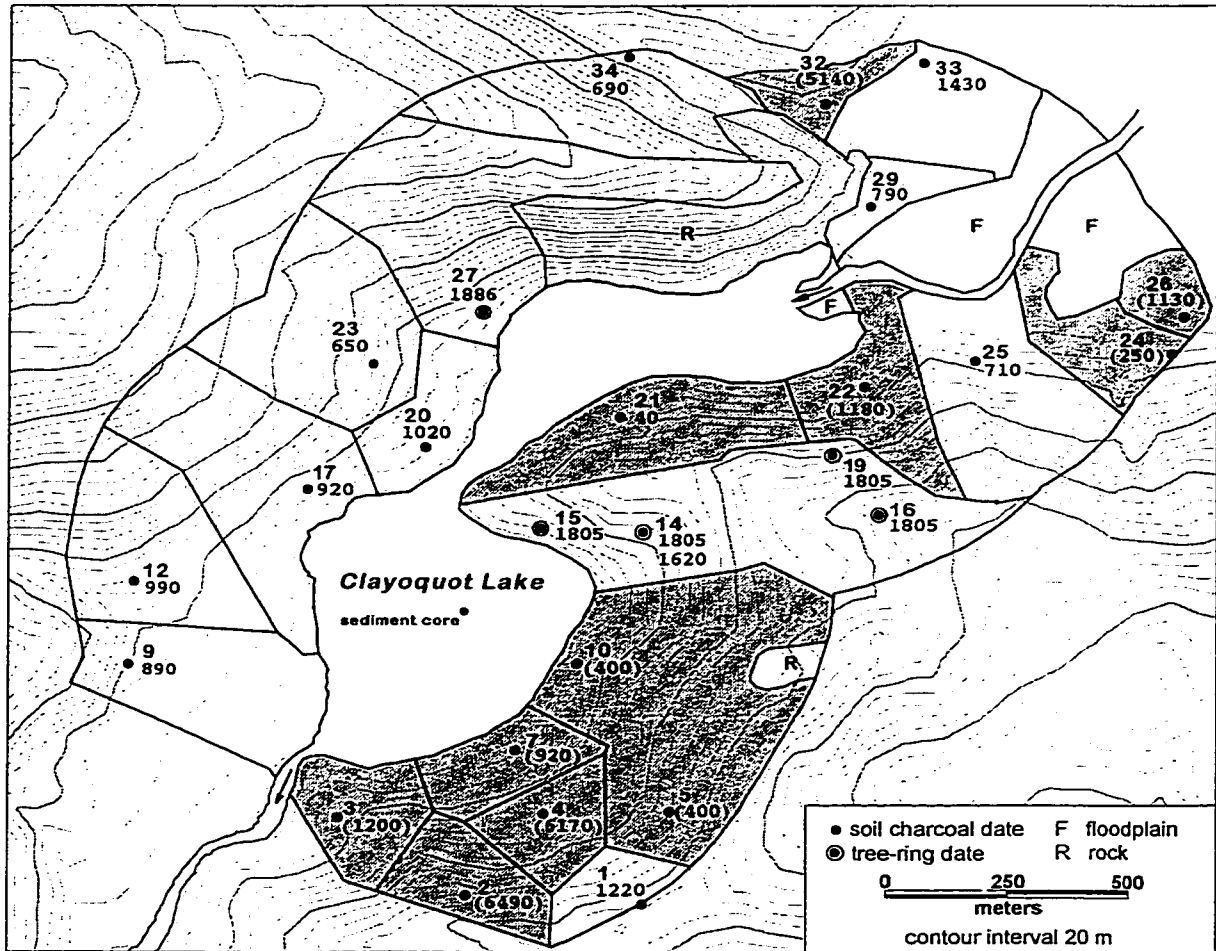


Figure 4.2 Date-of-last-fire map for the area within a 500 m buffer around Clayoquot Lake and parts of the Clayoquot River immediately upstream. Upper numbers in each polygon are site codes (Table 3.2). Lower numbers are the date of the last fire in years AD (BC in parentheses). Shaded polygons represent areas that have not burned since AD 200. Note that two tree-ring fire dates were obtained at site 14.

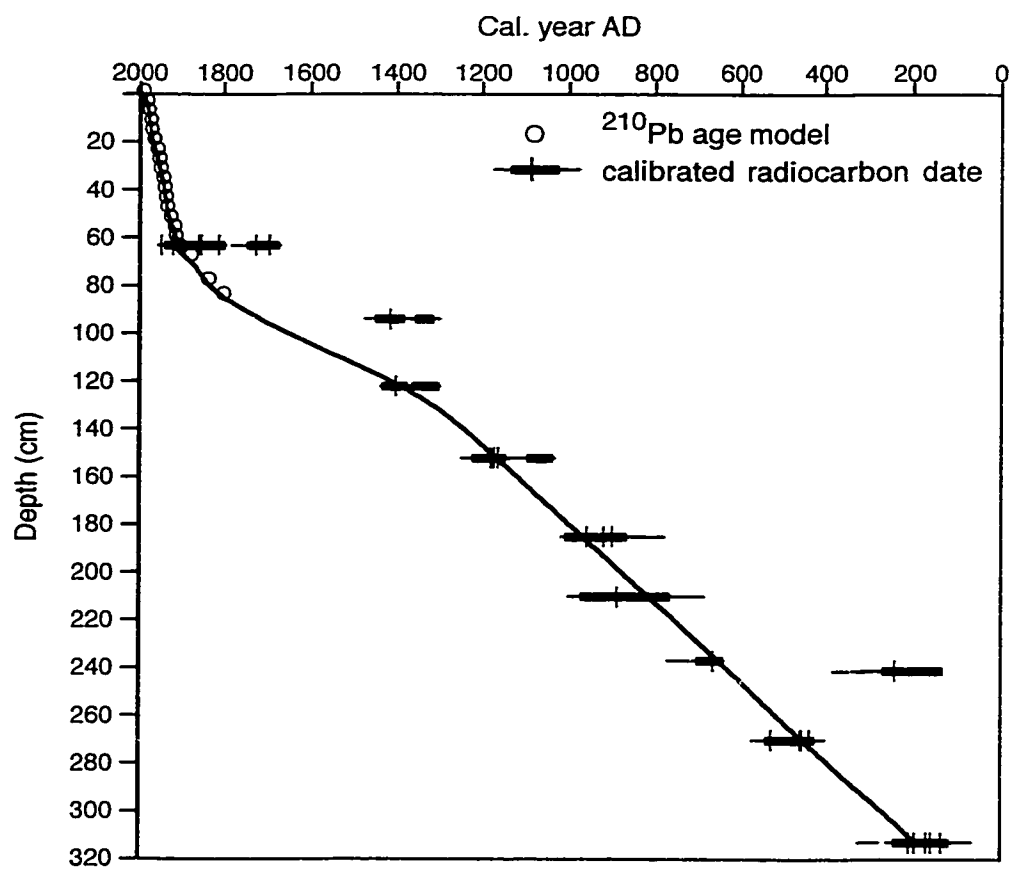


Figure 4.3 Age-depth relationship for the Clayoquot Lake sediment core. Calibrated radiocarbon dates show age intercepts and one and two standard deviations (Stuiver and Reimer 1993; Stuiver et al. 1998).

Table 4.1 Radiocarbon dates (a) and ^{210}Pb age determinations (b) from the Clayoquot Lake sediment core. All radiocarbon dates are AMS (accelerator mass spectrometry) dates on conifer needles.

a.

Depth (cm)	Radiocarbon age (BP)	Calibrated age ^a		Lab number (CAMS #)
		cal. AD	(-1 σ - +1 σ)	
63–64	120 \pm 50	1850	(1680 - 1950)	44474
94–95 ^b	520 \pm 60	1420	(1330 - 1440)	44475
122–123	560 \pm 60	1400	(1310 - 1430)	44476
152–153	880 \pm 50	1170	(1050 - 1220)	44477
185–186	1120 \pm 60	920	(830 - 1000)	44478
210–211	1170 \pm 80	890	(780 - 960)	44479
237–238	1340 \pm 40	670	(650 - 710)	45368
241–242 ^b	1780 \pm 50	240	(140 - 340)	44480
270–271	1580 \pm 40	460	(430 - 530)	44481
312–313	1840 \pm 50	170	(130 - 240)	39385

b.

Depth (cm)	Bulk density (g cm ⁻³)	^{210}Pb activity (DPM g ⁻¹) ^c	Modeled age at base of section (year AD) ^d
0–2	0.272	15.60 \pm 0.56	1992
4–6	0.266	8.35 \pm 0.42	1983
8–10	0.265	3.51 \pm 0.27	1973
12–14	0.252	2.73 \pm 0.24	1969
16–18	0.281	2.68 \pm 0.22	1966
20–22	0.280	3.92 \pm 0.30	1963
24–26	0.273	3.92 \pm 0.33	1956
28–30	0.284	2.68 \pm 0.24	1947
32–34	0.297	2.01 \pm 0.23	1941
36–38	0.273	2.43 \pm 0.22	1937
40–42	0.262	2.21 \pm 0.23	1930
44–46	0.250	1.70 \pm 0.17	1923
48–50	0.281	1.73 \pm 0.20	1919
52–54	0.287	2.16 \pm 0.21	1914
56–58	0.295	1.97 \pm 0.19	1902
60–62	0.309	1.42 \pm 0.17	1888
64–66	0.277	1.69 \pm 0.18	1883
68–70	0.305	1.66 \pm 0.19	1866
78–80	0.302	1.39 \pm 0.19	1833
84–86	0.289	1.29 \pm 0.20	1795

^a Calibrations following Stuiver and Reimer (1993) [version 4.1] and Stuiver et al. 1998.

^b Date rejected.

^c Analysis provided by Flett Research, 440 DeSalaberry Ave., Winnipeg, Manitoba, Canada.

^d The level of ^{210}Pb activity considered as supported by in situ decay of ^{226}Ra was determined by varying an estimate of supported ^{210}Pb until a best fit was achieved between log[unsupported ^{210}Pb] and cumulative dry weight of sediment (Flett Research Ltd., personal communication). This method yielded an r^2 of 0.84 corresponding to supported level of 1.215 DPM, and suggests that supported ^{210}Pb levels were nearly reached at a depth of 86 cm. Dates were assigned to each subsample using a model of ^{210}Pb activity that assumes a constant rate of supply of ^{210}Pb to the lake surface (Goldberg 1963).

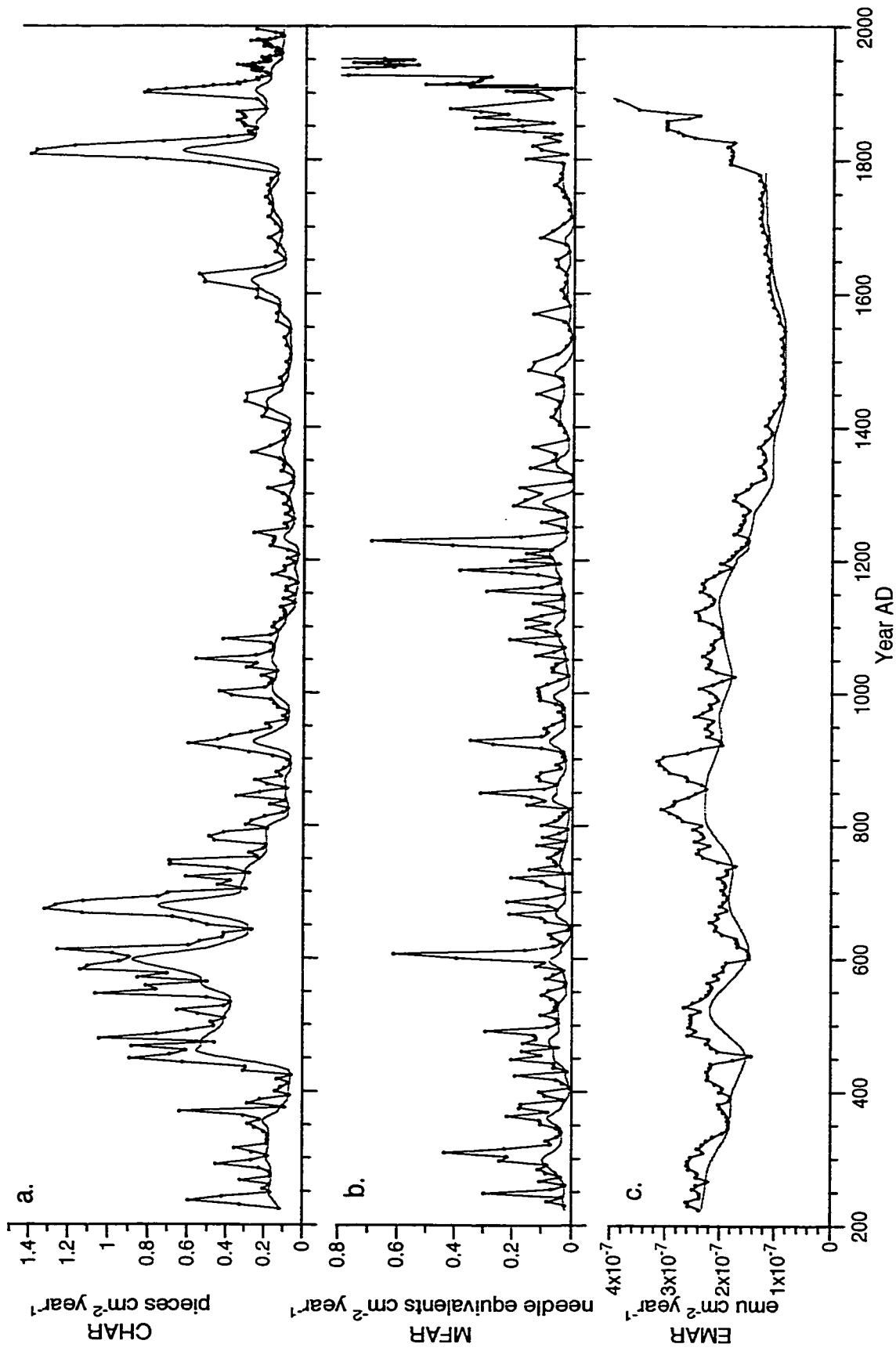


Figure 4.4 Charcoal, macrofossil, and magnetic susceptibility records from Clayoquot Lake. (a) Charcoal accumulation rate (CHAR), (b) macrofossil accumulation rate (MFAR), and (c) magnetic susceptibility accumulation rate (EMAR). The gray line indicates the background component that was subtracted from the accumulation rate to determine the peak component.

increasing sedimentation rates. Magnetic susceptibility in each subsample ranged between 1.04×10^{-5} and 2.25×10^{-5} emu (median = 1.52×10^{-5}). In contrast to the CHAR and MFAR records, EMAR varied more slowly over time and showed no distinct peaks. Background levels were high before AD 1200 (ca. 2×10^{-7} emu $\text{cm}^{-2} \text{year}^{-1}$), and then declined by ca. 50% for the period AD 1400–1800. Similar to the MFAR record, EMAR increased sharply at AD 1800.

Threshold values for local fires The total number of CHAR peaks detected was insensitive to a wide range of threshold values (0.16 to 0.22 pieces $\text{cm}^{-2} \text{year}^{-1}$; Figure 4.5), while small changes in threshold values outside of this range caused large changes in the number of CHAR peaks detected. These values (0.16 to 0.22) also correspond to a minimum in the frequency distribution of the CHAR peak component. Although the distribution is not distinctly bimodal, these results together indicate that large CHAR peaks may be separated from small peaks. A value of 0.20 pieces $\text{cm}^{-2} \text{year}^{-1}$ was chosen as the threshold that best identifies local fires.

The charcoal record shows 23 fires, with a large shift in fire frequency at AD 1100 (Figure 4.6). The average fire interval increased from 45 to 272 years from AD 200–1100 to AD 1100–present. The shortest fire intervals (ca. 20 years) and highest background component (ca. 0.5 pieces $\text{cm}^{-2} \text{year}^{-1}$) occurred between AD 400 and 600. The longest fire interval (ca. 500 years) and lowest background component (ca. 0.1 pieces $\text{cm}^{-2} \text{year}^{-1}$) occurred between AD 1100 and AD 1600. Although CHAR peaks could be identified visually during this period, they were distinctly smaller than during the other periods and may represent extra-local fires.

The peak components of CHAR, MFAR, and EMAR were positively correlated with corresponding background levels ($r = 0.583, 0.429$ and 0.384 , respectively; Table 4.2). Comparisons among the three records showed poor correlation. The magnitude of CHAR peaks was not correlated with EMAR ($r = -0.008$) or MFAR peaks ($r = 0.115$). Similarly, CHAR background levels were poorly correlated with background levels of EMAR ($r = 0.140$) and MFAR ($r = 0.180$). Correlation between records did not improve when using time-lags.

Charcoal source area

Three tree-ring dated fire events < 500 m from the lake coincided with large CHAR peaks (mean difference between the two methods = 6.3 years), indicating that large CHAR peaks were associated with these fires. In contrast, six tree-ring dated fires > 1000 m upstream did not match CHAR peaks, except where they coincided with fires < 500 m from the lake (mean difference = 33.8 years) (Figure 4.6). At a < 500 m-spatial scale, the sizes of CHAR peaks were inversely related to the distances of fires from the lake edge ($P = .010$; Figure 4.7), as would be expected if the quantity of charcoal dispersed from a fire decreases rapidly with distance. This relationship predicts that fires would need to occur within ca. 175–250 m from the lake edge in order to yield CHAR peaks > 0.20 pieces cm^{-2} year^{-1} . Therefore, based on a threshold of 0.20 pieces cm^{-2} year^{-1} to separate local fires from extra-local fires or random noise, the charcoal source area should be the area within ca. 175–250 m from the lake edge. This relationship is based on data from only the five most recent fires ($> \text{AD } 1100$) and strongly influenced by a single large fire near the lake in AD 1805; the relationship was not significant when sites with fire dates before AD 1100 were included ($P = .070$), probably because the actual extent of older fires may have been obscured by recent fires.

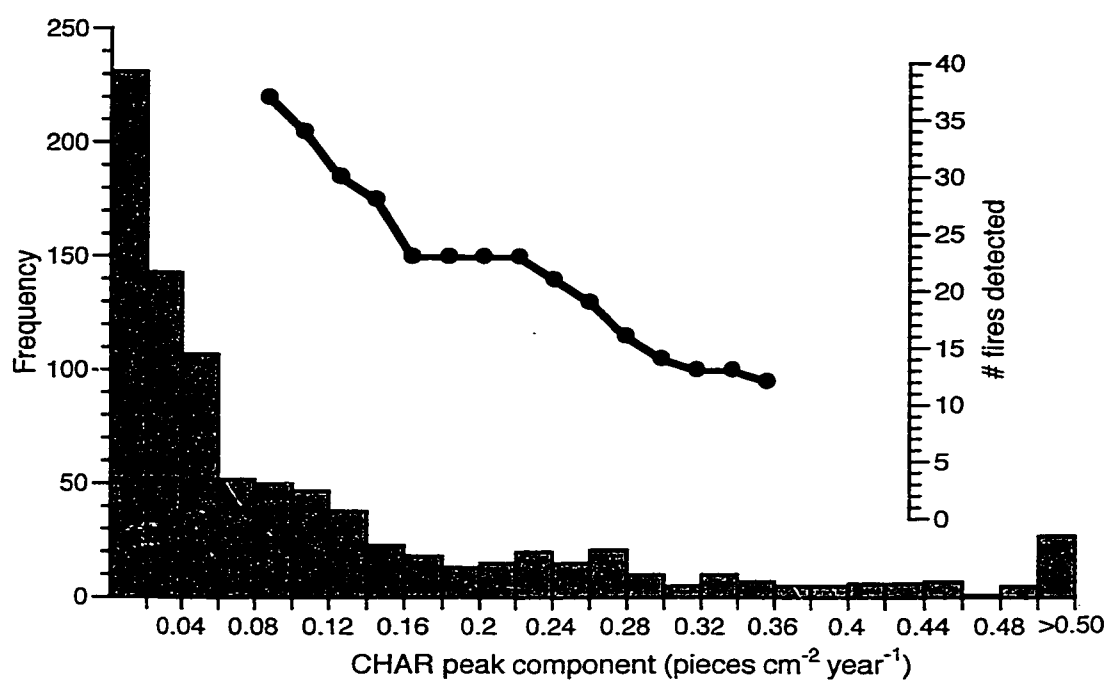


Figure 4.5 Frequency distribution of the charcoal peak component calculated as the positive residuals from a background curve (Figure 4.4). The CHAR record was first resampled to 2-year intervals. The upper curve shows the number of charcoal peaks (corresponding to local fires) detected using different threshold values.

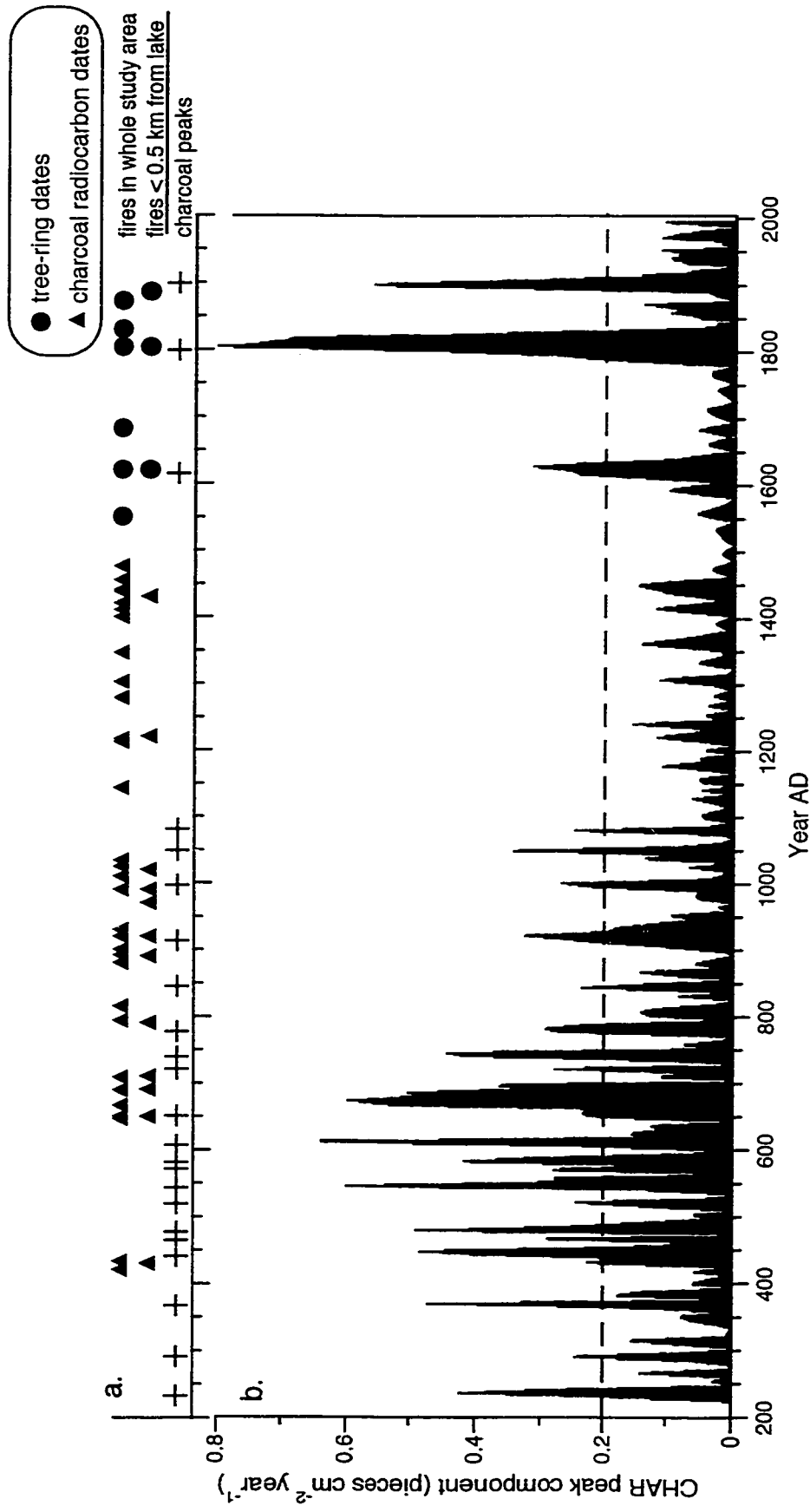


Figure 4.6 a. Fires in the Clayoquot Valley study area (83 sites) and limited to the vicinity of Clayoquot Lake (25 sites) detected by tree-ring records or radiocarbon dates of soil charcoal, compared to dates of fires detected by charcoal peaks in the sediment record. b. CHAR peak component, interpolated to 2-year intervals, showing the threshold used to determine local fires (dashed line).

Table 4.2 Cross-correlation of three time series from the Clayoquot Lake sediment record. Each series was separated into a background component and a peak component. CHAR=charcoal accumulation rate; EMAR=magnetic susceptibility accumulation rate; MFAR=macrofossil accumulation rate.

	CHAR		EMAR		MFAR	
	peak	back-ground	peak	back-ground	peak	back-ground
<u>CHAR</u>						
peak	1.000					
background	0.583	1.000				
<u>EMAR</u>						
peak	-0.008	0.060	1.000			
background	0.222	0.140	0.429	1.000		
<u>MFAR</u>						
peak	0.115	0.167	0.030	0.167	1.000	
background	0.124	0.180	0.114	0.221	0.384	1.000

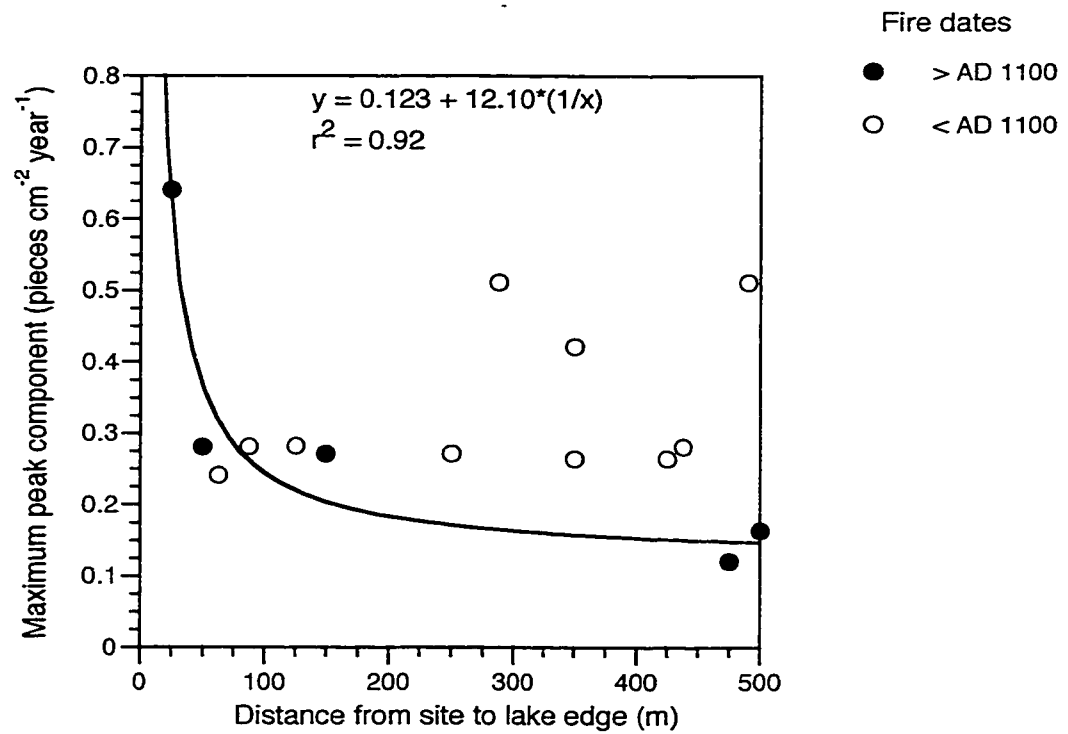


Figure 4.7 Comparison between the distance of fires to the lake edge and the height of the corresponding CHAR peak in the sediment core. The fitted curve is limited to fires occurring after AD 1100.

Fire-hazard ratio

Two sources of fire history may be combined to infer the spatial pattern of fire over time: (1) the lake sediment record indicates that 23 fires have occurred over the last 1800 years within a charcoal source area of 110 ha (250 m distance-to-lake), and (2) point samples of time-since-fire within the charcoal source area indicate that 43% of the charcoal source area did not burn at all over the last 1800 years (Figure 4.8a). This implies that the 23 fires were restricted to 57% of the area in which they could occur and still be detected in the sediment record. This pattern would have been very unlikely ($E = 4 \times 10^{-9}$; eq. 1) if fires were randomly distributed within this charcoal source area. A fire-hazard ratio was therefore used to quantify the range in fire susceptibility that results in the non-random pattern of fire within the charcoal source area. The fire-hazard ratio corresponding to a 50% probability of the observed outcome of all fires occurring in the burned areas (b_{50}) is 25; i.e., fires are 25 times more likely in burned than unburned areas (Figure 4.8b).

Defining a single fire-hazard ratio is difficult because the value of E is not known; the observed pattern of fire could have resulted by chance with a relatively low fire-hazard ratio ($b_{05} = 5$) or the observed pattern could have been ensured with a high fire-hazard ratio ($b_{95} = 345$). Limiting the period of analysis to after AD 1200 results in three fires that occurred in 21% of the charcoal source area, which is also an unlikely outcome if fires were randomly distributed ($E = .009$; eq. 1). For this period, the fire-hazard ratios b_{05} , b_{50} , and b_{95} , are 2, 14, and 212, respectively (Figure 4.8b).

Macrofossil record

The 1800-year macrofossil record was dominated by western hemlock and western redcedar (Figure 4.9). The relative abundance of western hemlock and western redcedar

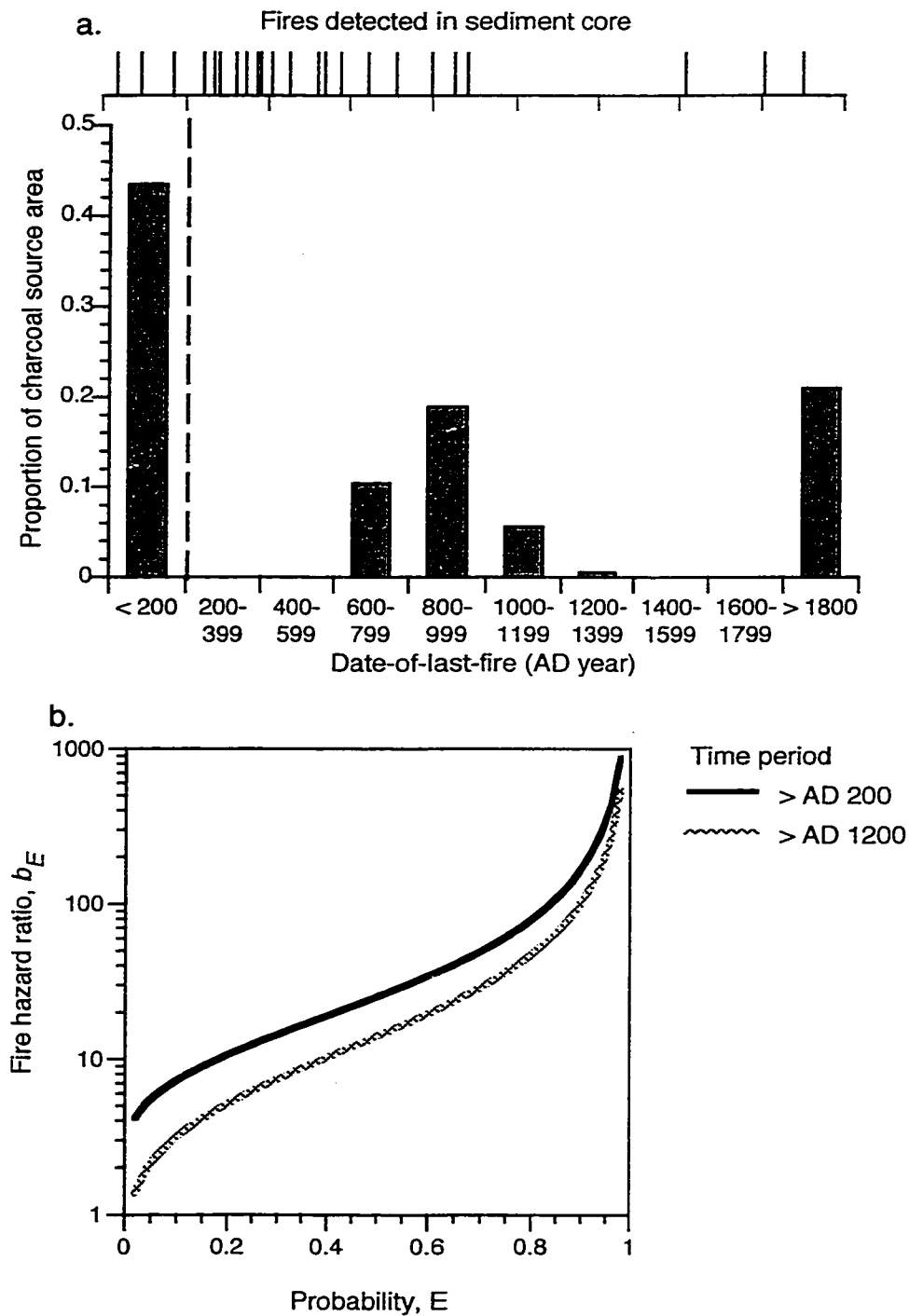


Figure 4.8

a. Fire history parameters used for the calculation of the fire hazard ratio. The proportion of the charcoal source area in each age class was computed from mapped date-of-last-fire using a charcoal source area based on a 250 m distance-to-lake (Figure 4.2) and fire dates were computed from the sediment core (Figure 4.6). b. The fire hazard ratio b_E represents the increased probability of fire in the portion of the area near Clayoquot Lake where fire could occur based on the age class structure in part (a). See *Methods* for the derivation of b_E .

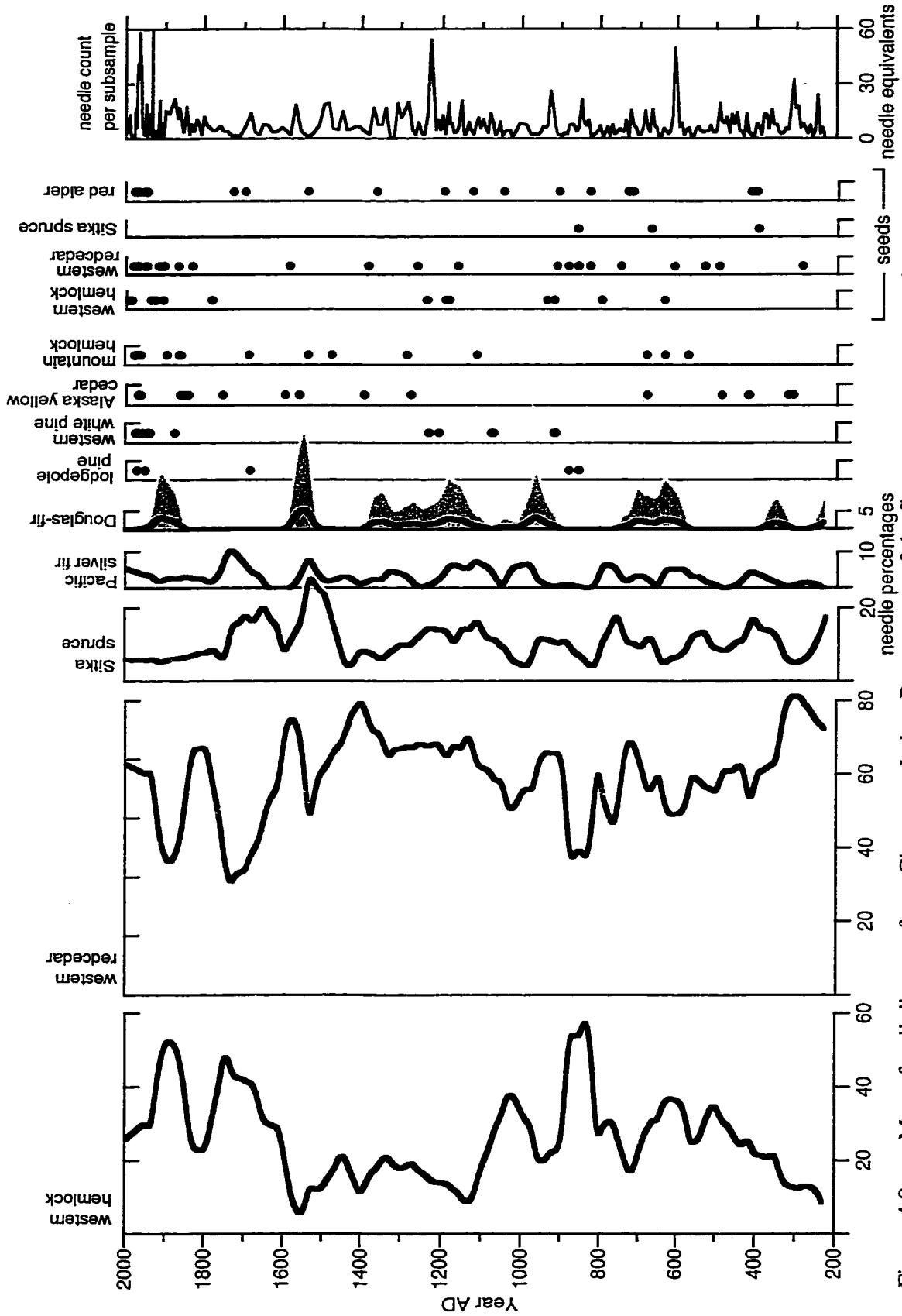


Figure 4.9 Macrofossil diagram from Clayoquot Lake. Percentages of the five most common species were calculated from needle concentrations interpolated to 2-year intervals and smoothed using a LOWESS filter with a 100-year window. Shaded area for Douglas-fir is 5x exaggeration.

fluctuated at high frequencies but showed no long-term trends other than a period of lower-than-average western hemlock during AD 1100–1600. Douglas-fir appeared most consistently during AD 900–1600. Sporadic occurrence of upland taxa such as mountain hemlock (*Tsuga mertensiana* (Bong.) Carr.) and Alaska yellow-cedar (*Chamaecyparis nootkatensis* (D. Don) Spach) likely represents transport of needles at least 800 m from the top of ridges around the lake.

Discussion

Correspondence between sediment and soil charcoal records

The major trends in the sediment charcoal record are mirrored by radiocarbon dates of soil charcoal. For example, of the soil charcoal analyzed within 500 m of the lake, few pieces were dated to the period of very few fires in the sediment record (AD 1100–1600), and several were dated to a period of frequent fires (AD 600–1100). Similar trends exist for the complete set of 83 sites in the entire study area (Figure 4.6). The DLF at these 83 sites (Chapter 3) shows few fires in the period AD 1150–1350 relative to adjacent periods (Figure 3.5). Although this finding is consistent with the sediment record, the trends in the soil charcoal record are much less pronounced than those in the sediment record.

The lack of a close match between the sediment and soil charcoal records is probably related to errors intrinsic to each method. The sediment record is dated by conifer needles that should closely represent the time of deposition and the time of charcoal incorporation into the sediment matrix. As a result, the sediment record should date fire events more accurately than soil charcoal radiocarbon dates, which are typically few to several centuries older than the date of the fire due to the length of time between wood formation and the fire event (Chapter 2). In addition, the soil charcoal record is

incomplete because charcoal from old fires may not be available if recent fires consume evidence of older fires (Ohlson and Tryterud 2000). The erasure of older fires may explain why very few soil charcoal radiocarbon dates coincide with the AD 400–600 period of frequent fires observed in the sediment record (Figure 4.6). Considering these limitations of the soil charcoal record, the sediment record allows for a more detailed interpretation of the temporal trends in fire occurrence over the last 1800 years.

Three aspects of the Clayoquot Lake sediment charcoal record make it especially useful for fire history studies. First, the high sedimentation rate, most likely due to sediment transport from the Clayoquot River, allowed fires closely spaced in time to be distinguished as separate fires. Specifically, for most of the record, fires 12 years apart could be detected as distinct peaks, assuming little secondary charcoal deposition and sediment mixing. Second, the poor correlation among sediment properties (charcoal, magnetic susceptibility, and macrofossils) suggests that charcoal accumulation is independent of the processes (e.g., flooding, erosional events) that affect sedimentation in Clayoquot Lake. This may be because sedimentation in the center of the lake is not affected by discrete events that deliver clastic materials into the lake. The unimportance of erosional events to sediment deposition at the coring site is supported by the lack of discrete peaks in the magnetic susceptibility record (Figure 4.4). Third, in this study, charcoal peaks could be matched with on-the-ground evidence of fires near the lake, allowing the estimation of the charcoal source area. The match of charcoal peaks to local fires verifies that large peaks are associated with local fires. In addition, the height of charcoal peaks was related to the distance-to-lake of corresponding fires, suggesting that charcoal dispersal declines rapidly with distance from fire (Figure 4.7). This relationship agrees qualitatively with direct measures of charcoal dispersal during a fire (Clark et al. 1998; Ohlson and Tryterud 2000). This relationship was only based on the five most

recent fires, because evidence of the extent of older fires was erased by more recent fires. Given this limitation, the charcoal source area determined by this study should be treated as only a first-approximation of charcoal dispersal (Figure 4.7).

Changes in fire frequency during the last two millennia

At centennial to millennial scales, the shift from frequent fires, AD 200–1100, to no fires, AD 1100–1600, suggests an abrupt change in the controls of forest fire (e.g., climate and ignition). This shift in fire frequency is contemporaneous with evidence for an onset of cool temperatures and glacial advances in the Canadian Rocky Mountains (AD 1101 and ca. AD 1140, respectively; Luckman 1995; Luckman et al. 1997) and for glacial advances in southern Alaska (ca. AD 1080; Wiles et al. 1999). Tree-ring reconstructions of climate and glacial advances synthesized for the entire northern hemisphere suggest the onset of cooler and wetter conditions of the “Little Ice Age” by ca. AD 1300 (Porter 1986; Mann et al. 1999). In addition, other proxies of paleoclimate from the central and western United States indicate that droughts were longer and more extensive prior to the “Little Ice Age” (Woodhouse and Overpeck 1998). One particularly detailed record of the salinity of a closed basin lake in North Dakota suggests a “regime shift” from predominately dry to wet conditions at AD 1200 (Laird et al. 1996; 1998). The correspondence of the decline in fire frequency at Clayoquot Lake with indicators of cooler or wetter conditions in Alaska, the Rocky Mountains, and central North America suggests that large-scale climate controls were responsible for shifts in fire frequency at Clayoquot Lake.

At decadal to centennial time scales, the periods of frequent fire prior to the “Little Ice Age” in the Clayoquot Lake core do not match other fire records or paleoclimate

evidence of drought from western North America. For example, the period of highest fire frequency at Clayoquot Lake (AD 300–800) does not coincide with high fire frequencies determined from fire-scarred trees in central California (AD 800–1300; Swetnam 1993) or from a lake sediment record in western Oregon (Long et al. 1998). In addition, this period of high fire frequency at Clayoquot Lake shows little correspondence with periods of drought inferred from tree-ring climate reconstructions (central California, AD 250–350 and AD 700–850; Hughes and Brown 1992), lake levels (eastern California, AD 900–1100 and AD 1200–1350; Stine 1994) or lake salinity (North Dakota, AD 200–370, AD 700–850, and AD 1000–1200; Laird et al. 1996). On the other hand, one tree-ring record from California (Hughes and Graumlich 1996) and a dust record from Minnesota (Dean 1997) do show evidence of severe drought between AD 400–600, corresponding to the period of frequent fires at Clayoquot Lake. This evidence for spatial variability of drought agrees with a review by Hughes and Diaz (1994) that the Medieval Warm Period (AD 900–1300) was not uniformly warm and dry across North America.

In addition to climatic changes, shifts in lightning strike frequency should also affect fire frequency, especially in landscapes where fire cannot spread easily among patches of susceptible sites (Turner and Romme 1994). In general, lightning is rare on the west coast of Vancouver Island because of the stability of onshore air flow. Lightning is most likely to occur during meteorological events that are associated with large-scale circulation features that also cause drought, such as offshore flow from central British Columbia and low moisture in the lower atmosphere (Rorig and Ferguson 1999). Therefore, ignition and climatic controls of fire may be correlated, making it difficult to identify the relative degree to which each controls fire frequency.

Anthropogenic ignitions probably had little effect on fire frequency. Although coastal peoples may have burned forest to enhance berry production (Turner 1991), the nearest villages (current and past) to the study area are 20 km away, and none of the reported culturally significant areas in the Clayoquot Valley, or any valley equally remote, suggest these areas were burned for berry crops (Scientific Panel 1995b). Such fires would have been controlled low intensity understory burns rather than the stand-replacing fires that occurred in the 19th century (Turner 1991), and thus not likely to have been recorded in lake sediments. Further evidence pointing to the role of lightning was the fortuitous finding of a lightning-scarred Douglas-fir with a scar date (AD 1886) matching the fire date in the surrounding stand (site 27). This site would have been a potential area for anthropogenic burning because it is located in an accessible area next to Clayoquot Lake.

Landscape patterns of fire susceptibility

Neither the sediment record nor the soil charcoal record alone can show the long-term landscape pattern of fire. The point samples of DLF capture only a rough approximation of the temporal variation in fire occurrence (Figure 4.8a), and the sediment record provides no information on the spatial pattern of fire. However, the combination of these records provides valuable information on how the fires recorded in the sediment core are patterned on the adjacent landscape. Specifically, the point samples suggest that all fires detected in the sediment core were restricted to ca. 60% of the area near the lake, a finding that is very unlikely if fires burn randomly over the landscape. The probability model used to examine the fire-hazard ratio suggests that the locations of fire were biased by one to two orders of magnitude among areas near the lake (Figure 4.8b).

The large fire-hazard ratio indicates a wide range in susceptibility to fire near Clayoquot Lake. Topography was probably most important at controlling fire susceptibility, as areas on north-facing slopes generally have not burned during the past 1800 years and areas on south-facing slopes burned in the last 200 years, and probably burned several times during the last 1800 years (Figure 4.2). The effect of topography on incoming solar radiation, and in turn on fuel moisture, may have caused south-facing slopes to be much more susceptible to fire than north-facing slopes (Chapter 3). Fuel loads were probably a secondary control on fire susceptibility. Before AD 1100, fires were frequent enough (20–50 year intervals) to reduce fuel loads if each fire reburned the same sites. To sustain a fire frequency of 20–50 years for several centuries, fires probably did not reburn exactly the same sites, but rather burned different south-facing sites at different times. Fire probably returned to burned areas as fuels accumulated > 200 years following the last fire (Agee and Huff 1987).

Ecosystem implications for differences in fire susceptibility

The wide range in susceptibility to fire indicated by this study has several implications for stand-level and landscape-level forest dynamics. In areas with low fire-susceptibility, late-successional communities probably persisted for several millennia. In contrast, areas with high fire-susceptibility may maintain spatially segregated communities of fire-dependent species, such as shore pine (*Pinus contorta*) and Douglas-fir. Large differences in fire susceptibility also may compound the effects of fire on forest structure and diversity. For example, the soil resource in some areas that burn repeatedly may be depleted of nutrients by nitrogen volatilization and erosion, thus contributing to stunted trees and a dense shrub layer of salal (*Gaultheria shallon*) (Chapter 3). If fire occurrence was spatially homogeneous, then fire frequency would be lower in areas that are currently

fire-susceptible, and thus may not be sufficient to maintain fire-dependent species in the stand. Therefore, the wide range in susceptibility to fire at Clayoquot Lake is an important process for maintaining species diversity at the landscape-scale.

Forest dynamics in areas with little fire-susceptibility would operate very differently than in areas experiencing stand-replacing fires. In the absence of fire, a change in climate would cause forest composition to change at a rate governed by the deaths of long-lived canopy dominant trees and the differential success of regenerating species in canopy gaps (Lertzman 1995). Such minimal change in forest composition at Clayoquot Lake was evident in the conifer needle macrofossil record, which sampled vegetation at a scale equivalent or greater than the charcoal record. The only long-term trends detected in this record was a slight decline of western hemlock during the 500-year absence of fire (AD 1100–1600) and increased Douglas-fir at AD 900 following a period of frequent fire (Figure 4.9). No other long-term trends in vegetation were detectable despite large changes in fire frequency, as would be expected if fire was spatially restricted to the same areas near the lake. Therefore, this study suggests that forest composition at the landscape scale was minimally impacted by changes in fire frequency.

Landscape ecologists have generally modeled the effects of disturbance on the landscape mosaic as related to disturbance size, frequency, and intensity (Shugart and West 1981; Urban et al. 1987; Turner et al. 1994). Although the role of terrain on differences in susceptibility to disturbance is widely recognized (Romme and Knight 1981; Camp et al. 1997; Heyerdahl et al. *in press*), most theoretical analyses of landscape dynamics consider fire susceptibility to be mainly dependent on fuel accumulation from earlier fires (e.g., Li et al. 1997; Wimberly et al. 2000). In areas with a strong topographic control on fire susceptibility such as the Clayoquot Valley, the pattern of disturbance is not spatially

homogeneous and yields a significantly different landscape mosaic of age classes than would be expected in the absence of these controls (Moloney and Levin 1996; Taulman 1998). This study shows that differences in fire susceptibility have had a strong influence on the distribution of fire for millennia, and thus should be incorporated into the theoretical framework used to model the fire disturbance regime.

LITERATURE CITED

- Agee, J. 1993. *Fire Ecology of Pacific Northwest Forests*. Washington, D.C., Island Press. 493 p.
- Agee, J. K. and Huff, M. H. 1980. First year ecological effects of the Hoh Fire, Olympic Mountains, Washington. *Fire and Forest Meteorology Conference Proceedings* **6**:175-181.
- Agee, J. K. and Huff, M. H. 1987. Fuel succession in a western hemlock/Douglas-fir forest. *Canadian Journal of Forest Research* **17**:697-704.
- Aitken, M. J. 1990. *Science-based Dating in Archaeology*. London, Longman Group UK Limited. 274 p.
- Alaback, P. B. 1996. Biodiversity patterns in relation to climate: the coastal temperate rainforests of North America. Pgs. 105-133 *in*: Lawford, R. G., Alaback, P. B. and Fuentes, E. (eds.) *High-Latitude Rainforests and Associated Ecosystems of the West Coast of the Americas*. New York, Springer-Verlag.
- Antonic, O. 1998. Modelling daily topographic solar radiation without site-specific hourly radiation data. *Ecological Modelling* **113**:31-40.
- Arno, S. F. and Sneek, K. M. 1977. A method for determining fire history in coniferous forests of the mountain west. USDA Forest Service, Intermountain Forest and Range Experiment Station. General Technical Report INT-42.
- Bassini, F. and Becker, P. 1990. Charcoal's occurrence in soil depends on topography in Terra firme forest near Manaus, Brazil. *Biotropica* **22**:420-422.
- Beers, T. W., Dress, P. E. and Wensel, L. C. 1966. Aspect transformation in site productivity research. *Journal of Forestry* **64**:691-692.
- Berli, S., Cherubini, P. and Schoch, W. 1994. Reconstruction of stand fluctuations, soil development and fire history over 7000 years BP by means of charcoal analysis. *Botanica Helvetica* **104**:17-30.
- Bormann, B. T., Spaltenstein, H., McClellan, M. H., Ugolini, F. C., Cromack K., Jr. and Nay, S. M. 1995. Rapid soil development after windthrow disturbance in pristine forests. *Journal of Ecology* **83**:747-757.
- Boyчук, D., Perera, A. H., TerMikaelian, M. T., Martell, D. L. and Li, C. 1997. Modelling the effect of spatial scale and correlated fire disturbances on forest age distribution. *Ecological Modelling* **95**:145-164.
- Burns, R. M. and Honkala, B. H. 1990. *Silvics of North America*. U.S. Department of Agriculture, Forest Service, Washington, D.C. Agriculture Handbook 654.
- Burrows, C. J. 1996. Radiocarbon dates for Holocene fires and associated events, Canterbury, New Zealand. *New Zealand Journal of Botany* **34**:111-121.
- Bussi eres, B., Payette, S. and Filion, L. 1996. Late Holocene deforestation and peat formation in Charlevoix highlands: Onset of the subalpine and alpine belts. *Geographie Physique et Quaternaire* **50**:257-269.
- Camp, A., Oliver, C., Hessburg, P. and Everett, R. 1997. Predicting late-successional fire refugia pre-dating European settlement in the Wenatchee Mountains. *Forest Ecology and Management* **95**:63-77.

- Carcaillet, C. 1998. A spatially precise study of Holocene fire history, climate and human impact within the Maurienne valley, North French Alps. *Journal of Ecology* **86**:384-396.
- Carcaillet, C. and Talon, B. 1996. A view of the wood charcoal stratigraphy and dating in soil: A case study of some soils from the French Alps. *Geographie Physique et Quaternaire* **50**:233-244.
- Carcaillet, C. and Thimon, M. 1996. Pedoanthracological contribution to the study of the evolution of the upper treeline in the Maurienne Valley (North French Alps): methodology and preliminary data. *Review of Palaeobotany and Palynology* **91**:399-416.
- Chandler, C., Cheney, P., Thomas, P., Trabaud, L. and Williams, D. 1983. Fire in forestry, Volume I: forest fire behavior and effects. New York, John Wiley & Sons. 450 p.
- Clague, J. J. and Mathewes, R. W. 1996. Neoglaciation, glacier-dammed lakes, and vegetation change in northwestern British Columbia, Canada. *Arctic and Alpine Research* **28**:10-24.
- Clark, J. S. 1988a. Stratigraphic charcoal analysis on petrographic thin sections: application to fire history in Northwestern Minnesota. *Quaternary Research* **30**:81-91.
- Clark, J. S. 1988b. Particle motion and the theory of charcoal analysis: source area, transport, deposition, and sampling. *Quaternary Research* **30**:67-80.
- Clark, J. S. 1988c. Effect of climate change on fire regimes in northwestern Minnesota. *Nature* **334**:233-235.
- Clark, J. S. 1990. Fire and climate change during the last 750 yr in northwestern Minnesota. *Ecological Monographs* **60**:135-159.
- Clark, J. S. and Royall, P. D. 1995. Transformation of a northern hardwood forest by aboriginal (Iroquois) fire: charcoal evidence from Crawford Lake, Ontario, Canada. *The Holocene* **5**:1-9.
- Clark, J. S. and Royall, P. D. 1996. Local and regional sediment charcoal evidence for fire regimes in presettlement north-eastern North America. *Journal of Ecology* **84**:365-383.
- Clark, J. S., Royall, P. D. and Chumbley, C. 1996. The role of fire during climate change in an eastern deciduous forest at Devil's Bathtub, New York. *Ecology* **77**:2148-2166.
- Clark, J. S. and Patterson, W. A. I. 1997. Background and local charcoal in sediments: scales of fire evidence in the paleorecord. Pgs. 23-48 *in*: Clark, J. S., Cachier, H., Goldammer, J. G. and Stocks, B. (eds.) *Sediment Records of Biomass Burning and Global Change*. Berlin, Springer-Verlag.
- Clark, J. S., Lynch, J., Stocks, B. J. and Goldammer, J. G. 1998. Relationships between charcoal particles in air and sediments in west-central Siberia. *Holocene* **8**:19-29.
- Clark, J. S., Gill, A. M. and Kershaw, A. P. *in press*. Spatial variability in fire regimes: its effects on recent and past vegetation. *in*: Bradstock, R. and Gill, A. M. (eds.) *Flammable Australia: the Fire Regimes and Biodiversity of a Continent*, Charles Sturt University.

- Cleveland, W. S. 1979. Robust locally weighted regression and smoothing scatterplots. *Journal of the American Statistics Association* 74:829-836.
- Cruikshank, J. G. and Cruikshank, M. M. 1981. The development of humus-iron podsol profiles, linked by radiocarbon dating and pollen analysis to vegetation history. *Oikos* 36:238-257.
- Cwynar, L. C. 1987. Fire and forest history of the North Cascade Range. *Ecology* 68:791-802.
- Daniels, L. D., Dobry, J., Klinka, K. and Feller, M. C. 1997. Determining the year of death of logs and snags of *Thuja plicata* in southwestern coastal British Columbia. *Canadian Journal of Forest Research* 27:1132-1141.
- Daniels, L. D., Marshall, P. L. and Klinka, K. 1995. Age structure of *Thuja plicata* in the tree layer of old-growth stands near Vancouver, British Columbia. *Northwest Science* 69:175-183.
- Davis, M. B. 1986. Climatic instability, time lags, and community disequilibrium. Pgs. 269-284 in: Diamond, J. and Chase, T. J. (eds.) *Community Ecology*. New York, Harper and Row.
- Dean, W. E. 1997. Rates, timing, and cyclicity of Holocene eolian activity in north-central U.S.: evidence from varved lake sediments. *Geology* 25:331-334.
- DeBell, D. S. and Franklin, J. F. 1987. Old-growth Douglas-fir and western hemlock: a 36-year record of growth and mortality. *Western Journal of Applied Forestry* 2:111-114.
- Diggle, P. J. 1983. *Statistical Analysis of Spatial Point Patterns*. London, Academic Press. 148 p.
- Dunwiddie, P. W. 1985. Dichotomous key to conifer foliage in the Pacific Northwest. *Northwest Science* 59:185-191.
- Dunwiddie, P. W. 1986. A 6000-year record of forest history on Mount Rainier, Washington. *Ecology* 67:58-68.
- Dunwiddie, P. W. 1987. Macrofossil and pollen representation of coniferous trees in modern sediments from Washington. *Ecology* 68:1-11.
- Earle, C. J., Brubaker, L. B. and Anderson, P. M. 1996. Charcoal in northcentral Alaskan lake sediments: Relationships to fire and late-Quaternary vegetation history. *Review of Palaeobotany and Palynology* 92:83-95.
- Environment Canada. 1998. *Canadian Climate Normals 1961-1990*. Ottawa, Environment Canada.
- Fahnestock, G. R. and Agee, J. K. 1983. Biomass consumption and smoke production by prehistoric and modern forest fires in western Washington. *Journal of Forestry*:653-657.
- Finney, M. A. 1995. The missing tail and other considerations for the use of fire history models. *International Journal of Wildland Fire* 5:197-202.
- Fowler, P. M. and Asleson, D. O. 1984. The location of lightning-caused wildland fires, northern Idaho. *Physical Geography* 5:240-252.
- Fox, J. F. 1989. Bias in estimating forest disturbance rates and tree lifetimes. *Ecology* 70:1267-1272.

- Franklin, J. F. and Dyrness, C. T. 1988. Natural Vegetation of Oregon and Washington. Corvallis, Oregon, OSU Press. 452 p.
- Franklin, J. F. and Hemstrom, M. A. 1981. Aspects of succession in the coniferous forests of the Pacific Northwest. Pgs. 212-229 *in*: West, D. C., Shugart, H. H. and Botkin, D. B. (eds.) Forest Succession: Concepts and Application. New York, Springer Verlag.
- Frazer, G. W., Trofymow, J. A. and Lertzman, K. P. 2000. Canopy openness and leaf area in chronosequences of coastal temperate rainforests. *Canadian Journal of Forest Research* 30:239-256.
- Gagnon, D. and Bradfield, G. E. 1986. Relationships among forest strata and environment in southern coastal British Columbia. *Canadian Journal of Forest Research* 16:1264-1271.
- Gholz, H. L., Grier, C. C., Campbell, A. G. and Brown, A. T. 1979. Equations for estimating biomass and leaf area of plants in the Pacific Northwest. Oregon State University Forest Research Lab. Research Paper 41.
- Goldammer, J. G. and Seibert, B. 1990. The impact of droughts and forest fires on tropical lowland rain forest of Eastern Borneo. Pgs. 11-31 *in*: Goldammer, J. G. (eds.) Fire in the Tropical Biota: Ecosystem Processes and Global Challenges. Berlin, Springer-Verlag.
- Goldberg, E. D. 1963. Geochronology with lead-210. Pgs. 121-122 *in*: Radioactive Dating. Vienna, International Atomic Energy Agency.
- Graham, R. L. and Cromack, K., Jr. 1982. Mass, nutrient content and decay rate of dead boles in rain forests of Olympic National Park. *Canadian Journal of Forest Research* 12:511-521.
- Gray, A. N. and Spies, T. A. 1996. Gap size, within-gap position and canopy structure effects on conifer seedling establishment. *Journal of Ecology* 84:635-645.
- Green, R. N. and Klinka, K. 1994. A field guide to site identification and interpretation for the Vancouver Forest Region. Victoria, B.C., Government of British Columbia, MOF Research Branch. 285 p.
- Hansen, B. C. S. and Engstrom, D. R. 1996. Vegetation history of Pleasant Island, southeastern Alaska, since 13,000 yr BP. *Quaternary Research* 46:161-175.
- Harmon, M. E., Franklin, J. F., Swanson, F. J., Sollins, P., Gregory, S. V., Lattin, J. D., Anderson, N. H., Cline, S. P., Aumen, N. G., Sedell, J. R., Lienkaemper, G. W., Cromack, K., Jr. and Cummins, K. W. 1986. Ecology of coarse woody debris in temperate ecosystems. *Advances in Ecological Research* 15:133-302.
- Hart, T. B., Hart, J. A., DeChamps, R., Fournier, M. and Ataholo, M. 1996. Changes in forest composition over the last 4000 years in the Ituri Basin, Zaire. Pgs. 545-563 *in*: van der Maesen, L. J. G., van der Burgt, X. M. and van Medenbrach de Rooy, J. M. (eds.) Biodiversity of African Plants. Dordrecht, Kluwer.
- Hemstrom, M. A. and Franklin, J. F. 1982. Fire and other disturbances of the forests in Mount Rainier National Park. *Quaternary Research* 18:32-51.
- Henderson, J. and Peter, D. 1981. Preliminary plant associations and habitat types of the Shelton Ranger District, Olympic National Forest. USDA Forest Service, Pacific Northwest Region.

- Hennon, P. E. and Loopstra, E. M. 1991. Persistence of western hemlock and western redcedar trees 38 years after girdling at Cat Island in Southeast Alaska. USDA Forest Service, Pacific NW Research Station. Research Note PNW-RN-507.
- Heusser, C. J. 1977. Quaternary palynology of the Pacific slope of Washington. *Quaternary Research* 8:282-306.
- Heusser, C. J., Heusser, L. E. and Peteet, D. M. 1999. Humptulips revisited: a revised interpretation of Quaternary vegetation and climate of western Washington, USA. *Palaeogeography, Palaeoclimatology, Palaeoecology* 150: 191-221.
- Heyerdahl, E. K., Brubaker, L. B. and Agee, J. K. 2000. Factors controlling spatial variation in historical fire regimes: a multiscale example from the interior west, USA. *Ecology in press*.
- Hoadley, R. B. 1990. *Identifying Wood: Accurate Results with Simple Tools*. Newtown, CT, Taunton Press. 223 p.
- Hopkins, M. S., Ash, J., Graham, A. W., Head, J. and Hewett, R. K. 1993. Charcoal evidence of the spatial extent of the Eucalyptus woodland expansions and rainforest contractions in North Queensland during the late Pleistocene. *Journal of Biogeography* 20:357-372.
- Hopkins, M. S., Head, J., Ash, J. E., Hewett, R. K. and Graham, A. W. 1996. Evidence of a Holocene and continuing recent expansion of lowland rain forest in humid, tropical North Queensland. *Journal of Biogeography* 23:737-745.
- Horn, S. P. and Sanford, R. L. 1992. Holocene fires in Costa-Rica. *Biotropica* 24:354-361.
- Huff, M. H. 1995. Forest age structure and development following wildfires in the western Olympic Mountains, Washington. *Ecological Applications* 5:471-483.
- Huff, M. H. and Agee, J. K. 1980. Characteristics of large lightning fires in the Olympic Mountains, Washington. In: *Proceedings of the Sixth Meteorology Conference, April 22-24, 1980*. Seattle, Washington; 117-123.
- Huggard, D. J. and Arsenault, A. 1999. Reverse cumulative standing age distributions in fire-frequency analysis - Comment. *Canadian Journal of Forest Research* 29:1449-1456.
- Hughes, M. K. and Brown, P. M. 1992. Drought frequency in central California since 101 B C recorded in giant sequoia tree-rings. *Climate Dynamics* 6:161-167.
- Hughes, M. K. and Diaz, H. F. 1994. Was there a 'Medieval Warm Period', and if so, where and when? *Climatic Change* 26:109-143.
- Hughes, M. K. and Graumlich, L. J. 1996. Multimillennial dendroclimatic studies from the western United States. Pgs. 109-124 *in*: Jones, P. D., Bradley, R. S. and Jouzel, J. (eds.) *Climatic Variations and Forcing Mechanisms of the Last 2000 Years*, Springer-Verlag.
- Ishii, H., Clement, J. P. and Shaw, D. C. 2000. Branch growth and crown form in old coastal Douglas-fir. *Forest Ecology and Management* 131:81-91.
- Johnson, E. A. and Gutsell, S. L. 1994. Fire frequency models, methods and interpretations. *Advances in Ecological Research* 25:239-287.
- Johnson, E. A. and Van Wagner, C. E. 1985. The theory and use of two fire history models. *Canadian Journal of Forest Research* 15:214-220.

- Jungen, J. R. 1985. Soils of Southern Vancouver Island. British Columbia Surveys and Resource Mapping Branch, Ministry of Environment.
- Keenan, R. J., Prescott, C. E., Kimmins, J. P., Pastor, J. and Dewey, B. 1996. Litter decomposition in western red cedar and western hemlock forests on northern Vancouver Island, British Columbia. *Canadian Journal of Botany* **74**:1626-1634.
- Kershaw, A. P., Bush, M. B., Hope, G. S., Weiss, K.-F., Goldammer, J. G. and Sanford, R. 1997. The contribution of humans to past biomass burning in the tropics. Pgs. 413-442 *in*: Clark, J. S., Cachier, H., Goldammer, J. G. and Stocks, B. (eds.) *Sediment Records of Biomass Burning and Global Change*. Berlin Heidelberg, Springer-Verlag.
- Kitzberger, T., Veblen, T. T. and Villalba, R. 1997. Climatic influences on fire regimes along a rain forest to xeric woodland gradient in northern Patagonia, Argentina. *Journal of Biogeography* **24**:35-47.
- Klinka, K., Qian, H., Pojar, J. and Meidinger, D. V. 1996. Classification of natural forest communities of coastal British Columbia, Canada. *Vegetatio* **125**:149-168.
- Laird, K. R., Fritz, S. C. and Cumming, B. F. 1998. A diatom-based reconstruction of drought intensity, duration, and frequency from Moon Lake, North Dakota: a sub-decadal record of the last 2300 years. *Journal of Paleolimnology* **19**:161-179.
- Laird, K. R., Fritz, S. C., Maasch, K. A. and Cumming, B. F. 1996. Greater drought intensity and frequency before AD 1200 in the Northern Great Plains. *Nature* **384**:552-554.
- Lavee, H., Kutiel, P., Segev, M. and Benyamini, Y. 1995. Effect of surface roughness on runoff and erosion in a Mediterranean ecosystem: the role of fire. *Geomorphology* **11**:227-234.
- Lertzman, K. P. 1992. Patterns of gap-phase replacement in a subalpine old-growth forest. *Ecology* **73**:657-669.
- Lertzman, K. P. 1995. Forest dynamics, differential mortality and variable recruitment rates. *Journal of Vegetation Science* **6**:191-204.
- Lertzman, K. P., Sutherland, G. D., Inselberg, A. and Saunders, S. C. 1996. Canopy gaps and the landscape mosaic in a coastal temperate rain forest. *Ecology* **77**:1254-1270.
- Lertzman, K. P., Spies, T. and Swanson, F. 1997. From ecosystem dynamics to ecosystem management. Pgs. 361-382 *in*: Schoonmaker, P. K., von Hagen, B. and Wolf, E. C. (eds.) *The Rain Forests of Home: Profile of a North American Bioregion*. Washington, D.C., Island Press.
- Lertzman, K. P. and Fall, J. 1998. From forest stands to landscapes: spatial scales and the roles of disturbances. Pgs. 339-367 *in*: Peterson, D. L. and Parker, V. T. (eds.) *Ecological Scale: Theory and Applications*. New York, Columbia University Press.
- Lertzman, K. P., Fall, J. and Dorner, B. 1998. Three kinds of heterogeneity in fire regimes: At the crossroads of fire history and landscape ecology. *Northwest Science* **72**:4-23.
- Li, C., TerMikaelian, M. and Perera, A. 1997. Temporal fire disturbance patterns on a forest landscape. *Ecological Modelling* **99**:137-150.

- Long, C. J., Whitlock, C., Bartlein, P. J. and Millspaugh, S. H. 1998. A 9000-year fire history from the Oregon Coast Range, based on a high-resolution charcoal study. *Canadian Journal of Forest Research* **28**:774-787.
- Lowe, D. J., McFadgen, B. G., Higham, T. F. G., Hogg, A. G., Froggatt, P. C. and Nairn, I. A. 1998. Radiocarbon age of the Kaharoa tephra, a key marker for late Holocene stratigraphy and archaeology in New Zealand. *The Holocene* **8**:499-507.
- Luckman, B. H. 1995. Calendar-dated, early Little-Ice-Age glacier advance At Robson Glacier, British Columbia, Canada. *Holocene* **5**:149-159.
- Luckman, B. H., Briffa, K. R., Jones, P. D. and Schweingruber, F. H. 1997. Tree-ring based reconstruction of summer temperatures at the Columbia Icefield, Alberta, Canada, AD 1073-1983. *Holocene* **7**:375-389.
- Lusk, C. H. 1996. Gradient analysis and disturbance history of temperate rain forests of the coast range summit plateau, Valdivia, Chile. *Revista Chilena de Historia Natural* **69**:401-411.
- MacDonald, G. M., Larsen, C. P. S., Szeicz, J. M. and Moser, K. A. 1991. The reconstruction of boreal forest fire history from lake sediments: a comparison of charcoal, pollen sedimentological, and geochemical indices. *Quaternary Science Reviews* **10**:53-74.
- Manly, B. F. J. 1997. *Randomization, Bootstrap and Monte Carlo Methods in Biology*, 2 ed. London, UK, Chapman & Hall. 399 p.
- Mann, M. E., Bradley, R. S. and Hughes, M. K. 1999. Northern hemisphere temperatures during the past millennium: Inferences, uncertainties, and limitations. *Geophysical Research Letters* **26**:759-762.
- Mathewes, R. W. 1973. A palynological study of post-glacial vegetation changes in the University Research Forest, southwestern British Columbia. *Canadian Journal of Earth Sciences* **19**:1185-1195.
- McFadgen, B. G. 1982. Dating New Zealand archaeology by radiocarbon. *New Zealand Journal of Science* **25**:379-392.
- McLachlan, J. and Brubaker, L. B. 1995. Local and regional vegetation change on the northeastern Olympic Peninsula during the Holocene. *Canadian Journal of Botany* **73**:1618-1627.
- McNabb, D. H. and Cromack, K. J. 1990. Effects of prescribed fire on nutrients and soil productivity. Pgs. 125-142 *in*: Walstad, J. D., Radosevich, S. R. and Sandberg, D. V. (eds.) *Natural and Prescribed Fire in the Pacific Northwest*. Corvallis, Oregon, Oregon State University Press.
- McNabb, D. H. and Swanson, F. J. 1990. Effects of fire on soil erosion. Pgs. 159-176 *in*: Walstad, J. D., Radosevich, S. R. and Sandberg, D. V. (eds.) *Natural and Prescribed Fire in the Pacific Northwest*. Corvallis, Oregon, Oregon State University Press.
- Meidinger, D. and Pojar, J. 1991. *Ecosystems of British Columbia*. British Columbia Ministry of Forests.
- Meyer, G. A., Wells, S. G., Balling, R. C., Jr. and Jull, A. J. T. 1992. Response of alluvial systems to fire and climate change in Yellowstone National Park. *Nature* **357**:147-150.

- Millspaugh, S. H. and Whitlock, C. 1995. A 750-year fire history based on lake sediment records in central Yellowstone National Park, USA. *The Holocene* **5**:283-292.
- Millspaugh, S. H., Whitlock, C. and Bartlein, P. J. 2000. Variations in fire frequency and climate over the past 17 000 yr in central Yellowstone National Park. *Geology* **28**:211-214.
- Ministry of Forests (British Columbia). 1995. Historical Fire 1950-1994. Victoria, BC: Protection Branch.
- Molloy, B. P. J., Burrows, C. J., Cox, J. E., Johnston, J. A. and Wardle, P. 1963. Distribution of subfossil forest remains, eastern South Island, New Zealand. *New Zealand Journal of Botany* **1**:68-77.
- Moloney, K. A. and Levin, S. A. 1996. The effects of disturbance architecture on landscape-level population dynamics. *Ecology* **77**:375-394.
- Muller, J. E. 1968. Geology and Mineral Deposits of Alberni Map Area, British Columbia. Geological Survey of Canada, Paper 68-50.
- Munger, T. T. 1940. The cycle from Douglas fir to hemlock. *Ecology* **21**:451-459.
- Niklasson, M. and Granstrom, A. 2000. Numbers and sizes of fires: Long-term spatially explicit fire history in a Swedish boreal landscape. *Ecology* **81**:1484-1499.
- Ohlson, M. and Tryterud, E. 2000. Interpretation of the charcoal record in forest soils: forest fires and their production and deposition of macroscopic charcoal. *Holocene* **10**:519-525.
- Okabe, A. 2000. Spatial tessellations : concepts and applications of Voronoi diagrams. New York, Wiley. 671 p.
- Ottmar, R. D., Burns, M. F., Hall, J. N. and Hanson, A. D. 1993. CONSUME Users Guide. USDA Forest Service, Pacific Northwest Region. General Technical Report PNW-GTR-304.
- Pearson, A. F. 2000. Natural Disturbance Patterns in a Coastal Temperate Rain Forest Watershed, Clayoquot Sound, British Columbia (Ph.D. Dissertation). Seattle, Washington, University of Washington.
- Pellatt, M. G., Smith, M. J., Mathewes, R. W. and Walker, I. R. 1998. Palaeoecology of postglacial treeline shifts in the northern Cascade Mountains, Canada. *Palaeogeography Palaeoclimatology Palaeoecology* **141**:123-138.
- Pickford, S. G., Fahnestock, G. and Ottmar, R. 1980. Weather, fuel, and lightning fires in Olympic National Park. *Northwest Science* **54**:92-105.
- Porter, S. C. 1986. Pattern and forcing of northern hemisphere glacier variations during the last millennium. *Quaternary Research* **26**:27-48.
- Prescott, C. E., Weetman, G. F. and Barker, J. E. 1996. Causes and amelioration of nutrient deficiencies in cutovers of cedar-hemlock forests in coastal British Columbia. *Forestry Chronicle* **72**:293-302.
- Reasoner, M. A. 1993. Equipment and procedure improvements for a lightweight, inexpensive, percussion core sampling system. *Journal of Paleolimnology* **8**:273-281.
- Reed, W. J., Larsen, C. P. S., Johnson, E. A. and MacDonald, G. M. 1998. Estimation of temporal variations in historical fire frequency from time-since-fire map data. *Forest Science* **44**:465-475.

- Reneau, S. L. and Dietrich, W. E. 1990. Depositional history of hollows on steep hillslopes, coastal Oregon and Washington. *National Geographic Research* 6:220-230.
- Rhodes, A. N. 1998. A method for the preparation and quantification of microscopic charcoal from terrestrial and lacustrine sediment cores. *Holocene* 8:113-117.
- Rich, P. M., Hetrick, W. A. and Saving, S. C. 1995. Modeling Topographic Influences on Solar Radiation: A Manual for the SOLARFLUX Model. Los Alamos National Laboratory. Manual LA-12989-M.
- Romme, W. H. and Knight, D. H. 1981. Fire frequency and subalpine forest succession along a topographic gradient in Wyoming. *Ecology* 62:319-326.
- Rorig, M. L. and Ferguson, S. A. 1999. Characteristics of lightning and wildland fire ignition in the Pacific Northwest. *Journal of Applied Meteorology* 38:1565-1575.
- Ryder, J. M. and Thomson, B. 1986. Neoglaciation in the southern Coast Mountains of British Columbia: chronology prior to the late Neoglacial maximum. *Canadian Journal of Earth Science* 23:273-287.
- Saldarriaga, J. G. and West, D. C. 1986. Holocene fires in the northern Amazon Basin. *Quaternary Research* 26:358-366.
- Sandberg, D. V. and Ottmar, R. D. 1983. Slash burning and fuel consumption in the Douglas-fir subregion. In: *Proceedings 7th Conference Fire and Forest Meteorology*. Ft. Collins, CO: Boston, American Meteorological Society; 90-93.
- Sanford, R. L., Saldarriaga, J., Clark, K. E., Uhl, C. and Herrera, R. 1985. Amazon rain forest fires. *Science* 227:53-55.
- Schmidt, R. L. 1960. Factors controlling the distribution of Douglas-fir in coastal British Columbia. *Quarterly Journal of Forestry* 54:155-160.
- Schmidt, R. L. 1970. A history of pre-settlement fires on Vancouver Island as determined from Douglas-fir ages. Pgs. 107-108 *in*: Smith, J. H. G. and Worrall, J. (eds.) *Tree-ring Analysis with Special Reference to Northwest America*. Vancouver, B.C., University of British Columbia Faculty of Forestry Bulletin No. 7.
- Shinneman, D. J. and Baker, W. L. 1997. Nonequilibrium dynamics between catastrophic disturbances and old-growth forests in ponderosa pine landscapes of the Black Hills. *Conservation Biology* 11:1276-1288.
- Shugart, H. H., Jr. and West, D. C. 1981. Long-term dynamics of forest ecosystems. *American Scientist* 69:647-652.
- Scientific Panel for Sustainable Forest Practices in Clayoquot Sound. 1995a. Report 5: Sustainable Ecosystem Management in Clayoquot Sound: Planning and Practices. Province of British Columbia, Cortex Consultants, Victoria, B.C.
- Scientific Panel for Sustainable Forest Practices in Clayoquot Sound. 1995b. Report 3: First Nations' Perspectives Relating to Forest Practices Standards in Clayoquot Sound. Province of British Columbia, Cortex Consultants, Victoria, B.C.
- Skinner, W. B., Stocks, B. J., Martell, D. L., Bonsal, B. and Shabbar, A. 1999. The association between circulation anomalies and the mid-troposphere and area burned by wildland fire in Canada. *Theoretical and Applied Climatology* 63:89-105.

- Soil Classification Working Group, Canadian Agricultural Services Coordinating Committee. 1998. *The Canadian System of Soil Classification*. Ottawa, NRC Research Press.
- Sollins, P. 1982. Input and decay of coarse woody debris in coniferous stands in western Oregon and Washington. *Canadian Journal of Forest Research* **12**:18-28.
- Sollins, P., Cline, S. P., Verhoeven, T., Sachs, D. and Spycher, G. 1987. Patterns of log decay in old-growth Douglas-fir forests. *Canadian Journal of Forest Research* **17**:1585-1595.
- Spies, T. A. and Franklin, J. F. 1989. Gap characteristics and vegetation response in coniferous forests of the Pacific Northwest. *Ecology* **70**:543-545.
- Spies, T. A., Franklin, J. F. and Thomas, T. B. 1988. Coarse woody debris in Douglas-fir forests of western Oregon and Washington. *Ecology* **69**:1689-1702.
- Sprugel, D. G. 1991. Disturbance, equilibrium, and environmental variability: What is 'natural' vegetation in a changing environment? *Biological Conservation* **58**:1-18.
- Stine, S. 1994. Extreme and persistent drought in California and Patagonia during mediaeval time. *Nature* **369**:546-549.
- Stocks, B. J. and Kauffman, J. B. 1997. Biomass consumption and behavior of wildland fire in boreal, temperate, and tropical ecosystems: parameters necessary to interpret historic fire regimes and future fire scenarios. Pgs. 169-188 *in*: Clark, J. S., Chachier, H., Goldammer, J. G. and Stocks, B. (eds.) *Sediment Records of Biomass Burning and Global Change*. Berlin, Springer Verlag.
- Stokes, M. A. and Smiley, T. L. 1996. *An Introduction to Tree-Ring Dating*. Tucson, AZ, University of Arizona Press. 73 p.
- Stone, J. N., MacKinnon, A., Parminter, J. V. and Lertzman, K. P. 1998. Coarse woody debris decomposition documented over 65 years on southern Vancouver Island. *Canadian Journal of Forest Research* **28**:788-793.
- Stuiver, M. and Reimer, P. J. 1993. Extended 14C database and revised CALIB radiocarbon calibration program. *Radiocarbon* **35**:215-230.
- Stuiver, M., Reimer, P. J. and Braziunas, T. F. 1998. High-precision radiocarbon age calibration for terrestrial and marine samples. *Radiocarbon* **40**:1127-1151.
- Sugita, S. and Tsukada, M. 1982. The vegetation history in western North America. I. Mineral and Hall Lakes. *Japanese Journal of Ecology* **32**:499-515.
- Swanson, F. J., Kratz, T. K., Caine, N. and Woodmansee, R. G. 1988. Landform effects on ecosystem patterns and processes. *BioScience* **38**:92-98.
- Swetnam, T. W. 1993. Fire history and climate change in giant sequoia groves. *Science* **262**:885-889.
- Taulman, J. F. 1998. Modification of a hierarchical model of forest disturbance. *Environmental Conservation* **25**:3-7.
- Teensma, P. D. A. 1987. *Fire History and Fire Regimes of the Central Western Cascades of Oregon* (Ph.D. Dissertation), University of Oregon, Eugene.
- Thompson, R. and Oldfield, F. 1986. *Environmental Magnetism*. London, Allen & Unwin.

- Thompson, R. S., Whitlock, C., Bartlein, P. J., Harrison, S. P. and Spaulding, W. G. 1993. Climatic changes in the western United States since 18,000 years BP. Pgs. 468-513 *in*: Wright, H. E., Jr., Kutzbach, J. E., Webb III, T., Ruddiman, W. F., Street-Perrott, F. A. and Bartlein, P. J. (eds.) *Global Climates Since the Last Glacial Maximum*. Minneapolis, University of Minnesota Press.
- Triska, F. J. and Cromack, K., Jr. 1979. The role of wood debris in forests and streams. *In*: *Forests: Fresh Perspectives From Ecosystem Analysis*; 40th Biol. Colloq. Waring, R. H., ed. Corvallis, Oregon: Oregon State University Press.
- Turner, J. 1984. Radiocarbon dating of wood and charcoal in an Australian forest ecosystem. *Australian Forester* **47**:79-83.
- Turner, M. G. and Romme, W. H. 1994. Landscape dynamics in crown fire ecosystems. *Landscape Ecology* **9**:59-77.
- Turner, M. G., Romme, W. H. and Gardner, R. H. 1994. Landscape disturbance models and the long-term dynamics of natural areas. *Natural Areas Journal* **14**:3-11.
- Turner, N. J. 1991. Burning mountainsides for better crops: Aboriginal burning in British Columbia. *Archaeology in Montana* **32**:57-93.
- Urban, D. L., O'Neill, R. V. and Shugart, H.H. 1987. Landscape Ecology. *BioScience* **37**:119-127.
- Veblen, T. T. and Alaback, P. B. 1996. A comparative review of forest dynamics and disturbance in the temperate rainforests of North and South America. Pgs. 173-213 *in*: Lawford, R. G., Alaback, P. B. and Fuentes, E. (eds.) *High-latitude Rainforests and Associated Ecosystems of the West Coast of the Americas*. New York, Springer-Verlag.
- Veblen, T. T., Kitzberger, T., Villalba, R. and Donnegan, J. 1999. Fire history in northern Patagonia: the roles of humans and climatic variation. *Ecological Monographs* **69**:47-67.
- Wainman, N. and Mathewes, R. W. 1987. Forest history of the last 12000 years based on plant macrofossil analysis of sediment from Marion Lake, southwestern British Columbia. *Canadian Journal of Botany* **65**:2179-2187.
- Waterbolk, H. T. 1983. Ten guidelines for the archaeological interpretation of radiocarbon dates. *PACT* **8**:57-70.
- Weisberg, P. J. 1998. *Fire History, Fire Regimes, and Development of Forest Structure in the Central Western Oregon Cascades*, (Ph.D. Dissertation) Oregon State University, Corvallis.
- Wells, R. W., Lertzman, K. P. and Saunders, S. C. 1998. Old-growth definitions for the forests of British Columbia, Canada. *Natural Areas Journal* **18**:279-292.
- Whitlock, C. 1992. Vegetational and climatic history of the Pacific Northwest during the last 20,000 years: implications for understanding present day biodiversity. *Northwest Environmental Journal* **8**:5-28.
- Whitlock, C., Bradbury, J. P. and Millspaugh, S. H. 1997. Controls on charcoal distribution in lake sediments: case studies from Yellowstone National Park and northwestern Minnesota. Pgs. 367-386 *in*: Clark, J. S., Cachier, H., Goldammer, J. G. and Stocks, B. (eds.) *Sediment Records of Biomass Burning and Global Change*. Berlin, Springer-Verlag.

- Whitlock, C. and Millspaugh, S. H. 1996. Testing the assumptions of fire history studies: An examination of modern charcoal accumulation in Yellowstone National Park, USA. *Holocene* **6**:7-15.
- Wiles, G. C., Barclay, D. J. and Calkin, P. E. 1999. Tree-ring-dated 'Little Ice Age' histories of maritime glaciers from western Prince William Sound, Alaska. *Holocene* **9**:163-173.
- Wimberly, M. C., Spies, T. A., Long, C. J. and Whitlock, C. 2000. Simulating historical variability in the amount of old forests in the Oregon Coast Range. *Conservation Biology* **14**:167-180.
- Woodhouse, C. A. and Overpeck, J. T. 1998. 2000 years of drought variability in the central United States. *Bulletin of the American Meteorological Society* **79**:2693-2714.
- Young, J. A. and Young, C. G. 1992. *Seeds of woody plants in North America*. Portland, Or., Dioscorides Press. 407 p.

VITA

Daniel G. Gavin

EDUCATION

- Ph.D. 2000 Division of Ecosystem Sciences, College of Forest Resources, University of Washington, Seattle, WA.
- M.S. 1997 College of Forest Resources, University of Washington, Seattle, WA.
- B.A. 1992 Dartmouth College, Hanover, NH.

PEER-REVIEWED PUBLICATIONS

- Gavin, D.G., J.S. McLachlan, L.B. Brubaker, and K. Young. (2001) Post-glacial history of subalpine forests on the Olympic Peninsula, WA, USA. The Holocene: in press.
- Gavin, D.G. and L.B. Brubaker. (1999) A 6000-year soil pollen record of subalpine meadow vegetation in the Olympic Mountains, Washington, USA. Journal of Ecology 87: 106-122.
- Gavin, D.G. and D.R. Peart. (1999) Vegetative life history of a dominant rain forest canopy tree. Biotropica 31: 288-294.
- Gavin, D.G. and D.R. Peart. (1997) Spatial structure and regeneration of *Tetramerista glabra* in peat swamp rain forest in Indonesian Borneo. Plant Ecology 131: 223-231.
- Gavin, D.G., D.R. Peart and M. Leighton. (1996) Canopy structure in peat swamp forest in West Kalimantan, Indonesia. Tropical Biodiversity. 3(3): 243-249.
- Gavin, D.G. and D.R. Peart. (1993) Effects of beech bark disease on the growth of American beech (*Fagus grandifolia*). Canadian Journal of Forest Research 23: 1566-1575.

PUBLISHED ABSTRACTS

- Gavin, D.G. (1999) Holocene fire history in a coastal temperate rainforest, Vancouver Island. Bulletin of the Ecological Society of America 80:
- Gavin, D.G., Lertzman, K.P., Brubaker, L.B. and Nelson, E. (1997) Holocene fire size and frequency in a coastal temperate rainforest. Bulletin of the Ecological Society of America 78(4):93.
- Gavin, D.G., Lertzman, K.P., Brubaker, L.B. and Nelson, E. (1996) Long term fire histories in a coastal temperate rainforest. Bulletin of the Ecological Society of America 77(3):157.
- Gavin, D.G., Lertzman, K.P., Brubaker, L.B. and Nelson, E. (1996) Long-term fire histories in a coastal temperate rainforest. AMQUA: Program and Abstracts of the 14th Biennial Meeting, Flagstaff, NM.